

RICE UNIVERSITY



JOHN S. OLDOW  
Professor and Head  
Geology and Geological Engineering  
University of Idaho  
Moscow, Idaho 83844-3022  
Phone: 208-885-6192  
E-Mail: oldow@uidaho.edu

USE OF A THREE-DIMENSIONAL FLOW MODEL  
TO DETERMINE THE POSITION AND SHAPE OF A SALTY

by

SHAWN M. PAQUETTE

A THESIS SUBMITTED  
IN PARTIAL FULFILLMENT OF THE  
REQUIREMENTS FOR THE DEGREE

MASTER OF SCIENCE

APPROVED, THESIS COMMITTEE

RECEIVED

JAN 08 1993

SRAKIT COUNTY  
HEALTH DEPT.

A handwritten signature in cursive script, likely belonging to Philip B. Bedient.

Philip B. Bedient, Professor, *Chair*,  
Environmental Science and Engineering

A handwritten signature in cursive script, likely belonging to Mark R. Wiesner.

Mark R. Wiesner, Associate Professor,  
Environmental Science and Engineering

A handwritten signature in cursive script, likely belonging to John B. Anderson.

John B. Anderson, Professor, *Chair*,  
Geology and Geophysics

Houston, Texas  
January, 1997

## ABSTRACT

# USE OF A THREE-DIMENSIONAL FLOW MODEL TO SIMULATE THE POSITION AND SHAPE OF A SALTWATER INTERFACE

by

SHAWN M. PAQUETTE

Use of a standard three-dimensional flow model to simulate the saltwater interface in coastal and island aquifers as a no flow boundary is introduced. The method was used to simulate flow in a generic circular island aquifer. The results of this model compared favorably with those generated by an analytical solution and a numerical simulation. The method was used to investigate the freshwater resources of Guemes Island, Skagit County, Washington. The model showed that the northern region of the island is most vulnerable to saltwater intrusion. However, it was determined from the modeling exercise that with careful planning Guemes Island can sustain substantial development of its aquifer system without significant saltwater intrusion. The use of a standard flow model can not simulate changes in well discharge concentration but can be a valuable tool in managing groundwater development in island and coastal aquifers

## Acknowledgments

I wish to thank Dr. Phil Bedient for the opportunity to study at Rice University. I also would like to thank the other members of my thesis committee, Dr. Mark Weisner and Dr. John Anderson for their guidance. For their help in the development of this thesis, I would like to thank: Dr. Maged Hamed for his guidance and technical support; John Bradford for his role in the acquisition of field data; Gary Raven for his modeling expertise; and last but not least, Paul Nelson for the countless hours he spent trying to figure out why our computer wasn't working and for helping make this thesis as aesthetically pleasing as possible.

I want to thank all of my friends in Houston, Greg, Raq, Tariq, Paul, Amy, Cathy, Nelson, and the rest of you clowns that helped make Houston home. I doubt I would be sane (as sane as I am now anyway) if it hadn't been for all of you. Thanks to all my friends and family (especially my sisters Lesley and Heather) back in the great state of Vermont who were never more than a phone call away.

I especially want to thank my parents for their love and support, for the guidance that they gave me from day one of life, for teaching me to always believe in myself, and for making me who I am today.

Lastly, I want to thank Tracey for her love and support during the last few years. Without her this never would have come to pass.

## Table of Contents

ABSTRACT.....	ii
ACKNOWLEDGMENTS.....	iii
TABLE OF CONTENTS.....	iv
LIST OF FIGURES.....	viii
LIST OF TABLES.....	ix
1. INTRODUCTION .....	1
2. BACKGROUND AND LITERATURE REVIEW.....	8
2.1 BACKGROUND: GENERAL CONCEPTUAL MODELS .....	8
2.2 EARLY ANALYTICAL MODELS.....	11
2.2.1 The Ghyben-Herzberg Relationship.....	11
2.2.2 Potential Flow Theory.....	14
2.2.3 The Zone of Mixing and Dispersion .....	15
2.3 SHARP-INTERFACE MODELING .....	17
2.3.1 Single Phase Sharp-Interface Approximations: Analytical.....	17
2.3.2 Single Phase Sharp-Interface Approximations: Numerical.....	19
2.3.3 Two Phase Sharp-Interface Approximations .....	22
2.3.4 Multilayed Sharp Interface Approximations .....	24
2.4 USE OF FLOW MODELS AND SIMULATION OF THE INTERFACE AS A NO FLOW BOUNDARY.....	26

2.4.1 Two-Dimensional Studies.....	27
2.4.2 Quasi Three-Dimensional Studies .....	28
2.4.3 Full Three-Dimensional Studies .....	29
2.5 DENSITY-DEPENDENT, MIISCIBLE FLUID, MODELING .....	30
2.5.1 General Concept.....	31
2.5.2 Specific Applications of Miscible Flow Modeling .....	32
2.5.3 USGS Density-Dependent Codes.....	34
2.5.4 Applications of SUTRA .....	35
<b>3. MODELING METHOD AND VERIFICATION .....</b>	<b>37</b>
3.1 MODELING METHOD .....	37
3.1.1 The General Equation of Flow.....	38
3.1.2 Simulation of the Interface as a No Flow Boundary .....	40
3.1.3 Use of the Ghyben-Herzberg Relationship .....	41
3.2 FLOW MODEL SELECTION: MODFLOW .....	43
3.2.1 The Numerical Method.....	45
3.2.2 Treatment of Boundary Conditions.....	46
3.2.3 Treatment of Three-Dimensional Flow.....	47
3.3 VERIFICATION OF THE METHOD ON A GENERIC CIRCULAR ISLAND .....	48
3.3.1 Fetter's Solution for the Position of the Saline Interface Beneath Oceanic Islands.....	49

3.3.2 Analytical Solution to Fetter's Equation for a Circular Island.....	52
3.3.3 Numerical Solution to Fetter's Differential Equation.....	53
3.3.4 No Flow Boundary 3-D Solution to the Circular Island.....	55
3.3.5 Comparison of the Solution Methods.....	59
4. CASE STUDY: GUEMES ISLAND.....	66
4.1 BACKGROUND OF GUEMES ISLAND.....	66
4.1.1 Hydrogeologic Units .....	68
4.1.2 Hydraulic Conductivity Values.....	71
4.1.3 Approximate Water Budget.....	74
4.1.4 Quality of Groundwater.....	78
4.2 ADDITIONAL DATA COLLECTED.....	82
4.2.1 Data Collection.....	83
4.2.2 Elevation of Bedrock.....	83
4.2.3 Head Distribution in the Double Bluff Aquifer.....	84
4.3 MODEL CONSTRUCTION AND GRID DESIGN.....	87
4.3.1 Three-Dimensional Grid Layout.....	87
4.3.2 Representation of the Aquifer System in MODFLOW .....	92
4.3.3 Boundary Conditions .....	93
4.3.4 MODFLOW Parameters .....	94
4.4 MODEL CALIBRATION .....	95
4.4.1 Calibration Process .....	96

4.4.2 Sensitivity Analysis .....	101
4.5 FUTURE PREDICTIONS OF GROUNDWATER DEVELOPMENT ....	104
4.5.1 Case One .....	104
4.5.2 Case Two.....	105
4.5.3 Case Three.....	105
4.5.4 Case Four.....	107
4.5.5 Case Five.....	110
4.5.6 Case Six .....	110
4.5.7 Freshwater Resources of Guemes Island.....	113
5. CONCLUSIONS .....	116
6. REFERENCES .....	120
APPENDIX A: Matlab Code for Numerically Model of the Circular Island.....	126
APPENDIX B: IBOUND Conditions for the MODFLOW Solution to the Circular Island.....	129
APPENDIX C: Extent and Thickness of the Vashon Aquifer.....	131
APPENDIX D: Double Bluff Aquifer Well Information.....	133
APPENDIX E: Water Quality Summary of Guemes Island.....	134
APPENDIX F: Conceptual Model and IBOUND Conditions in MODFLOW for Guemes Island.....	136

## List of Figures

Figure 2.1: Conceptual Model of a Coastal Aquifer in Connection with the Sea .....	10
Figure 2.2: Conceptual Model of an Island Aquifer in Connection with the Sea .....	10
Figure 2.3: The Ghyben-Herzberg Relationship    Source: Strack, 1989 .....	13
Figure 2.4: Glover's Potential Flow Relationship    Source: Todd, 1980 .....	16
Figure 3.1: Elemental Control Volume .....	39
Figure 3.2: Vertical Cross-Section of a Typical Island .....	42
Figure 3.3: Computational Finite Element Molecule .....	46
Figure 3.4: Control Volume for Two-Dimensional Dupuit Flow .....	50
Figure 3.5: Circular Island Heads: Analytical Solution .....	53
Figure 3.6: Numerical Solutions to the Circular Island, Heads in ft msl .....	56
Figure 3.7: MODFLOW Solution to the Circular Island: 17x17x10 Grid .....	60
Figure 3.8: MODFLOW Solution to the Circular Island, 17x17x20 Grid .....	61
Figure 3.9: MODFLOW Solution to the Circular Island, 32x32x20 Grid .....	62
Figure 4.1: Inventoried Wells on Guemes Island .....	67
Figure 4.2: Six Main Hydrogeologic Units Beneath Guemes Island .....	68
Figure 4.3: Estimated Hydraulic Conductivity Values .....	75
Figure 4.4: Relation of Precipitation to Groundwater Recharge on Guemes Island, Source: Kahle and Olsen, 1995 .....	77



Figure 4.5: Areal Distribution of Chloride Concentrations, Source: Kahle and Olsen, 1995.....	80
Figure 4.6: Seasonal Variation of Chloride Concentration in Select Wells.....	81
Figure 4.7: Point Elevations of Bedrock Estimated by the Gravity Survey.....	85
Figure 4.8: Bedrock Elevation Distribution Beneath Guemes Island.....	86
Figure 4.9: Measured Heads within the Double Bluff Aquifer .....	88
Figure 4.10: Measured Head Distribution: Double Bluff Aquifer.....	90
Figure 4.11: Grid Layout for MODFLOW Model: Guemes Island .....	91
Figure 4.12: The Initial MODFLOW Run Using Average Values of Conductivity .....	98
Figure 4.13: Calibrated Head Map: Double Bluff Aquifer.....	99
Figure 4.14: The Calibrated Conductivity Values: Double Bluff Aquifer .....	102
Figure 4.15: Sensitivity Analysis: RMS vs. Adjustment Factor.....	103
Figure 4.16: Drawdown in the Double Bluff Aquifer: Case 1.....	106
Figure 4.17: Drawdown in the Double Bluff Aquifer: Case 2.....	108
Figure 4.18: Drawdown in the Double Bluff Aquifer: Case 3.....	109
Figure 4.19: Drawdown in the Double Bluff Aquifer: Case 4.....	111
Figure 4.20: Drawdown in the Double Bluff Aquifer: Case 5.....	112
Figure 4.21: Drawdown in the Double Bluff Aquifer: Case 6.....	114
Figure B.1: IBOUND Conditions for Circular Island: Layer 1.....	129
Figure B.2: IBOUND Conditions for Circular Island: Vertical X-Section.....	130

Figure C.1: Extent and Thickness of the Double Bluff Aquifer.....	131
Figure F.1: Conceptual Model: Layer Six.....	136
Figure F.2: Conceptual Model: Row 32.....	137
Figure F.3: IBOUND Conditions: Layer Six.....	138
Figure F.4: IBOUND Conditions: Row 32.....	139

## List of Tables

Table 1.1: Composition of "Average" Seawater .....	4
Table 1.2: Brewing and Distilling Requirements for TDS.....	6
Table 3.1: MODFLOW Parameters for the Generic Circular Island.....	58
Table 3.2: Maximum Head Values Determined in Each Simulation.....	63
Table 4.1: Average Horizontal Conductivities for the Hydrogeologic Units, Guemes Island.....	74
Table 4.2: Approximate Water Budget for Guemes Island .....	76
Table 4.3: Vertical Leakance Terms: Guemes Island .....	94
Table 4.4: Comparison of Generated and Measured Head Values.....	100
Table D.1: Double Bluff aquifer Well Information.....	133
Table E.1: Summary Concentrations of Common Constituents, Guemes Island, June 1992.....	134
Table E.2: Median Concentrations by Unit, Guemes Island, June 1992.....	135

## 1. INTRODUCTION

Coastal and island regions are some of the most densely populated areas of the world. Demand for freshwater in these regions has increased and the development of groundwater aquifers has left these areas susceptible to saltwater intrusion. In many areas where groundwater is the only source of freshwater, particularly small oceanic islands and arid coastal areas where surface water sources may not be available, this problem is of major concern. Saltwater intrusion **effects** human health and welfare in a number of ways. A decrease in water quality, due to intrusion, can adversely **effect** the potability of a water resource. Salinity in agricultural irrigation water results in a decrease in crop productivity and may require a switch to more salt tolerant crops. High salinity is also undesirable for many industrial purposes.

In order to adequately plan groundwater development the dynamics of the flow system must be understood. The portion of this system which is most difficult to understand is the interaction between the saltwater and freshwater. There are a number of approaches for estimating the position of the interface between the two liquids, which will be summarized in Chapter Two. An accurate groundwater model of the aquifer system is a vital tool in development of a groundwater strategy ensuring the longevity of the freshwater resource.

The purpose of this research is to establish a groundwater model capable of estimating changes in the freshwater/saltwater system due to development of the freshwater lens in small oceanic islands. The modeling method focuses on the use of a standard three-dimensional flow model, MODFLOW (McDonald and Harbaugh, 1984), and estimation of the interface position as a no flow boundary. Specifically the objectives of this research are the following:

1. Develop a modeling methodology for using a standard flow model to estimate both the position and the shape of the saltwater/freshwater interface as a no flow boundary.
2. Verify that this modeling methodology generates results similar to those generated by an analytical model of a generic circular island
3. Use the modeling methodology to construct a flow model of Guemes Island, Skagit County, Washington.
4. Calibrate the flow model of Guemes Island to present day head values.
5. Use the flow model of Guemes Island to show that with proper planning it can sustain significant development while maintaining the integrity of its fresh groundwater resource.

Saltwater intrusion can come from a variety of different sources. The most common and well know source, the focus of this research, is the sea. Seawater intrudes into a coastal aquifer due to the direct hydraulic connection

of the sea to the freshwater aquifer. Maintaining the freshwater resource in coastal and island regions requires careful planning of aquifer development to decrease its effect on intrusion. A model of the flow system, like the one used in this research, is a valuable tool for estimating the response of coastal aquifers to changes in recharge and freshwater withdrawal.

Surface sources of saline water include, brine disposal pits and leaching of road salts used during storm events. In coastal regions, tide waters may invade freshwater supplies from above through wells or by other pathways. Minerals deposited along the shoreline can also leach into aquifers from above. Crop irrigation is a major source of saline water intrusion. Salts accumulate on the soils through irrigation waters and then can be leached into underlying groundwater supplies.

There are a number of underground sources of saltwater other than seawater. Intrusion of brine waste from petroleum exploration can occur through leaking injection wells (Miller, 1980). Poorly designed brine disposal pits cause leaching into surrounding aquifers. There is also a large amount of naturally occurring saline groundwater. This saline groundwater may intrude into new regions when the flow dynamics of the system are changed.

There is no primary drinking water standard for chloride or total dissolved solids, both of which are associated with the presence of saline water. However, these contaminants may adversely affect the aesthetic quality of drinking water and therefore the USEPA has set nonenforceable

guidelines for them. The SMCL for chloride is set at 250 mg/l, and TDS is 500 mg/l (AWWA, 1990). It has been estimated that for seawater as little as two percent in freshwater may render the water unpotable (Todd, 1980).

In order to evaluate seawater intrusion compared to other sources of TDS, the chloride-bicarbonate ratio has been recommended as a criterion (Todd, 1980). Chloride is the dominant anion in seawater, and normally occurs in only small amounts in groundwater. On the other hand, bicarbonate is the **dominate** anion in groundwater and occurs in minor

Table 1.1: Composition of "Average" Seawater

<u>Ion</u>	<u>Percent Composition</u>	<u>Amount in "Average"</u> <u>Seawater (mg/l)</u>
Chloride	55.04	18,980
Sodium	30.61	10,556
Sulfate	7.68	2649
Magnesium	3.69	1727
Calcium	1.16	400
Potassium	1.10	380
Bicarbonate	0.41	140
Bromide	0.19	65
Boric Acid	0.07	26
Strontium	0.04	13

Others	0.01	2
Total	100	34,483

amounts in seawater. The ratio of the two anions in a water supply may be used to indicate the presence of seawater intrusion. The composition of dissolved solids and amount of major ions in "average" seawater can be found in Table 1.1 (Chow, 1964). TDS and chloride concentrations have an effect on more than just the potability of a water resource. Maas (1984) did an extensive investigation of crop tolerances for salinity. This study listed the maximum soil salinity for certain crops without a loss of yield and also the percent decrease in yield at soil salinity above the threshold. In arid areas the decrease in crop production can have a devastating effect on the availability and price of food. The use of groundwater for livestock water consumption requires TDS values ranging from 3000 mg/l for poultry to as much as 12,000 mg/l for sheep (USEPA, 1973). Many industries have TDS standards for the water used in both cooling and production. High TDS values can cause significant problems with some equipment such as boilers due to scaling. Water is also used as an ingredient in much of the processed food industry which may require low TDS values. As an example of industrial quality requirements, Table 1.2 list TDS requirements for brewing and distilling (Atkinson 1986). Water treatment cost to meet TDS requirements may discourage business from locating in areas with intrusion problems.



Table 1.2: Brewing and Distilling Requirements for TDS

<u>Use</u>	<u>Limit in mg/l</u>
Boiler Feed Water	50-3000 (pressure dependent)
Brewing, light beer	500
Brewing, dark beer	1000
Brewing and Distilling, general	500-1500

Saltwater intrusion is a problem in many areas of the world, as well as in the United States. China, Japan, and the Middle East, to mention but a few, have all experienced a decrease in water quality due to the effects of intrusion. In the United States saltwater intrusion is of concern not only along the coast and on islands but also in regions where there are large amounts of shallow saline groundwater. It has been reported that 41 of the 50 states has some form of saltwater intrusion (Atkinson et al., 1986).

Methods for controlling intrusion varies depending upon the source of saline water, the extent of intrusion, local geology, water use, and economic factors. Raising and maintaining freshwater heads through artificial freshwater recharge can be an effective method (Todd, 1974). However, this necessitates development of a supplemental water source and may be economically unfeasible. Head barriers can be introduced into an aquifer through either injection or extraction wells. These head barriers can induce either flows seaward or landward in order to counteract the process of saltwater intrusion. An impermeable subsurface barrier can be constructed

throughout the vertical extent of the aquifer to prevent the inflow of seawater into the freshwater lens. The best and most cost effective method to prevent saltwater intrusion is through adequate planning of groundwater development in order to minimize its effect on the natural state of equilibrium between the freshwater and saltwater in the aquifer.

## 2. BACKGROUND AND LITERATURE REVIEW

The purpose of this chapter is to review and summarize contributions to the understanding of the interaction between freshwater and saltwater in coastal and island aquifers. Although many of these concepts may be applicable to other forms of saltwater contamination, discussed in Chapter 1, the main emphasis will be on coastal and island aquifers in direct hydrologic connection with the sea. There are a number of different approaches to modeling saltwater intrusion. Assumptions about the physics of the mixing process lead to either a sharp-interface approximation of the system, immiscible fluids, or a density-dependent miscible fluids solution. The flow system may be described using only the freshwater equation. Alternatively, both the freshwater and saltwater equations may be handled simultaneously. The position of the interface can be estimated with an analytical or numerical solution in either two or three dimensions. The time frame, scale of the flow system, and desired results will influence the choice of models, as will the physical characteristics of the aquifer system.

### 2.1 BACKGROUND: GENERAL CONCEPTUAL MODELS

The occurrence of seawater in island and coastal aquifers can be visualized with simple conceptual models, see Figures 2.1 and 2.2. The main elements of these models include: recharge of the freshwater lens, the intrusion of saltwater, and the transition zone. It should be noted that the

term *saltwater intrusion* does not necessarily imply dynamic conditions, it has historically been used to simply imply the presence of saltwater (Handbook of Hydrology, 1993). The recharge of freshwater, generally horizontal for coastal aquifers and vertical for island aquifers, forms a lens of freshwater that floats on top of a base of seawater. Owing to its greater density the saltwater tends to force its way inland forming a wedge beneath the freshwater lens. The freshwater in the lens flows toward the sea where it is discharged at a seepage face. At the interface separating the two liquids the pressure of the saltwater, caused by its density, is counterbalanced by the hydraulic gradient of the freshwater flowing to the sea. These forces bring the system to a natural state of equilibrium. As the piezometric head of the freshwater is decreased by either pumping or changes in recharge, due to urbanization, there is less flow to the sea, which allows intrusion to occur.

Under natural conditions the position of the interface will remain relatively fixed. In many instances the two liquids can be treated as immiscible and the interface can be viewed as abrupt or sharp (Rielly and Goodman, 1985). Freshwater and seawater are actually miscible fluids and therefore the zone of contact between them takes on the form of a transition zone caused by hydrodynamic dispersion (Bear, 1979). Across this zone the density varies from that of freshwater to that of seawater. The mixed liquid within the transition zone flows toward the sea causing saltwater to flow

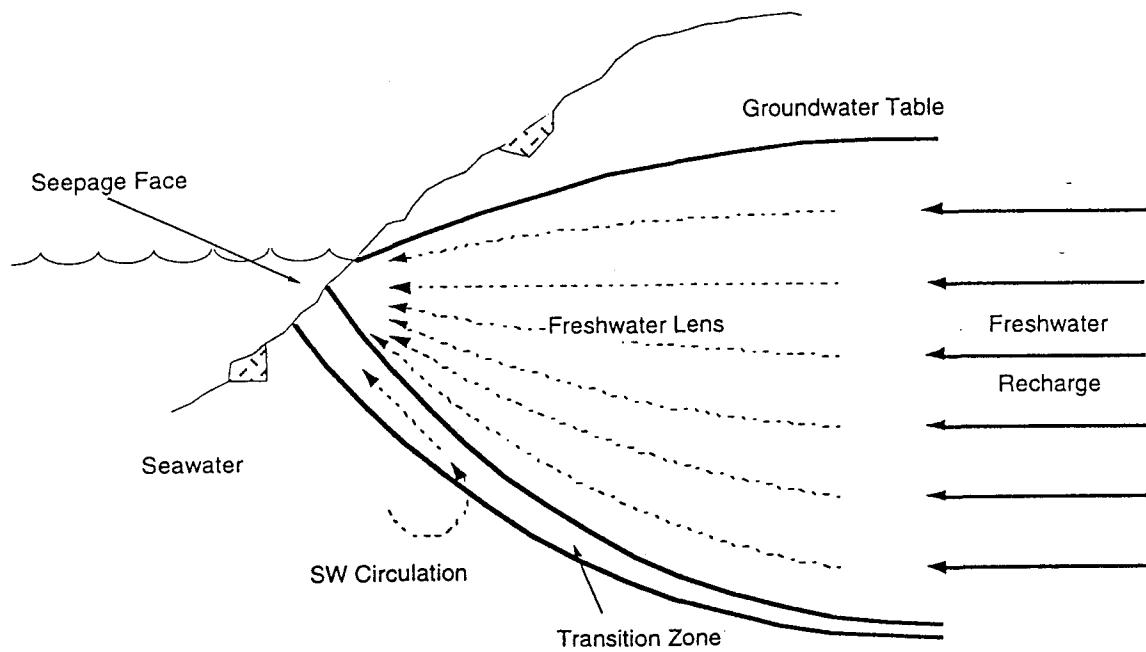


Figure 2.1: Conceptual Model of a Coastal Aquifer in Connection with the Sea

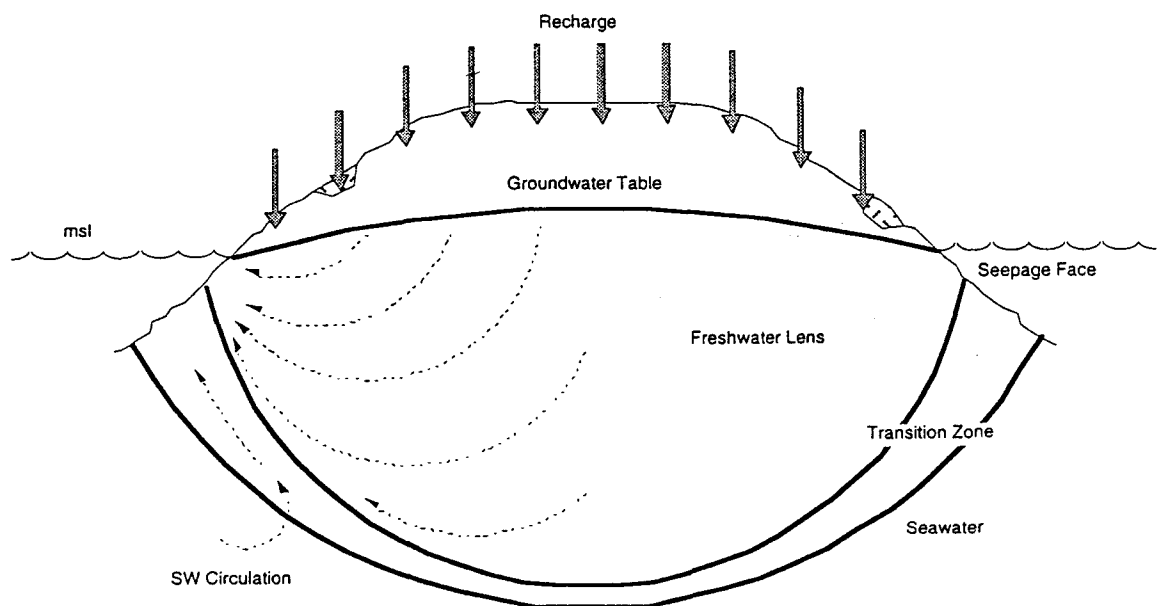


Figure 2.2: Conceptual Model of an Island Aquifer in Connection with the Sea

toward the area of mixing forming a small circulation of saltwater around this area.

The position and size of the transition zone can be affected by a number of factors. Large tidal variations can increase the thickness of the transition zone near the shore. Increased pumping can cause *upconing* of the saltwater and increase the thickness of the zone in localized areas. In an extreme case, concentrated pumping in the Honolulu-Pearl Harbor area of Hawaii has created a localized transition zone more than 300 m thick, essentially the entire thickness of the aquifer (Todd and Meyer, 1971). Variability in recharge and discharge rates can also affect the mixing process and therefore increase the thickness of the transition zone.

## 2.2 EARLY ANALYTICAL MODELS

The earliest estimation of the position of the saltwater interface was developed independently by two European **scientist**, Badon Ghyben and Herzberg, in the late 1800's. Although these two **scientist** are credited with the first statement of this interface relationship, it was later discovered in 1963 by Carlston that the relationship may have been derived by Du Commom as early as 1828 (Rielly and Goodman, 1985).

### 2.2.1 The Ghyben-Herzberg Relationship

The *Ghyben-Herzberg Relationship*, see Fig. 2.3, assumes hydrostatic equilibrium of the system. The aquifer is bounded from above by either the

water table for an unconfined aquifer, or the piezometric surface for a confined aquifer. The lower boundary is the assumed sharp-interface separating the freshwater lens from the saltwater. The distance between the upper boundary and sea level is denoted,  $h_f$ , and from msl to the lower boundary,  $h_s$ .  $H_s$  is the depth below msl to some reference level, and  $Z$  is the height of a point on the interface from the same reference level. The head in the freshwater,  $\phi$ , is expressed in terms of the pressure and elevation by:

$$\phi = \frac{p_f}{g * \rho_f} + Z \quad \text{Eq 2.1}$$

where  $p_f$  is the pressure of the freshwater,  $\rho_f$  the density of freshwater, and  $g$  the acceleration due to gravity. The head in the saltwater can be written in similar terms.

$$\phi_s = \frac{p_s}{g * \rho_s} + \bar{Z} \quad \text{Eq 2.2}$$

The pressure at any point on the interface must be a single value and the value of  $Z$  at that point will be  $H_s - h_s$ . By substitution and setting  $p_f = p_s$ , the following equation results:

$$g * \rho_f (\phi - H_s + h_s) = g * \rho_s (\phi_s - H_s + h_s) \quad \text{Eq 2.3}$$

If the resistance to vertical flow is neglected, *Dupuit's Assumption*, so that the equipotentials are vertical then,  $\phi = H_s + h_f$ . If the analysis is further limited to the case where the saltwater is at rest, the head in the saltwater equals the elevation of sea level above the reference level,  $\phi_s = H_s$ . By rearranging terms

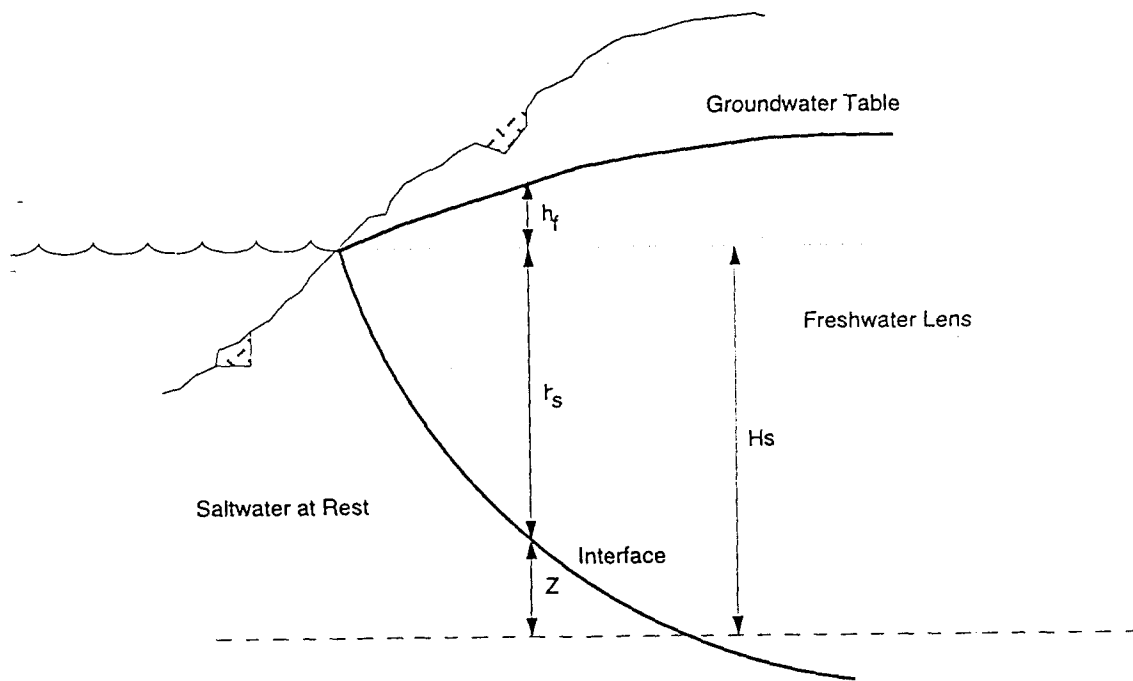


Figure 2.3: The Ghyben-Herzberg Relationship Source: Strack, 1989

and dividing by  $g \cdot \rho_f$ , we are left with the Ghyben-Herzberg Equation (Bear, 1979; Freeze and Cherry, 1979; Strack, 1989).

$$h_f = h_s \frac{\rho_s - \rho_f}{\rho_f} \quad \text{Eq 2.4}$$

Assuming typical values for freshwater and seawater density, this relationship indicates that for every foot of head above sea level there is approximately 40 feet of freshwater lens below sea level to the interface.

This relationship has been generalized by the work of Hubbert and others for the condition where the underlying saltwater is in motion with heads above or below sea level. The result for nonequilibrium conditions has the form:



$$Z = \frac{\rho_f}{\rho_s - \rho_f} h_f - \frac{\rho_f}{\rho_s - \rho_f} h_s \quad \text{Eq 2.5}$$

The variable  $h_f$  is the level of water in a well drilled into the freshwater lens to a depth of  $Z$ , and  $h_s$  is the altitude of the water level in a well drilled into the saltwater wedge to the same depth  $Z$ . If the value of  $h_s = 0$ , then this equation reduces to the Ghyben-Herzberg equation.

Bear and Dagan (1964b) investigated the validity of the Ghyben-Herzberg relationship. They found that for a confined horizontal aquifer with steady flow the approximation was within an error of 5 percent, for determining the position of the interface toe. As the shore is approached *Dupuit's Assumption* becomes less valid. Vertical flow of the freshwater to the seepage face allows the depth to interface to be greater than that predicted by the Ghyben-Herzberg relationship (Bear, 1979). Another problem with the relationship assumptions is that it does not allow for a seepage face for discharge of the freshwater, which is a critical component of the flow system.

### 2.2.2 Potential Flow Theory

Glover (1959) developed a formula to describe the shape of the sharp interface in a coastal aquifer accounting for discharge of the freshwater. His formula was derived from potential flow theory and has the form:

$$Z^2 = \frac{2qx}{\Delta\rho K} + \left( \frac{q}{\Delta\rho K} \right)^2 \quad \text{Eq 2.6}$$

where  $Z$  and  $x$  are as shown in Figure 2.4. The  $\Delta\rho$  is the difference in the densities of the fresh and saltwater,  $K$  is the hydraulic conductivity, and  $q$  is the discharge per unit length of shoreline.

### 2.2.3 The Zone of Mixing and Dispersion

In the early 1960's, Kohout (1960a)(1960b) discovered the importance of the mixing zone while doing research in the Biscayne aquifer of southeastern Florida, one of the most intensely studied aquifers in North America. Field data indicated that the saltwater front undergoes transient changes in position and composition due to seasonal changes in recharge and the resulting water table fluctuations. This field data confirmed the necessity of considering dispersion in both steady-state and transient analyses.

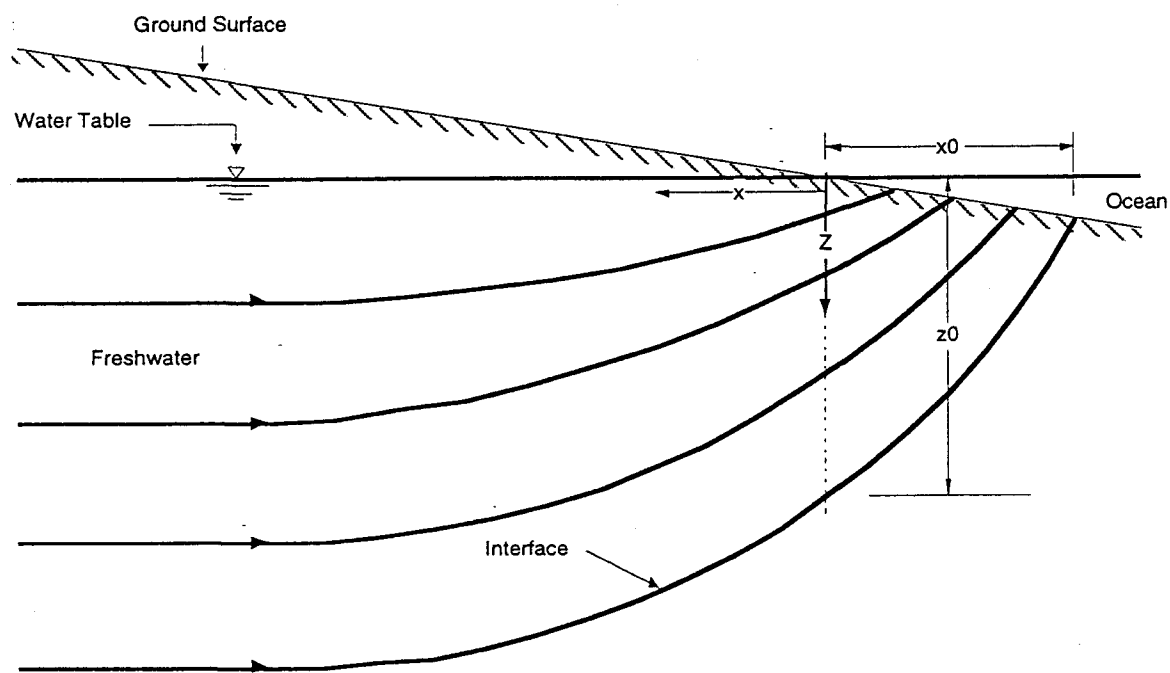


**Figure 2.4: Glover's Potential Flow Relationship**      **Source: Todd, 1980**

Cooper (1959) developed a hypothesis to explain the zone of dispersion by the movement of the saltwater front inducing a circulation of saltwater from the sea into the zone of dispersion and back to the sea. Included in his analysis, Cooper attempts to define the amount of mixing attributed to tidal fluctuations in coastal aquifers. Henry (1964) made the first attempt to quantify the effects of dispersion and density-dependent fluid flow on saltwater intrusion. Henry's work was significant in that it was the first miscible fluids, as opposed to sharp interface, approach to the saltwater problem. Henry's approximate solution was often used to validate early numerical codes for density-dependent flow.

Cooper et al. (1964) summarized early work in the area of saltwater intrusion giving insight into the role of hydrodynamic dispersion, transient movement of the interface, and providing direction for future advances in the understanding of saltwater intrusion. Since 1965, the understanding of the flow system has increased dramatically. Advances in both sharp interface and density dependent flow modeling have progressed rapidly. The following sections outline some of the work done in each of the different approaches to the saltwater intrusion problem.

## **2.3 SHARP-INTERFACE MODELING**

One approach to modeling saltwater intrusion is based on the well known assumption of an abrupt or sharp-interface. Although this approach does not provide information about the transition zone and therefore concentrations cannot be determined, it does provide information on the regional flow dynamics and can predict the response of the freshwater/saltwater interface to applied stresses. The sharp-interface assumption has been proven to be a valuable tool in evaluating water resources in coastal and island regions. This approach can be viewed in two different ways. The first describes the system using only the equation of freshwater flow, the second handles the equations of freshwater and saltwater flow simultaneously.

### **2.3.1 Single Phase Sharp-Interface Approximations: Analytical**

The single phase sharp-interface approximation assumes that the saltwater is static and the system is described using only the equation of freshwater flow. The key modeling assumption in this approach is the Ghyben-Herzberg relationship. Although for most aquifer systems the complexity of the geometry warrants a numerical solution, analytical solutions have been derived for problems with simple domains and are useful in validating numerical models.

Many of the single phase investigations assume that the system is under steady state conditions and that the interface in the aquifer reaches a stationary equilibrium. Bear and Dagan (1964a) attempted to derive approximate expressions for the movement of the interface in a single confined coastal aquifer caused by changes in the freshwater flow rate to the sea. This study was able to predict the landward movement of the interface as decreases in the freshwater heads were induced by pumping. The major restriction to the problem was that the outward flow to the sea had to remain sufficiently large. Errors were produced when simulating shallow aquifers with a thin freshwater lens. For a similar case, expressions were derived by dividing the aquifer into zones defined by the type of flow occurring (Strack, 1976). By dividing the aquifer into zones, the technique was better able to represent flow in shallow aquifers. This analytical technique was applied to two interface flow problems, confined and unconfined, in a shallow coastal aquifer with a fully penetrating well. Each problem was divided into two zones, confined/unconfined flow, and confined/unconfined interface flow. The technique assumed a single potential which is defined throughout all zones of the aquifer. It was shown that saltwater intrusion occurred in the well when the discharge rate exceeded a certain value and the conditions that must be met in order to prevent intrusion were established.

Fetter (1972) developed a technique to define the three-dimensional position of the interface beneath oceanic islands. The position was described by one differential equation:

$$K \left( 1 + \frac{\gamma_f}{\gamma_s - \gamma_f} \right) \left( \frac{\delta^2 h^2}{\delta x^2} + \frac{\delta^2 h^2}{\delta y^2} \right) = -2W \quad \text{Eq 2.7}$$

where  $K$  is the average hydraulic conductivity,  $W$  the recharge,  $x$  and  $y$  the areal position,  $\gamma$  the density of freshwater or saltwater, and  $h$  the freshwater head in the aquifer at position  $xy$ . The expression was derived by using the Ghyben-Herzberg relationship and considering two-dimensional Dupuit flow through a control volume bounded on top by the water table and on the bottom by the no flow saltwater interface. Analytical expressions for an infinite strip island and a circular island were developed as well as a numerical solution for problems with irregular boundaries. The model was successfully used to generate the known position of the saline interface beneath the South Fork of Long Island, New York. This analytical technique will be discussed in more detail in Chapter 3, and will be used as a comparison for the modeling technique developed in this research.

### 2.3.2 Single Phase Sharp-Interface Approximations: Numerical

For most actual situations the boundary conditions and other parameters are too complicated to derive an analytical solution to the intrusion problem. In this case it is necessary to use a numerical simulation. The numerical simulations discussed here all involve solving only the

freshwater flow equation and assume the saltwater as static. All of the models are based on both the Ghyben-Herzberg relationship and Dupuit's assumption, which simplifies the three-dimensional flow pattern around the interface to two-dimensions. A number of numerical solutions have been developed for the sharp-interface problem. The examples discussed in this section represent a cross-section of the accomplished work in this subject.

Shamir and Dagan (1971) presented partial differential equations that describe the motion of the seawater interface and of the free surface in an unconfined coastal aquifer. The two regions of the aquifer, the intrusion length and the rest of the aquifer, were treated separately both in the equations used and in the grid spacing. The spacing over the intrusion length was adjusted as the position of the toe moved in order to have the interface defined by the same number of grid points at all times. The model takes into account the geometry of the vertical cross-section of the aquifer, as well as spatial variations in recharge and pumping. An implicit numerical scheme was used to solve the set of equations and the numerical solutions compared favorably with simple analytical solutions and laboratory experiments.

The boundary integral equation method was used to study intrusion problems into a freshwater aquifer (Taigbenu et al., 1984). A transient solution was solved for intrusion into a deep aquifer, and a steady state solution was used into a shallow aquifer. Both solutions were compared to analytical solutions for aquifers with simple boundaries.

A two-dimensional numerical model was developed in order to simulate changes in the shape of the water table for an island under unsteady flow conditions (Ayers and Vacher, 1983). Finite difference equations were developed for the governing flow equation and solved by an implicit procedure. The model was applied to simulate changes in the undeveloped freshwater lens of Somerset Island, Bermuda. The results were in good agreement with field observations and the model successfully predicted changes in the lens configuration due to seasonal variations in recharge.

The effects of upconing in unconfined aquifers by use of the finite element method were studied under both transient and steady state conditions (Wirojanagud and Charbeneau, 1985). The position of the sharp interface was estimated below the pumping well in order to establish the optimal pumping rate and well depth. The model established the need for skimming of freshwater from the top of the lens in order to minimize the upconing of the interface. This skimming procedure has been used effectively in many areas as a method to control saltwater intrusion. Due to the effects of gravity an upconed interface will return to its original position although the process is slow and requires abandoning the aquifer for a long period of time.



### 2.3.3 Two Phase Sharp-Interface Approximations

When the dynamics of the saltwater become important both the equations for freshwater and saltwater flow must be solved simultaneously. Most of the work done in this area have investigated intrusion into single aquifers. The complexity of the system has made developing analytical solutions difficult and therefore most studies have relied on numerical methods.

An areal finite element model was applied to North Haven, a small island off the Coast of Long Island, New York (Pinder and Page, 1977). The model was based on the sharp-interface assumption in order to target areas of potential intrusion so that a more stringent density-dependent transport model could be applied to those specific areas. The governing non-linear equations were developed by vertical integration of the flow equations for both the freshwater and saltwater. The requirement that the pressure along the interface of the two fluids remain constant was also used in order to develop the equations.

The governing equations were developed in a similar manner by (Mercer et al., 1980). In this study the equations were solved for the freshwater head, saltwater head, and the elevation of the interface by finite difference techniques. The results showed that the model was in good agreement with a simple analytical solution. The model was then used to test the validity of Dupuit's approximation. As expected, under conditions of a

steep interface the use of Dupuit's assumption becomes inappropriate due to the increased importance of vertical flow. The model was later applied to a field site at Kahului, Maui, Hawaii. The finite difference method was used in another study of the intrusion problem and was found to be unconditionally convergent and stable (Polo and Ramis, 1983). This model was found to generate its own boundary conditions along the coast and to be a good fit with unsteady analytical solutions.

Wilson and Costa (1982) used a finite element model to study the case where the freshwater is cut off from the sea by the intruded saltwater and therefore must leak upward through an overlying aquitard. The freshwater and saltwater domains were defined over the entire domain instead of splitting the aquifer into the two sections, the intrusion length and a freshwater only sections. Application of the model showed that it handled the sharp interface accurately in the absence of ambient flow. The addition of ambient throughflow leads to numerical dispersion of the problem. The solution to the problem also showed that the method worked equally well for advancing and retreating saltwater wedges.

An areal two-dimensional model to describe the unsteady motion of the freshwater/saltwater interface and of the groundwater surface was developed and applied to the confined groundwater in the estuaries of the Naka and Kiki rivers in Japan (Inouchi et al., 1985). Two separate equations were derived from the basic equations of groundwater flow. One equation

describes the rapid change in the freshwater head, and the other the slow variation in the position of the interface over time. Changes in the pumping rates over the years have caused the inland migration of the interface in the aquifers. The model was able to match the observed movement of the saltwater front to the present and to predict possible future movement.

In a study of the El Viejon Aquifer along the gulf coast of Mexico, a single phase model was used in order to calibrate the parameters of the finite difference model (Rivera et al., 1990). These calibrated parameters were then used in a two phase model to predict the position and movement of the saltwater interface within the aquifer as the demand for groundwater in the area increased. The method showed that calibration by the less numerically demanding single phase equation led to parameter values that when used in the two phase model gave head values very close to the calibration values. This approach can save considerable time in the calibration process.

#### **2.3.4 Multilayered Sharp Interface Approximations**

Few models have been reported for saltwater intrusion in multilayered systems, and most of these are limited extensions of single layered models. An extension of a single layered, single phase model to simulate intrusion in a layered coastal aquifer was developed in order to look at the case where the freshwater under a semiimpervious layer is directly below the saline toe in the upper aquifer (Muallem and Bear, 1974). This situation has been shown to

occur in both laboratory results with the Hele-Shaw analogue and in field observations. The model was tested against the Hele-Shaw analogue, which has been used as a simple tool to give direct visual solutions for a moving interface in aquifers (Bear, 1979), and the results compared favorably. Results from this experiment showed that the separation of the interface into two parts, above and below the impervious layer, became less significant as the length of the inland intrusion increased. Bear and Kapuler (1981) developed a two phase finite difference model to study the coastal aquifer of Israel, which is divided into a number of subaquifers by impervious clay layers. The effect of changing the discharge to the sea, on the position of the interface in each of the aquifers was modeled. This study also revealed that the separation of the interfaces in each of the aquifers became less significant as intrusion moved further inland.

Essaid (1990) was the first to develop a general purpose quasi three-dimensional, sharp-interface model to simulate saltwater intrusion in multiple aquifer systems. In this model, the block centered finite difference method was used to simulate the coupled saltwater and freshwater flow equations. This was a major step forward in improving the numerical modeling of interfaces in complex aquifer systems. However, the method used to deal with the leakance between aquifers led to schemes that were inconsistent with the key assumptions for sharp interface modeling. An attempt to enhance this approach through changes in the numerical

formulation was conducted by (Huyakorn et al., 1996). Test results from this study indicted that the new computational algorithms were accurate and efficient in predicting the locations, lateral movement, and upconing of the freshwater/saltwater interface.

Although the sharp interface models represented here cover a wide range of saltwater intrusion problems, there is at the present time no single model that may be used to solve the number of different intrusion scenarios that may occur in a coastal flow system. The next section discusses the use of flow models and simulation of the interface as a no flow boundary. This is the general principle used in the method developed in this research. By utilizing the versatility of a standard flow model, the flow system as a whole should be better understood than in the case specific studies presented here.

#### ***2.4 USE OF FLOW MODELS AND SIMULATION OF THE INTERFACE AS A NO FLOW BOUNDARY***

Rigorous treatment of the saltwater interface requires a model that allows for density effects as well as diffusion and dispersion of the saltwater. The sharp-interface approximation ignores the dynamics of the transition zone. In the last section a number of sharp-interface modeling studies were introduced. Another approach to the sharp-interface problem is the use of standard flow codes to simulate the saltwater interface approximately as a streamline boundary represented by no flow conditions. This has been

demonstrated in two-dimensional profile, quasi-three-dimensional, and fully three-dimensional case studies.

This application has mostly been used in large scale regional flow applications where the approximate position of the boundary has been simulated in order to approximate flow conditions. The technique developed in Chapter 3 uses this approach although on a much finer scale. The position and shape of the interface will be simulated by a full three-dimensional model. The interface position in a single aquifer will be simulated by a relatively large number of vertical grid points in order to accurately define the shape. The following are some examples of studies using flow models with the no flow boundary technique.

#### **2.4.1 Two-Dimensional Studies**

Bush (1988) simulated saltwater movement in the Floridian Aquifer system, Hilton Head Island, South Carolina, by using the density-dependent flow model SUTRA (Voss, 1984). The study was done on 8 mile by 810 feet cross section of the aquifer. In the predevelopment steady state simulation, with a standard flow model, the results showed that the freshwater flowed toward the Port Royal Sound over an intruding wedge of saltwater that meets the freshwater in a zone of mixing. The saltwater mixes with the freshwater, reverses direction, and is cycled back toward Port Royal Sound. This process was shown to be very slow with an average velocity of 1.3 ft/yr. If the mixing

zone was small this process of mixing could be neglected and the freshwater flow over the wedge could be simulated by treating the wedge as a no flow boundary without significant error. Areal digital models of the Floridian flow system, made as part of the Floridian Regional Aquifer-System Analysis (Bush and Johnston, 1986) used this technique to simulate boundaries along the sea.

#### **2.4.2 Quasi Three-Dimensional Studies**

A quasi-three dimensional flow model was used to simulate the six main water bearing units along the coast of South Carolina (Aucott, 1988). In this study the eastern boundary of the aquifer system, the Atlantic Ocean, was simulated as a no flow boundary. It was shown that the position of the seawater interface in each of the aquifers was dependent on the aquifer freshwater head values along the coast. In a similar study of the coastal plain of southeastern Virginia, the interface along the Atlantic Ocean was simulated as a stationary no flow boundary in order to predict the effects of future groundwater development (Hamilton and Larson, 1988). A transient quasi three-dimensional study model was used to determine the reliability of the groundwater supply in three layers of the Pajaro Valley aquifer system, Santa Cruz and Monterey Counties, California (Johnson et al., 1988). In this study the use of constant head and constant flux boundaries along the coast

were used. These boundaries were shifted and inflows and outflows adjusted in an attempt to simulate conditions along the coast.

#### 2.4.3 Full Three-Dimensional Studies

Guswa and LeBlanc (1985) used a fully three-dimensional flow model of the Cape Cod aquifer system, Massachusetts, in order to evaluate the hydrologic impacts of regional groundwater development. A finite difference code was used to simulate flow in five regions of the aquifer system. In this study the boundary between the fresh and saline groundwater along the coast was treated as a no flow boundary under steady state pumping conditions. Hubbert's equation was used to determine the position of the interface by means of an iterative approach to produce an equilibrium interface position. The study was done under steady state conditions for two important reasons: insufficient long term records of head and stress changes in the region, and the static no flow approximation used to represent the boundary between the fresh and saline water is valid only for equilibrium conditions. MODFLOW (McDonald and Harbaugh, 1984) was used in three dimensions for a study in southern Spain in order to better understand the hydrodynamics of the aquifer system before a miscible fluid model could be employed (Calvache and Pulido-Bosch, 1991).

In a study of the impact of future groundwater withdrawals from the Bolson-Fill aquifer, White Sands Missile Range, New Mexico, Risser (1988)



simulated water quality, as well as water level changes, for a number of possible pumping scenarios. A full three-dimensional finite difference flow code was used to calibrate the model and to predict water level changes. In the initial model construction the eastern edge of the grid, which is bounded by a natural saline groundwater reservoir, was simulated as a constant head boundary. This boundary condition was shown not to be an adequate simulation of the actual field conditions. It was determined that the freshwater flowed over the denser saline water and that the boundary condition must be simulated as a no flow boundary. Once the flow model was calibrated water quality changes were simulated using the two-dimensional density-dependent flow model SUTRA in vertical cross-section.

## ***2.5 DENSITY-DEPENDENT, MISCIBLE FLUID, MODELING***

Simulation of the transition zone separating freshwater and saltwater requires simultaneous solution of the governing equations of fluid flow and solute transport. This approach leads to density-dependent transport models. These models are useful in the case when concentrations in wells are being simulated and therefore sharp interface approximations are insufficient. In areas where the thickness of the transition zone is significantly large, due to variations in recharge, tidal fluctuations, and/or pumping, this approach may be more appropriate than the sharp interface approximation. Besides saltwater intrusion, other examples of density-dependent flow involving

miscible fluids include seepage of some types of landfill leachate, waste injection into saline aquifers, heat storage in aquifers, brine disposal, and liquid phase geothermal flow (Anderson and Woessner, 1992).

#### 2.5.1 General Concept

Standard flow models assume that the density of groundwater is constant and equal to 1.0 gm/cu. cm. This assumption is appropriate for groundwaters with low TDS and temperatures in the range of most aquifers. When the TDS of a groundwater is increased, or the temperature changed significantly, the effects of the change in groundwater density on the flow field must be accounted for. Problems involving miscible fluids of variable density are complex in that the density of the solution is dependent on the mixed concentration and temperature. Excluding the equation for heat transport, the solution to this problem involves the equations of flow and solute transport. As the concentration of the groundwater increases due to the transport of dissolved solids, the density of the groundwater increases. The new density of the groundwater at each node must therefore be inputted into the equation of flow. The iterative process is repeated, with new concentrations and densities calculated at each time step inputted into the next time step. A number of numerical models have been produced to solve the problem of density-dependent flow both for specific applications and for public use, the following are a few examples.

### 2.5.2 Specific Applications of Miscible Flow Modeling

An early attempt to simulate two-dimensional transient flow including the effects of dispersion, used the method of characteristics to solve the solute transport equation and an iterative approach to solve the groundwater flow equation (Pinder and Cooper, 1970). This solution yielded the motion of the saltwater body and the distribution of concentration for a particular problem. It was found that in general the numerical computations were too lengthy and that the difficulties could be expected in a narrow transition zone in which there are large concentration gradients. Herbert et al. (1988) modeled the groundwater flow over a hypothetical salt dome. In this study the high gradients of salt concentration caused the problem to be highly nonlinear. The problems were dealt with by starting with a relatively simple problem and stepping through smaller problems to reach the desired goal. These two modeling studies solved the problem well when the fluids were highly miscible, but as the problem approached a sharp interface they broke down numerically.

A study on Gogo Island, Japan used two different models in order to study the effects of the tides on the position and characteristics of the interface (Inouchi et al., 1990). The sharp interface model showed, as expected, that the intrusion was furthest inland at high tide. The dispersion, density-dependent model, showed that at this same time the thickness of the transition zone separating the saltwater from the freshwater was its widest. Extensive

monitoring in the coastal area of Laizhou Bay, China was conducted to track the intrusion of saltwater (Wu et al. 1993). The interface characteristics were found to vary within the aquifer. Some areas involved wide transition zones while others proved to have a distinct, sharp interface. In a later study, (Xue et al., 1995), this region was modeled using a three-dimensional miscible transport model. The effects of variable density, precipitation, and pumping were taken into account. The model was able to predict the observed values of the earlier monitoring study quite well, even though the interface characteristics varied within the aquifer system.

In order to estimate the velocity field around the injection zone of waste into a saltwater aquifer beneath the city of St. Petersburg, Florida, a density-dependent flow model was used (Hickey, 1989). The model took into account not only the densities of the two liquids but also the mixed solution of the native saline water and the chloride injectant. This model was calibrated using the data from a 91-day test and then used to simulated the flow field for a full 366-day injection period.

In another example of density-dependent modeling not involving seawater, an analytical model, which takes into account hydrodynamic dispersion, was used in order predict the migration of landfill leachate (Huyakorn et al., 1987). The model assumed a three-dimensional uniform flow field, taking into account the effects of partial penetration of the contaminant source and a finite aquifer thickness. It was found that this

model was a good screening instrument for a preliminary evaluation of the dilution potential of waste sites.

### 2.5.3 USGS Density-Dependent Codes

There are a number of public-domain USGS codes dealing with density-dependent flow modeling. The most popular and applicable is SUTRA (Voss, 1984). SUTRA combines finite elements and integrated finite differences to simulate two-dimensional problems under saturated and partially saturated conditions. Applications of this model are discussed in the next section. MOCDENSE (Sanford and Konikow, 1985) is a two-dimensional finite difference code developed for saturated conditions from the USGS solute transport code MOC (Konikow and Bredehoeft, 1978). This code assumes that the density of the solution is a function only of the concentration and that the constituents are chemically conservative. MOCDENSE was used in vertical cross section to simulate intrusion along the coast of southern Spain (Calvache and Pulido-Bosch, 1991). HST3D (Kipp, 1987) is a three-dimensional finite difference model for groundwater flow taking into account both solute transport and heat transport. VARDEN (Kuiper, 1983; Kuiper, 1985) is a three-dimensional finite difference code for steady state groundwater flow in which water density varies with spatial position and is treated as a known spatially dependent parameter. A

modification to the model was made in order to take into account the effects of multiaquifer wells (Kontis and Mandle, 1988).

#### 2.5.4 Applications of SUTRA

SUTRA is the most widely used density dependent flow model. It is often used to simulate intrusion after the hydrologic characteristics are evaluated with a flow model. (Bush, 1988) simulated saltwater movement in the Floridian Aquifer system, Hilton Head Island, South Carolina using SUTRA. (Risser, 1988) used the model in vertical cross-section to try to study the impacts of future groundwater withdrawals on the Bolson-Fill aquifer, White Sands Missile Range, New Mexico. Discussion of these studies can be found in Section 2.4.

Most of the time the density-dependent flow model is used in order to simulate a situation where the transition zone is wide. Inaccuracies in the modeling approach tends to lead to poor results for a narrow transition zone. Voss and Souza (1987) were able to simulate the narrow transition zone in an aquifer in Oahu, Hawaii using SUTRA. Care was taken in the spatial discretization in order to accurately represent the narrow interface. SUTRA has been used in the modeling of the interface beneath atoll islands. Atoll islands are reef islands with a small seawater lagoon in the center. Tidal effects are very strong in these aquifers making the Ghyben-Herzberg-Dupuit model inappropriate. The effects of the tide on atoll islands was investigated

by Oberdorfer et al. (1990) with use of the SUTRA model. SUTRA was also used in order to simulate the upconing of saltwater beneath a pumping well (Rielly and Goodman, 1987). Two modeling approaches were used, the sharp-interface method, and the density-dependent transport method. This study showed that significant amounts of saltwater could be discharged from a pumping well even if the sharp-interface below remains stable.

There is no one model or method that has been developed to solve all the problems involved with saltwater intrusion. Sharp-interface models fail to take into account the complexity of the mixing zone. Density-dependent models solve for concentrations within the transition zone but may become numerically unstable as the interface becomes thin. The complexity of the system involving saltwater intrusion and the necessity of managing these systems to maintain water resources, dictates the need for future advances in this field of study.

### 3. MODELING METHOD AND VERIFICATION

The objective of this chapter is to introduce and verify the modeling method to be utilized in this study. As required by the method, a standard flow model is selected to solve the equations of flow in three dimensions. The position and shape of the interface is estimated from head values and simulated in the flow model as a no flow boundary. Once developed, the method is used to simulate flow in an unconfined aquifer beneath a generic circular oceanic island. The results of this simulation will be compared to those of analytical and numerical solutions to the same problem. Once verified, this method will be used in Chapter 4 to investigate present and future water resources for an island in the Pacific Northwest.

#### 3.1 MODELING METHOD

The modeling method introduced here is a steady state, single phase, full three-dimensional, sharp interface model. The main elements of the method are: 1) the general equations of flow in three dimensions, 2) simulation of the saltwater/freshwater interface by use of a no flow boundary, and 3) estimation of the position of that interface by the *Ghyben-Herzberg Relationship*. The first and second elements mentioned above are implemented by the use of a standard full 3-D flow model, a discussion of the model chosen for this study is conducted in Section 3.2. The third element is



solved analytically and the position and shape of the no flow boundary inputted into the model manually.

### 3.1.1 The General Equation of Flow

The modeling method uses the single phase approach, utilizing only the equations of flow for the freshwater. The three-dimensional movement of groundwater, density assumed constant, through porous earth material can be described by the following partial-differential equation (Bedient et al., 1994):

$$\frac{\partial}{\partial x} \left( K_x \frac{\partial h}{\partial x} \right) + \frac{\partial}{\partial y} \left( K_y \frac{\partial h}{\partial y} \right) + \frac{\partial}{\partial z} \left( K_z \frac{\partial h}{\partial z} \right) - W = S_s \frac{\partial h}{\partial t} \quad \text{Eq 3.1}$$

where,

$K_x, K_y, K_z$	=	hydraulic conductivity along the x,y,z axes
$h$	=	potentiometric head
$W$	=	volumetric flux per unit volume and represents
$S_s$	=	specific storage of the porous material
$t$	=	time

The numerical method used by MODFLOW, to solve this equation is discussed in Section 3.2. This partial differential equation can be derived by combining the equation of continuity from fluid mechanics and Darcy's Law in three dimensions.

For the case of steady state flow, consider the elemental control volume, Figure 3.1, a unit volume of porous media. The law of conservation of mass requires that

$$\text{mass in} - \text{mass out} = \text{change in storage per unit time}$$

For steady state conditions in saturated soil the right side of the equation becomes zero. The equation of continuity can be expressed as:

$$-\frac{\partial}{\partial x}(\rho V_x) - \frac{\partial}{\partial y}(\rho V_y) - \frac{\partial}{\partial z}(\rho V_z) = 0 \quad \text{Eq 3.2}$$

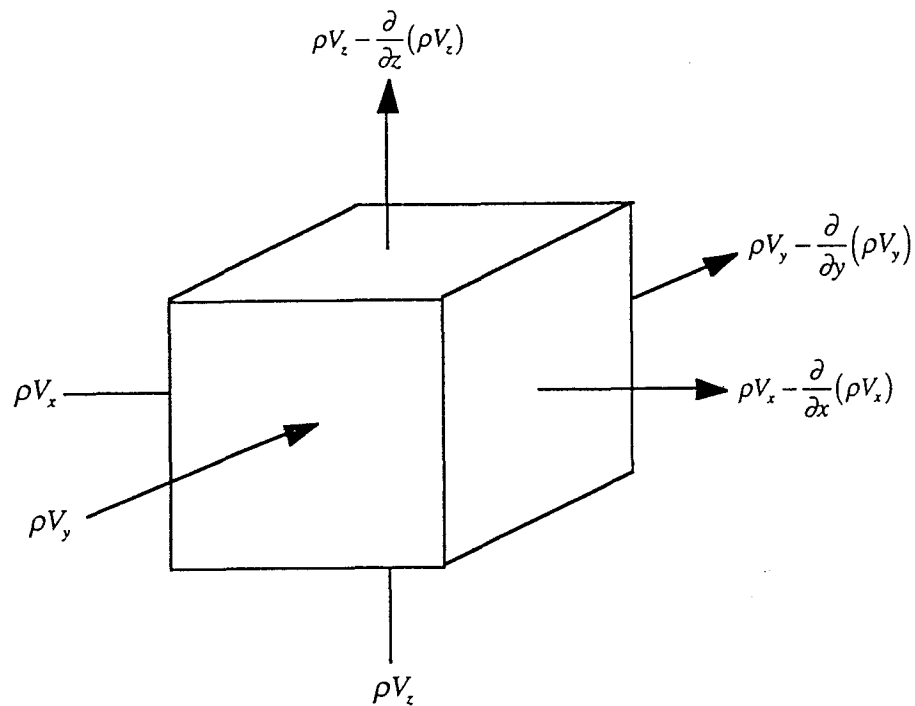


Figure 3.1: Elemental Control Volume

Assuming an incompressible fluid, the density will remain constant at all times,  $\rho$  can be divided out. Darcy's law,  $V = -K(dh/dL)$ , can be substituted into the equation yielding the final partial differential equation.

$$\frac{\partial}{\partial x} \left( K_x \frac{\partial h}{\partial x} \right) + \frac{\partial}{\partial y} \left( K_y \frac{\partial h}{\partial y} \right) + \frac{\partial}{\partial z} \left( K_z \frac{\partial h}{\partial z} \right) = 0 \quad \text{Eq 3.3}$$

### 3.1.2 Simulation of the Interface as a No Flow Boundary

The interface between the freshwater and the saltwater is treated as a no flow boundary. This sharp interface approach to the saltwater intrusion problem has been used successfully to investigate water resources in coastal areas. Although the assumption of a sharp interface does not simulate changes in concentration within the transition zone it can be used to simulate intrusion of the saltwater front due to changes in recharge and/or pumping. Under steady state conditions this boundary is simulated as stable and static.

In order to accurately simulate freshwater flow along the interface, a number of layers in a single aquifer are used to define the position and shape of the interface. The depth to the interface at each x-y node is established using the Ghyben-Herzberg Relationship, see section 3.1.3. The no flow boundary condition is manually inputted for all cells below the estimated position of the interface. The coast is treated as a constant head boundary and cells above the interface within the aquifer are active general flow cells. Figure 3.2 is a vertical cross-section of the boundary conditions in a typical island aquifer as they are treated in this model. As the number of vertical layers within the aquifer is increased, the shape of the interface will be more accurately defined. However, as the number of layers increases so does the computational time and the necessary number of input values, both initially and during the calibration process. An acceptable number of layers should be used in order to balance these two factors.

During the calibration process it is assumed that the position of the interface can be estimated from measured head values within the aquifer. This position remains constant during the steady state calibration of the model and is inputted initially. When the steady state model is used to predict future water resources, the final head values are unknown and therefore the final position of the interface is unknown. For this study the final position is determined on a trial and error basis. For a single simulation of future head values a number of trial runs may be necessary. After each model run new head values are determined and the interface position adjusted accordingly. This process continues until the position of the interface and the corresponding freshwater head values no longer change after subsequent model runs. It is possible that in the future a code could be implemented to solve for the moving no flow boundary iteratively as the heads are solved.

### 3.1.3 Use of the Ghyben-Herzberg Relationship

The Ghyben-Herzberg Relationship is the key modeling assumption for most sharp interface models. The equation, which was derived in Chapter 2, can be rewritten in the following form:

$$z = \frac{\rho_f}{\rho_s - \rho_f} h \quad \text{Eq 3.4}$$

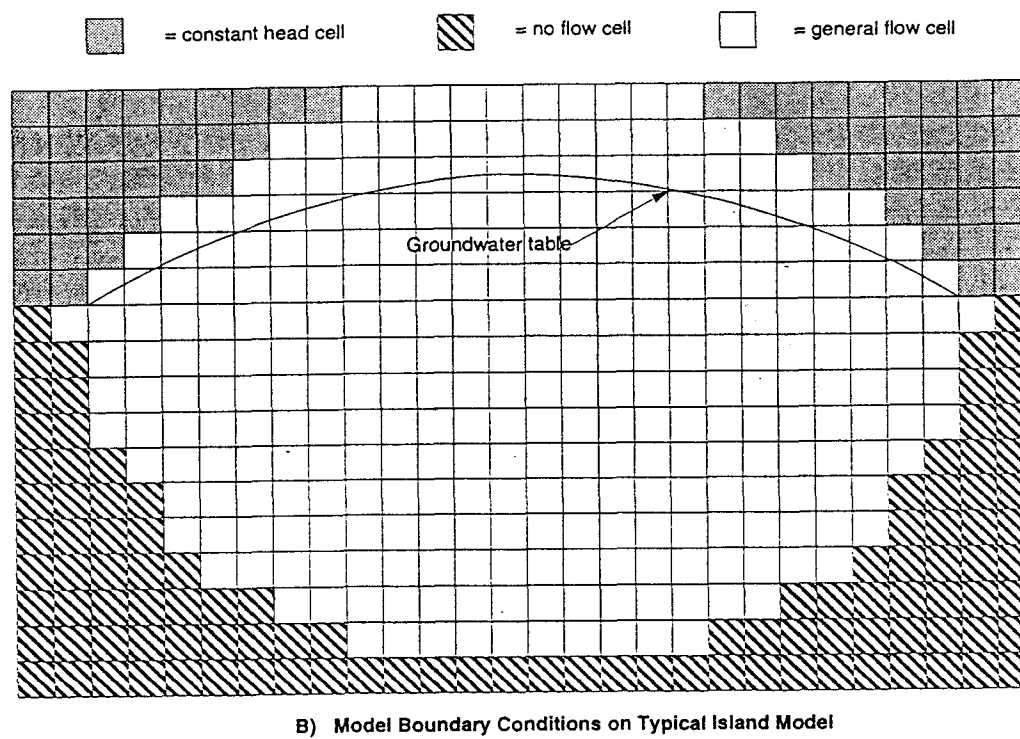
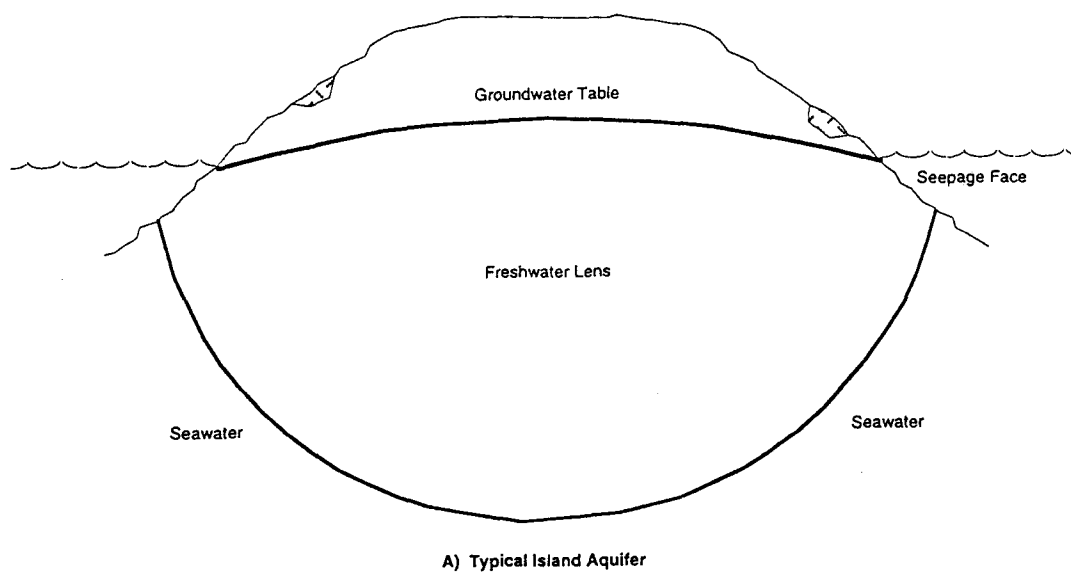


Figure 3.2: Vertical Cross-Section of a Typical Island

where  $\rho_f$  and  $\rho_s$  are the densities of the freshwater and saltwater,  $h$  is the freshwater head at any point, and  $z$  is the depth below sea level to the interface. Assuming typical densities of 1.00 and 1.025 kg/l for the freshwater and saltwater respectively (Chow, 1964), the ratio of  $z$  to  $h$  is approximately 40:1. This ratio has been proven to give a quick and fairly accurate approximation of the saltwater interface position in island and coastal aquifers. The ratio is used to determine the initial position of the interface for the calibration process and also to determine the interface position for each step of the trial and error process during prediction of its future position.

### **3.2 FLOW MODEL SELECTION: MODFLOW**

The three-dimensional flow model chosen for this study is MODFLOW (McDonald and Harbaugh, 1984). This model was chosen because it is well documented, versatile, and has been used to successfully model numerous sites. MODFLOW is the most widely used three-dimensional flow model at this time. MODFLOW is a modular block-centered finite difference code developed by the USGS. It can simulate two-dimensional, quasi three-dimensional, and full three-dimensional flow. The primary output from the model is the hydraulic head distribution in each of the model layers.

The model is designed in such a way that the user can select a series of packages or modules, each dealing with a specific hydrologic feature, to be used during a given simulation. The main packages necessary for all

simulations are the Basic Package and the Block-Centered Flow Package. Optional packages deal with the following; rivers, recharge, wells, drains, evapotranspiration, general-head boundary conditions, and numerical methods to solve the finite-difference equation set.

The Basic Package is an administrative package. It reads data on the number of rows, columns, layers, and stress periods to be used in the simulation. The modular packages to be used in the modeling exercise are specified here and assigned a location for the input data to be stored. The overall water budget is dealt with in this package. Initial starting heads and boundary conditions are specified here along with specifications for model output.

The name Block-Centered Flow Package comes from the assumption that for all calculations the node of the cell is located at its center. All data and calculations dealing with the conductance of the system are dealt with in this package. The type of each layer is chosen in this package, either confined, unconfined, or a combination of the two depending upon calculated head data in each cell. Data is inputted for conductivity, bottom elevation of the layer, leakance, transmissivity, and/or specific storage depending upon the type of simulation.

### 3.2.1 The Numerical Method

The computer code approximates the general flow equation in three dimensions and then solves the resulting matrix equation. MODFLOW approximates the flow equation by the finite difference method. The formulation of the finite difference equations used in the model will not be presented in this thesis. The general form of the finite difference expression for the flow equation is written for the computational molecule shown in Figure 3.3 as follows (Anderson and Woessner, 1992):

$$\begin{aligned}
 Bh_{i-1,j,k} + Ch_{i,j+1,k} + Dh_{i+1,j,k} + Eh_{i,j-1,k} + Fh_{i,j,k+1} \\
 + Gh_{i,j,k-1} + Hh_{i,j,k} = RHS_{i,j,k}
 \end{aligned}
 \tag{Eq 3.5}$$

The equation for the head at the node  $i,j,k$  ( $h_{i,j,k}$ ) involves the head at the node itself as well as heads at the six surrounding nodes. Each head is multiplied by a coefficient (B,C,D,E,F,G, or H) that is a function of the hydraulic conductivity between the nodes. The coefficient H also is a function of the storage term. The RHS includes the terms for storage, recharge, and other inputs to the flow system. The finite element equations developed in MODFLOW are similar to this simplified equation.

MODFLOW allows the user to choose the iterative method used to solve the resulting matrix. Choices include the strongly implicit procedure (SIP), slice-successive overrelaxation, or the preconditioned conjugate



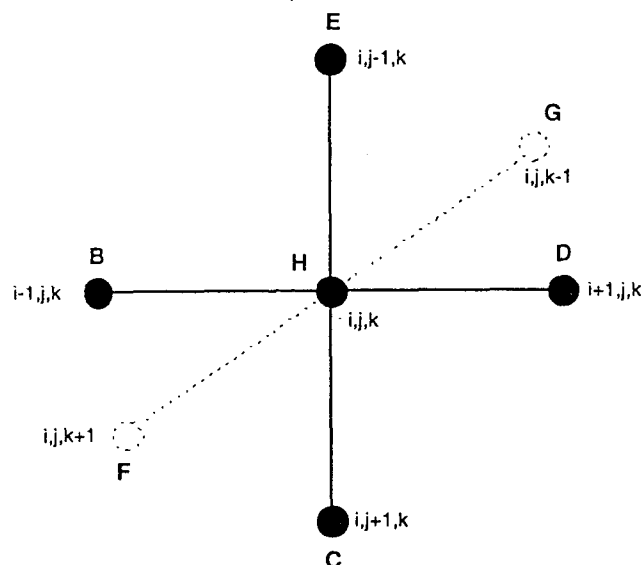


Figure 3.3: Computational Finite Element Molecule

gradient method (PCG). Details of the theory behind each of the numerical methods used to solve the matrix will not be presented here.

### 3.2.2 Treatment of Boundary Conditions

Boundary conditions are specified in the IBOUND array. There are two basic boundary conditions, constant head and no flow. Constant head cells are identified by assigning a value less than zero to the node in the IBOUND array. A value of zero identifies a no flow boundary and any value greater than zero identifies an active variable head cell.

Constant head boundaries act as an inexhaustible supply of water. The head in these cells will not change and the groundwater system may either pull water from or discharge water into the constant head cell depending upon the conditions in the adjacent variable head cells. In the saltwater

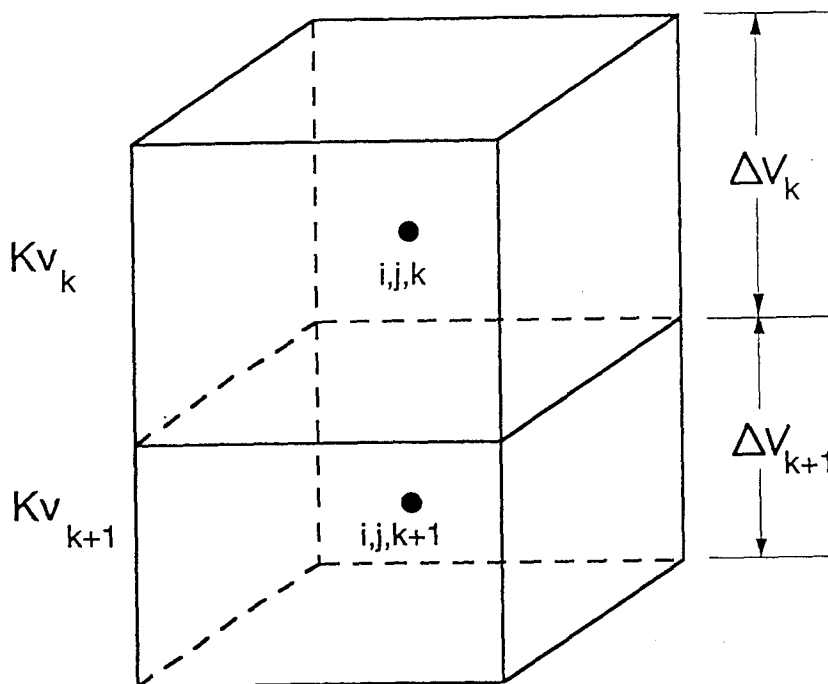
intrusion systems studied here the entire island is surrounded by a constant head boundary representing mean sea level. The freshwater lens will discharge to these constant head cells through the seepage face. No flow boundaries are inactive cells that neither discharge to or pull water from the groundwater system and water will flow around these cells. The saltwater interface is simulated by this boundary condition.

### 3.2.3 Treatment of Three-Dimensional Flow

MODFLOW deals with three-dimensional flow by use of a leakance term. Flow from one layer to another, whether the layers are in separate aquifers or the same aquifer, is simulated by this term. For MODFLOW simulations involving more than one layer, the user must calculate the vertical transmission or leakage term, VCONT, for each nodal block in the grid, excluding the bottom layer. The model assumes that the bottom layer is underlain by impermeable material and VCONT in this layer is zero. Computing VCONT depends on whether the simulation is quasi or fully three-dimensional. In this study the MODFLOW simulations are full three-dimensional. The following equation is the most general for a full three-dimensional simulation, see Figure 3.4.

$$VCONT_{i,j,k+1/2} = \frac{2}{\frac{\Delta v_k}{(K_z)_{i,j,k}} + \frac{\Delta v_{k+1}}{(K_z)_{i,j,k+1}}} \quad \text{Eq 3.6}$$

The  $K$  terms are the conductivities of the adjacent layers and the  $v$  term is the thickness of each layer.



### **3.3 VERIFICATION OF THE METHOD ON A GENERIC CIRCULAR ISLAND**

In this section the modeling method is implemented on a generic circular island. MODFLOW is used to approximate the unconfined aquifer and the interface is simulated as a no flow boundary. The resulting heads are compared to those resulting from an analytical solution of the same circular island, as well as a numerical solution of the differential equation used to derive the analytical equation.

### 3.3.1 Fetter's Solution for the Position of the Saline Interface Beneath Oceanic Islands

Fetter (1972) described the three-dimensional position of the interface beneath oceanic islands by one differential equation. The solution was a sharp interface, single phase model. The key modeling assumptions are the Ghyben-Herzberg relationship and Dupuit's assumption. Dupuit's assumption is used so that the governing flow equation is reduced to two dimensions. An analytical solution was derived for circular islands, as well as for an infinite strip island. For islands of irregular shape a numerical solution to the differential equation is introduced. The numerical solution was used on the South Fork of Long Island to accurately simulate the position of the saltwater interface underlying that portion of the island.

Fetter's differential equation can be derived by looking at the control volume for two-dimensional Dupuit flow. This control volume is a vertical section of porous material saturated with fresh groundwater. The control volume is bounded on top by the water table and below by the no flow saltwater interface. The x-y plane represents mean sea level. At any x-y point, the total thickness of the freshwater lens, Eq. 3.7, is equal to the sum of the freshwater head and the depth from mean sea level to the interface, defined by the Ghyben-Herzberg relationship.

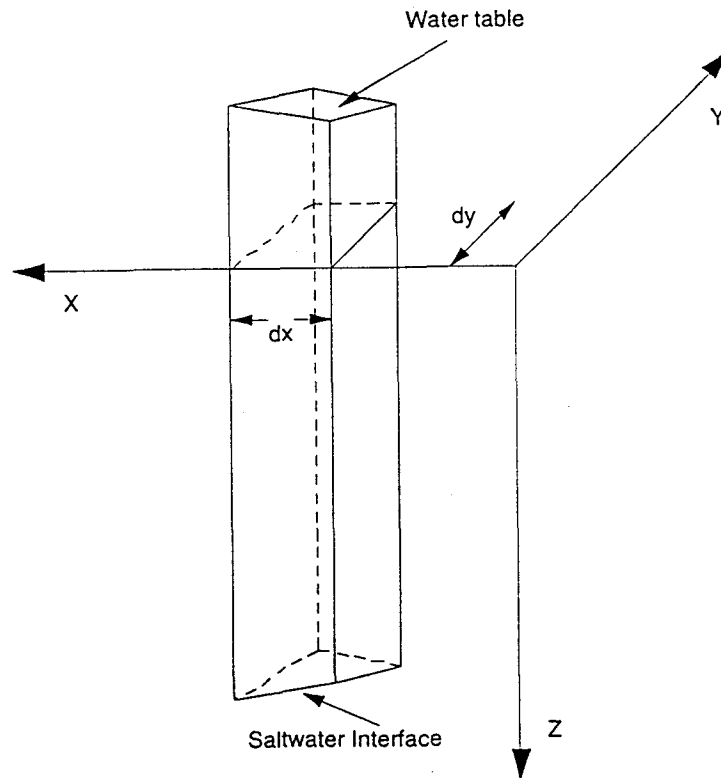


Figure 3.4: Control Volume for Two-Dimensional Dupuit Flow

$$h(i, j) + \frac{\rho_f}{\rho_s - \rho_f} h(i, j) \quad \text{Eq 3.7}$$

The flow rate through the left face of the control volume is equal to the area multiplied by the velocity, velocity being defined by Darcy's law.

$$-K \left[ \left( h + \frac{\rho_f}{\rho_s - \rho_f} h \right) \frac{\partial h}{\partial x} \right]_{x+dx} dy \quad \text{Eq 3.8}$$

The parameter  $h$  is the average value of the head along the  $x$  axis within the length  $dy$ .  $K$  is the average hydraulic conductivity within the aquifer(s) of concern. The flow rate through the left side of the control volume can be

similarly derived. The difference in flow per unit time between the amount of fluid flow in the x direction through the left and right faces is:

$$dq_x = (q_{x+dx} - q_x)dy \quad \text{Eq 3.9}$$

The change in flow rate in the direction of the x axis can be given by the truncated Taylor's expansion as:

$$(q_{x+dx} - q_x)dy = \left( \frac{\partial q_x}{\partial x} \right) dx dy = \quad \text{Eq 3.10}$$

$$-K \frac{\partial}{\partial x} \left[ \left( h + \frac{\rho_f}{\rho_s - \rho_f} h \right) \frac{\partial h}{\partial x} \right] dx dy$$

The flow in the y direction is defined by a similar expression. For steady flow of an incompressible fluid the law of continuity requires the change in flow rate through the sides of the control volume to equal the inflow or outflow through the top and bottom. The bottom is assumed to be a no flow surface and the only addition to the control volume is the vertical recharge,  $W$ , across the phreatic surface. The average daily recharge, dimensions  $LT^{-1}$ , is assumed to be a steady state addition to the control volume equal to  $W \cdot dx dy$ . The law of continuity can be written in terms of hydraulic head as:

$$K \left[ \left( 1 + \frac{\rho_f}{\rho_s - \rho_f} \right) \frac{\partial}{\partial x} \left( h \frac{\partial h}{\partial x} \right) \right] + \quad \text{Eq 3.11}$$

$$K \left[ \left( 1 + \frac{\rho_f}{\rho_s - \rho_f} \right) \frac{\partial}{\partial y} \left( h \frac{\partial h}{\partial y} \right) \right] = -W$$

This equation may be rewritten in the form of Eq 2.7, or in the following form:

$$\frac{\partial^2 h^2}{\partial x^2} + \frac{\partial^2 h^2}{\partial y^2} = \frac{-2W}{K \left[ 1 + \left( \rho_f / (\rho_s - \rho_f) \right) \right]} \quad \text{Eq 3.12}$$

### 3.3.2 Analytical Solution to Fetter's Equation for a Circular Island

In order to derive the analytical solution for a circular island Eq. 3.12 must be expressed in polar coordinates. It is assumed that the island has an axis of radial symmetry located at the center and has the following boundary conditions. The slope of the phreatic surface is zero,  $dh/dr=0$ , at the center of the island,  $r=0$ . At the edge of the island,  $r=R$ , the head is equal to mean sea level,  $h=0$ . The solution yields the equation for the head in a circular island at any distance,  $r$ , from the center. The depth to the interface can be determined by using this head and the Ghyben-Herzberg Relationship.

$$h^2 = \frac{W(R^2 - r^2)}{2K \left[ 1 + \left( \rho_f / (\rho_s - \rho_f) \right) \right]} \quad \text{Eq 3.13}$$

This analytical solution is used to solve for the heads in a generic circular island. Heads will be generated for this same island using a finite difference solution to Fetter's differential equation, and then with the method outlined in this chapter using MODFLOW. The circular island has the following characteristics: average hydraulic conductivity,  $K$ , of 50 ft/day, average recharge of 0.02 ft/day, and a radius of 1 mile. Average values for the

densities of freshwater and saltwater will be assumed. The heads determined by the analytical solution can be found in Figure 3.5.

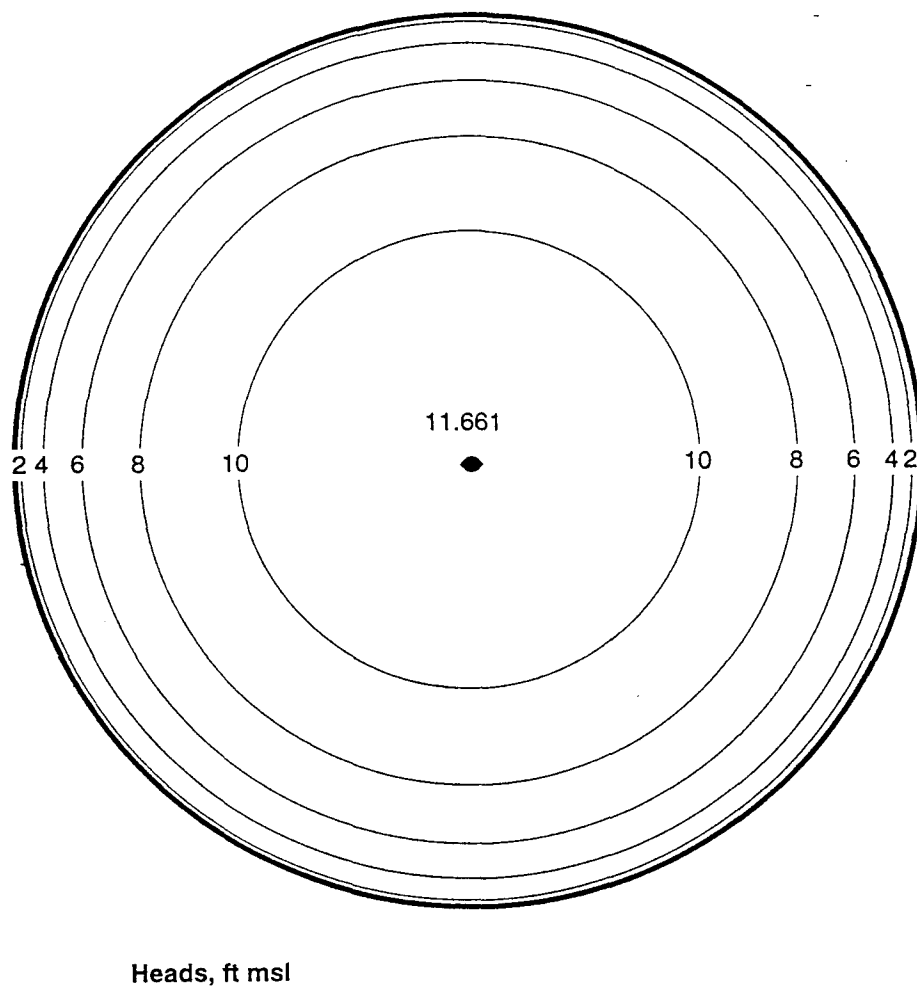


Figure 3.5: Circular Island Heads: Analytical Solution

### 3.3.3 Numerical Solution to Fetter's Differential Equation

Equation 3.12 may be approximated by the following finite difference equation (Fetter, 1972):



$$h^2(x, y) = 0.25 * [h^2(x + n, y) + \quad \text{Eq 3.14}$$

$$h^2(x - n, y) + h^2(x, y + n) + h^2(x, y - n)]$$

$$-0.25n^2 \left[ \frac{-2W}{K \left[ 1 + \left( \rho_f / (\rho_s - \rho_f) \right) \right]} \right]$$

where  $n$  is the distance between nodal points on the grid, all grid cells are assumed to be square. As the value of  $n$  decreases, the grid becomes finer and the head values computed approach the heads that would be obtained by a corresponding analytical solution.

The finite difference equation is used to estimate head values for the generic circular island. A program written in MATLAB, see Appendix A, is used to solve for heads by an iterative approach. The circle is approximated by a set of square cells within a square grid. Cells within the circle are active variable head cells and all cells outside are constant head cells,  $h=0$ . Initial values for head were estimated to be 10 ft and were inputted for the interior active cells. The first iteration solves the finite difference equation for each cell using the constant exterior, as well as the estimated interior head values. These new interior values are then used to solve the equation in the next iteration. The maximum error, difference between the new head value and the head value obtained in the previous iteration, at each cell are compared with an error limit to determine when the grid has been solved to the required accuracy.

The circle was approximated using two grids. The first was a 17x17 grid with a value for  $n$  of 704 ft. The second simulation cut the value of  $n$  in half creating a 32x32 grid. As the grid spacing decreases, the numerical solution approaches the analytical solution for a circular island. The numerical approximations of the heads beneath a generic circular island  $s$  can be found in Figure 3.6.

### 3.3.4 No Flow Boundary 3-D Solution to the Circular Island

The modeling method introduced in this study is now used to estimate the head distribution for the generic circular island. The steady state position of the interface is estimated initially by using the heads determined by the analytical method and is adjusted as needed. All cells within the island boundary and above the interface will be active variable head cells. The cells below the interface are no flow cells and the cells outside of the island are constant head cells representing the sea,  $h=0$ . The input values to the model are the grid layout, the hydraulic conductivity, vertical recharge to the top layer, and the vertical conductance. The vertical conductance can be found by the following formula discussed earlier in this chapter.

$$VCONT_{i,j,k+1/2} = \frac{2}{\frac{\Delta v_k}{(K_z)_{i,j,k}} + \frac{\Delta v_{k+1}}{(K_z)_{i,j,k+1}}} \quad \text{Eq 3.15}$$

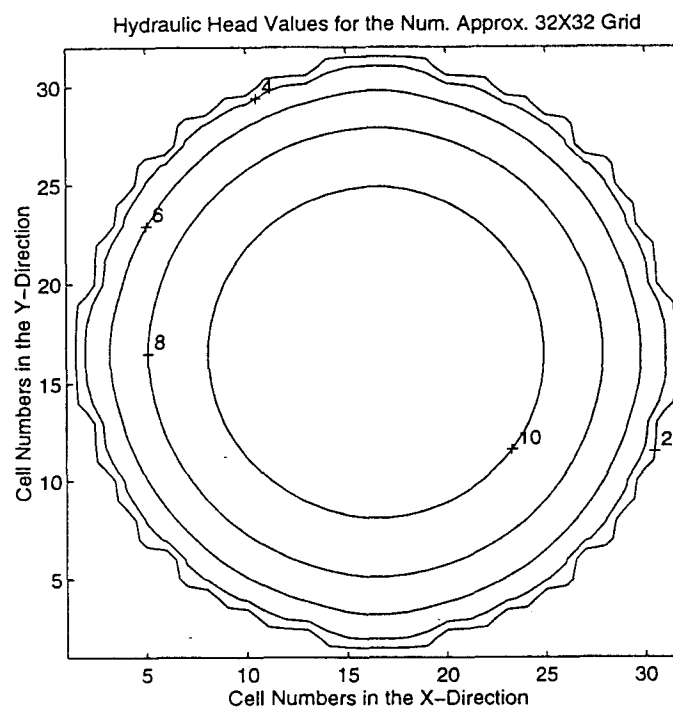
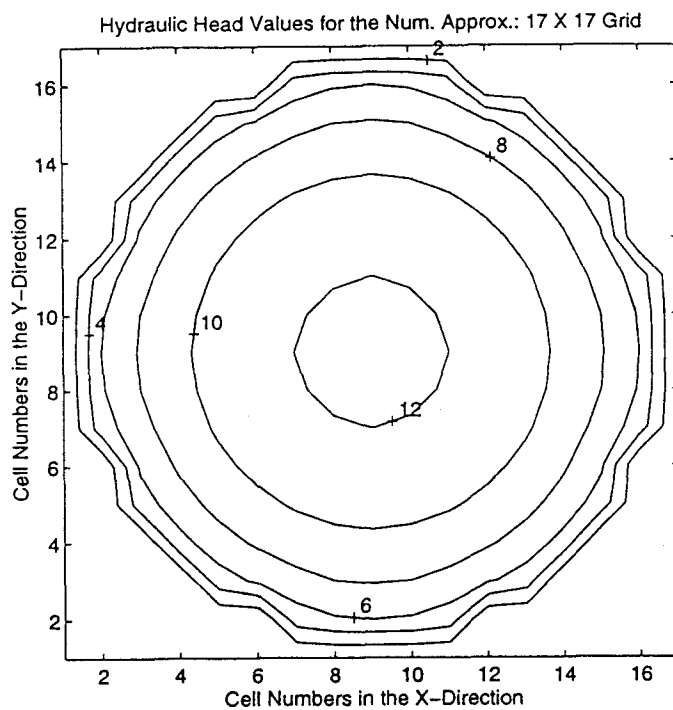


Figure 3.6: Numerical Solutions to the Circular Island, Heads in ft msl

This equation is reduced to the following form when dealing with vertical layers of equal width and the two adjacent layers represent the same hydrogeologic unit.

$$VCONT_{i,j,k+1/2} = \frac{K_{z(i,j)}}{\Delta z_{k+1/2}} \quad \text{Eq 3.16}$$

The vertical hydraulic conductivity used in this simulation is assumed to be the same as the horizontal. This value was chosen for comparison purposes because in Fetter's equation the K value is assumed to be an average conductivity in all dimensions.

Fetter's simulation assumes that at the shoreline the head is zero and, by the Ghyben-Herzberg Relationship, the corresponding depth to the interface is also zero, which does not allow for a seepage face. The MODFLOW model must have a seepage face to allow for discharge to the sea. The width of this discharge face will be determined by using Glover's potential flow theory, see Chapter 2.

$$Z^2 = \frac{2qx}{\Delta \rho K} + \left( \frac{q}{\Delta \rho K} \right)^2 \quad \text{Eq 3.17}$$

The width of the submarine zone,  $x_o$ , through which freshwater discharges into the sea can be obtained from Eq 3.17 for the case when the depth to the interface,  $z$ , is zero. This yields the following equation:

$$x_o = -\frac{q}{2\Delta \rho K} \quad \text{Eq 3.18}$$

where the term  $q$  is the discharge per unit length of shoreline. This term can be determined, in the steady state case, by multiplying the recharge in ft/day by the surface area, and then dividing by the length of shoreline.

Three grids were used to simulate the circular island. Three separate grids were chosen in order to investigate the effect of the grid spacing on the generated heads. The first is a 17x17x10 grid with layer widths equal to 50 ft. In the second grid the width of each layer is cut in half to create a 17x17x20 grid. The third grid doubles the number of cells in both the x and y directions to form a 32x32x20 grid. The model parameters inputted for each run can be found in Table 3.1.

**Table 3.1: MODFLOW Parameters for the Generic Circular Island**

<u>Parameter</u>	<u>17x17x10 Grid</u>	<u>17x17x20 Grid</u>	<u>32x32x20 Grid</u>
<i>Conductivity</i>	50 ft/day	50 ft/day	50 ft/day
<i>Transmissivity</i>	2500 ft <sup>2</sup> /day	1250 ft <sup>2</sup> /day	1250 ft <sup>2</sup> /day
<i>Vcont</i>	1/day	2/day	2/day
<i>Recharge</i>	0.02 ft/day	0.02 ft/day	0.02 ft/day
<i>Seepage Face</i>	21 ft	21 ft	21 ft
<i>Width</i>			

The other input for each simulation is the IBOUND array which defines the boundary condition of each cell. A separate array must be inputted for each of the model layers because at each depth within the aquifer

the size of the freshwater region changes due to the presence of saltwater. An example of the boundary conditions for the circular island model can be found in Appendix B.

The generated heads from each model run can be found in Figures 3.7, 3.8, and 3.9. The MODFLOW model output matches the head distributions calculated in the analytical and numerical solutions to Fetter's model. The head distribution approached the analytical solution as both the horizontal and the vertical grid spacings were decreased. A complete discussion and comparison of the circular island model results can be found in the next section.

### **3.3.5 Comparison of the Solution Methods**

Head distribution for the generic circular island has been solved using three methods, an analytical method, a numerical method with two separate grid spacings, and the three-dimensional no flow boundary method introduced in this study, with three grid spacings. A qualitative analysis of all the plots show the shape of the head distributions to be quite similar. The spacing between the equipotentials is constant for all simulations, with the phreatic surface changing gradually in the center of the island and rapidly at the edge near the sea. The shape of the equipotential lines in all of the

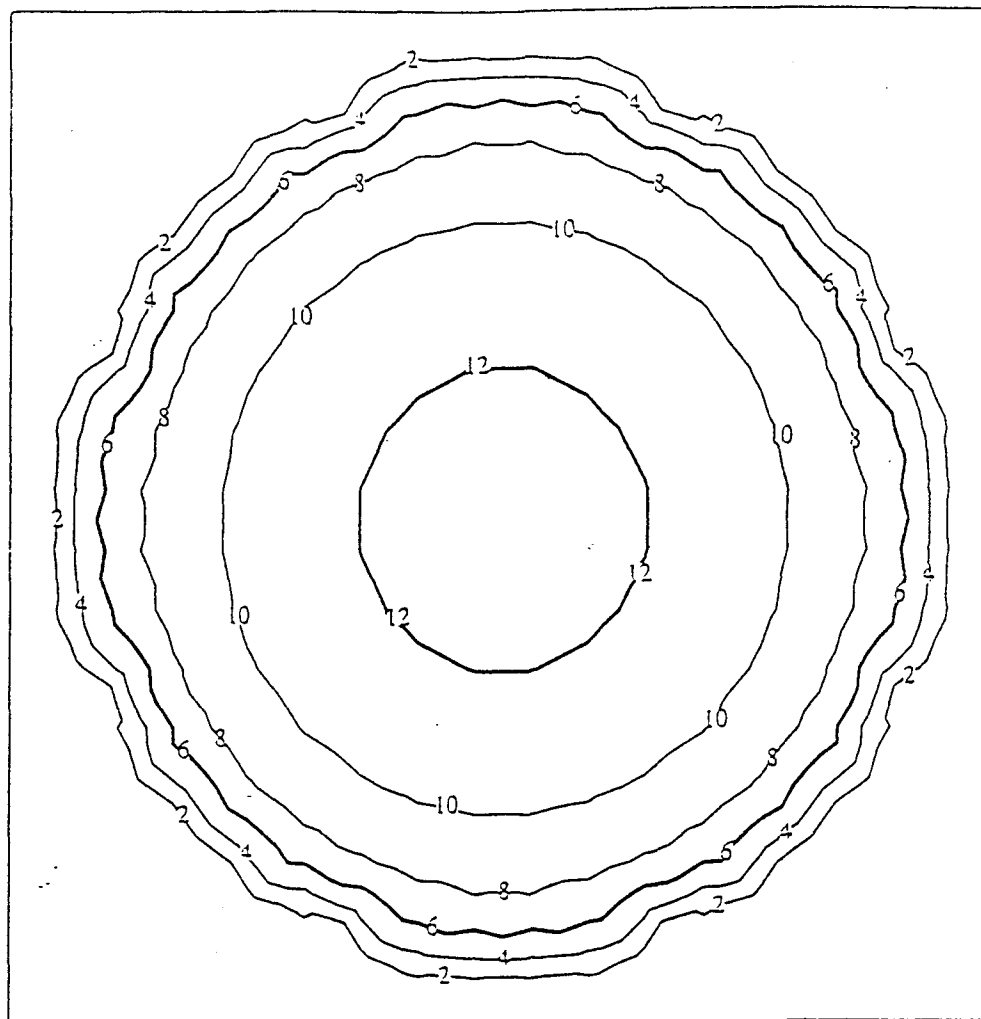


Figure 3.7: MODFLOW Solution to the Circular Island: 17x17x10 Grid

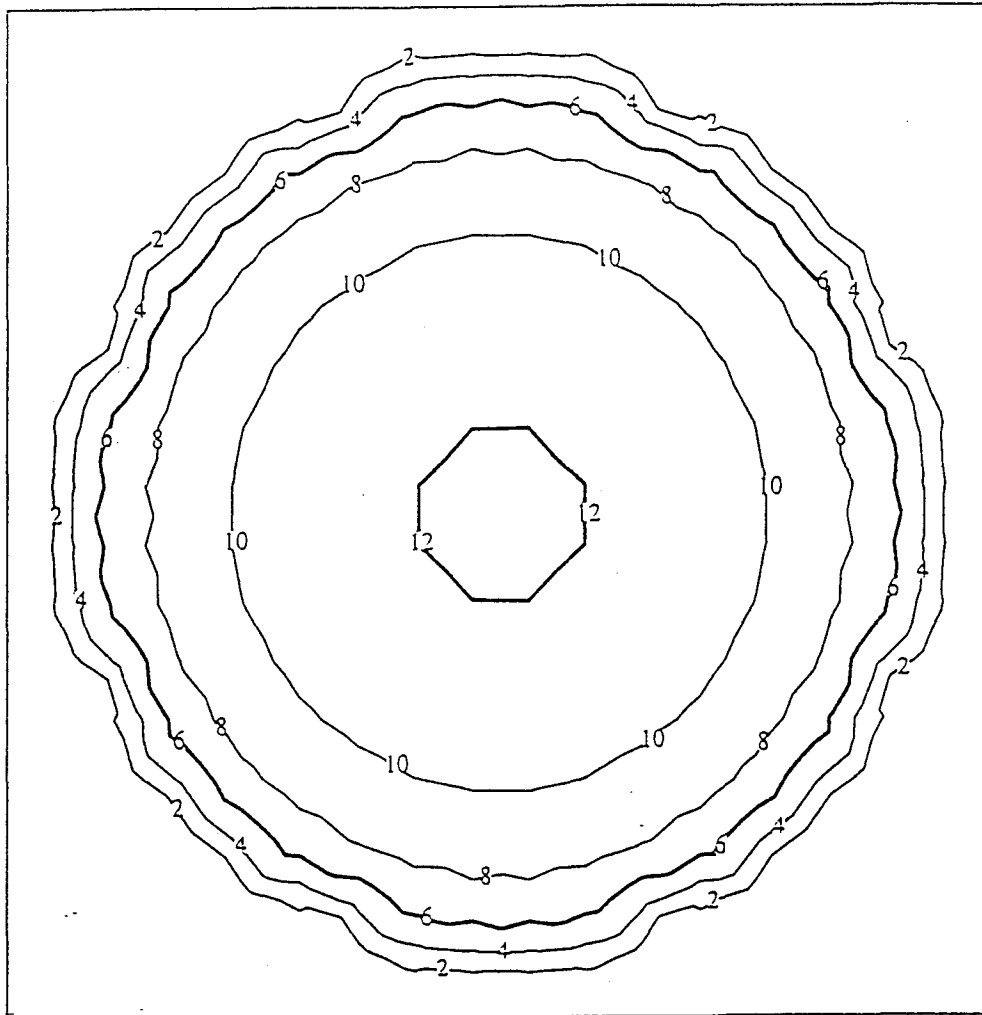


Figure 3.8: MODFLOW Solution to the Circular Island, 17x17x20 Grid



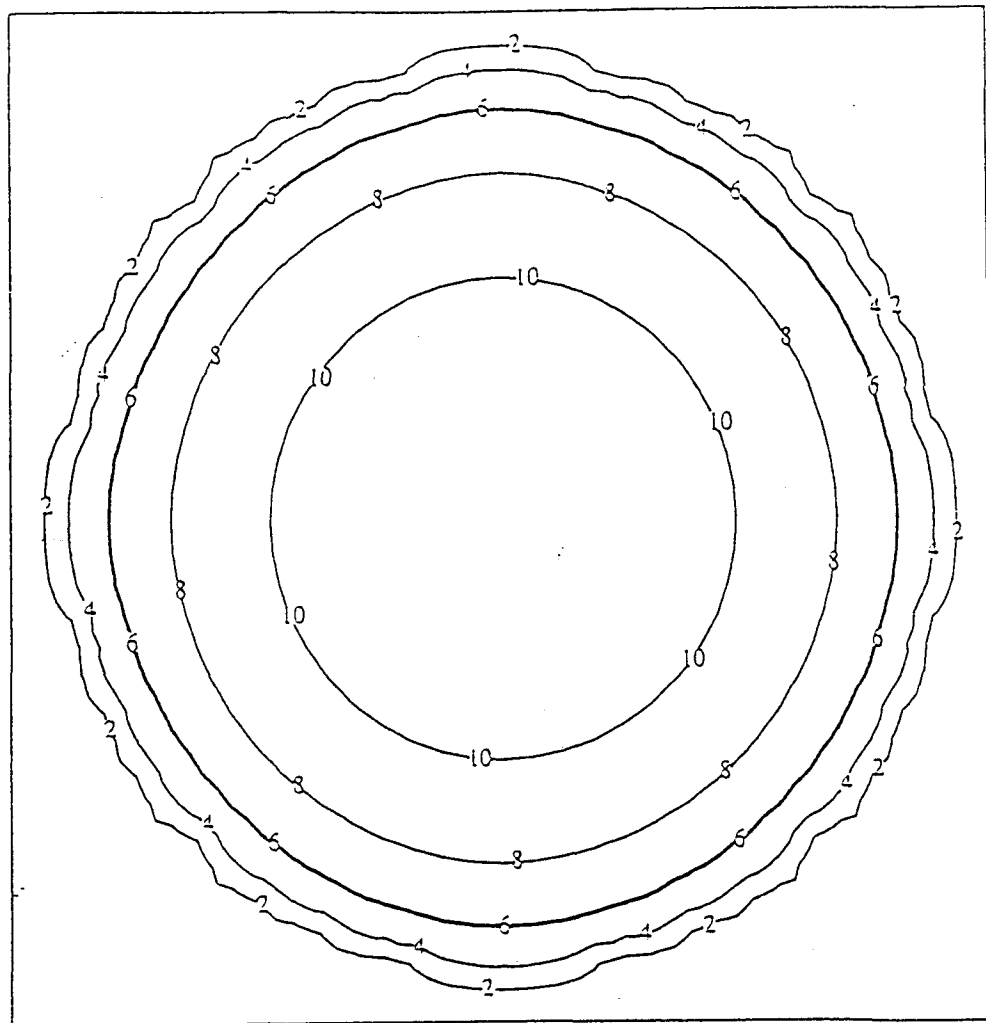


Figure 3.9: MODFLOW Solution to the Circular Island, 32x32x20 Grid

solutions approximated the circular equipotentials of the analytical solution. The maximum head value, located at the center of the island, for each of the solutions, and its deviation from the analytical, can be found in Table 3.2.

Table 3.2: Maximum Head Values Determined in Each Simulation

<u>Solution Method</u>	<u>Grid Spacing</u>	<u>Maximum Head</u> <u>Value</u>	<u>Percent Difference</u> <u>from Analytical</u>
<i>Analytical:</i>	n/a	11.661 ft	0
<i>Numerical:</i>	17x17	12.416 ft	6.47
	32x32	11.887 ft	1.94
	17x17x10	12.578 ft	7.86
	17x17x20	12.161 ft	4.29
	32x32x20	11.591 ft	.60

The maximum head values at the center of the island for the numerical and MODFLOW simulations were all within ten percent of the analytical solution. As expected for the numerical solution, as the grid spacing was decreased the solution approached that of the analytical. The same was true for the MODFLOW solution. This improvement in the results is due to the fact that as the grid spacing decreases the number of square cells used to represent the island increases and the shape is therefore better approximated by the model. The MODFLOW solution was also improved as the thickness of each layer was decreased. The shape of the interface is

defined by the nodes along its length. As the number of nodes is increased the shape of the interface, and the flow along the no flow boundary are more accurately defined.

The method introduced in this research, modeling the position and shape of the saltwater interface as a no flow boundary in a three-dimensional flow model, has been shown to match both a numerical and an analytical solution to a simple circular island quite well. The advantages of this method are that it takes into account the vertical flow component. For islands with multiple aquifer systems the vertical flow within and between these aquifers can be simulated. Fetter's method deals with only two-dimensional flow and uses an average conductivity value to deal with multiple aquifer systems. the full three-dimensional approach will better simulate the amount of recharge to actually reach the deeper aquifers.

Fetter's solution also accounts for all inputs and outputs to the flow system as changes in recharge. It doesn't take into account the flow dynamics around wells, drains, and no flow boundaries. By using MODFLOW, the versatility of the flow model can better simulate the actual flow system and therefore the position of the interface can be determined more accurately. The model also takes into account the presence of a seepage face, which occurs in the real flow system. In general, the full-three dimensional no flow boundary model is as versatile as the flow code used in its implementation

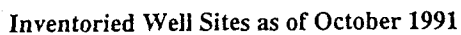
and therefore better represents the entire flow system. It can be a valuable tool in the investigation of water resources in both coastal and island regions.

#### **4. CASE STUDY: GUEMES ISLAND**

The modeling method introduced in Chapter 3, use of MODFLOW and simulation of the saltwater interface as a no flow boundary, is used in this chapter to investigate the water resources on Guemes Island, Skagit County, Washington. The full three-dimensional island model uses aquifer and well data collected by the USGS in their 1994 study (Kahle and Olsen, 1995), as well as additional data collected by the author in conjunction with the Department of Geology and Geophysics at Rice University. The model takes into account the complex geometry of the aquifer system, vertical recharge of freshwater to that system, withdrawals from the freshwater aquifers due to pumping, and the position of the saltwater interface. The calibrated model of Guemes Island is used to predict the drawdown and the related movement of the of the saltwater interface within the main water bearing aquifer of the island, for six possible future pumping scenarios.

##### **4.1 BACKGROUND OF GUEMES ISLAND**

Guemes Island is an 8.2 square mile island located in the northern section of the Puget Sound, western Washington State. The fresh groundwater resources of the island provide all of the freshwater used by the 535 year-round residents, as well as an additional 1,605 seasonal residents, Figure 4.1 shows a map of the island and the position of the inventoried



wells. The island population has increased rapidly over the last couple of years, 55 building permits were issued in 1995 compared to an average of ten

annually over the past ten years. As the population of the island increases the demand for fresh drinking water has caused concerns over the integrity of the island's fresh groundwater supply.

#### 4.1.1 Hydrogeologic Units

Guemes Island is composed of six main hydrogeologic units. The relative position of each layer beneath the island can be found in a hypothetical cross section of the flow system, Figure 4.2.

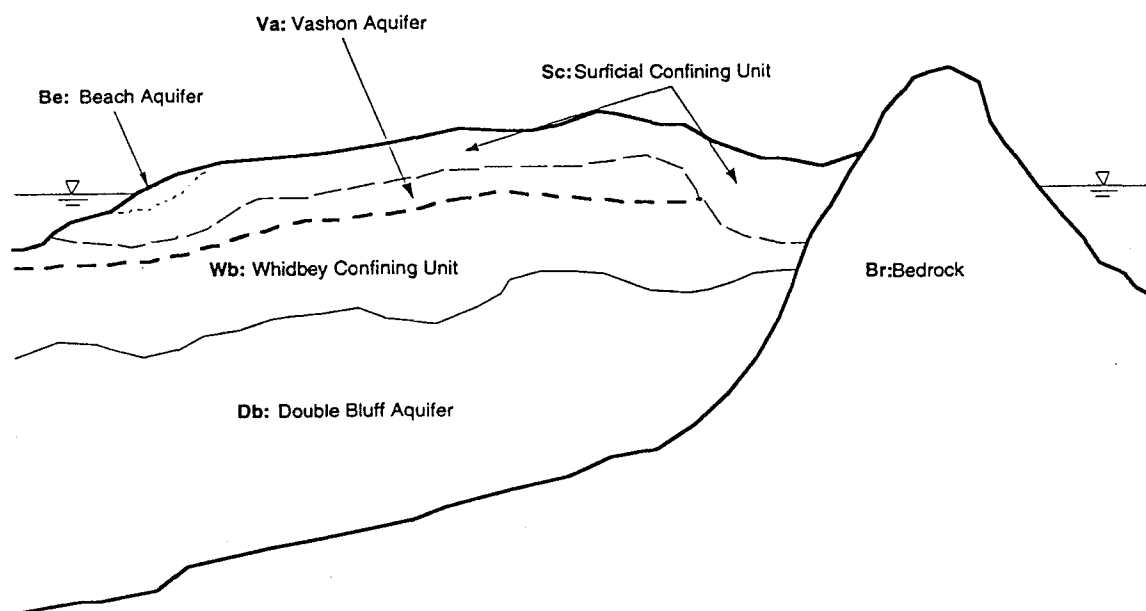


Figure 4.2: Six Main Hydrogeologic Units Beneath Guemes Island

The Beach aquifer consists of sand and gravel accumulated along the coast due to longshore drift. Although a small number of wells are using this aquifer for freshwater the aquifer is not included in this modeling study for

two reasons. First, the wells in this unit are mostly hand dug, shallow wells located directly on the beach. Any high TDS and/or chloride values in these wells could easily be attributed to seawater minerals entering the well through the well casing from above due to beach mineral deposits or by ocean spray. The second reason is that the aquifer is insignificant in both its vertical and areal extent compared to the other hydrogeologic units of the island. The aquifer extends inland only a little beyond the visible beach and its thickness is estimated to be 10 to 20 ft.

The surficial confining unit extends over the entire surface of the island. It is a low permeability unit consisting of compacted sand, gravel, silt and clay. The unit does contain some water bearing lenses and five inventoried wells are completed in this unit. The Vashon aquifer is a water bearing aquifer that consists of partially saturated sands and gravels. The unit does not occur island wide but rather in two separate areas of the island, see Figure C.1 in Appendix C. The thickness of this aquifer is commonly between 40 and 80 feet and twenty-eight inventoried wells are completed within the unit. The Whidbey confining unit is composed mostly of floodplain clay. It occurs over much of the island and is located directly above the Double Bluff aquifer. A total of 17 wells are inventoried in this unit and are tapped into small water bearing lenses. These wells generally have a low yield due to the relatively small size of these lenses.



The Double Bluff aquifer is the main water bearing unit of the island. Fifty-four wells are inventoried within this unit, including all of the public supply wells. This aquifer consist of a sand and gravel outwash that underlies most of the island. The Double Bluff aquifer is the main focus of this modeling study. It is the aquifer with the greatest vertical extent and therefore is the aquifer that will be the source of any significant, future withdrawal of fresh groundwater. The southeastern end of the island is an outcropping of bedrock. This bedrock underlies the entire island and for all general purposes is impermeable. The few wells drilled into the outcropping have been able to yield small amounts of freshwater due to fractures within the rock.

The USGS study estimated the extent, the elevation of the top of the unit, and the thickness of the unit for the surficial confining unit, the Vashon aquifer, the Whidbey confining unit, and the Double Bluff aquifer. The thickness of the Double Bluff aquifer was not estimated by the USGS because all of their estimations were done from the well driller's logs and drilling was generally stopped once the Double Bluff aquifer was significantly penetrated to produce the required freshwater withdrawal. A sample of the maps generated by the USGS can be found in Appendix C. These maps were used along with an estimation of the bedrock elevation, discussed later in this chapter, to produce the conceptual model of Guemes Island's flow system.

#### 4.1.2 Hydraulic Conductivity Values

The hydraulic conductivity of each of the units was estimated in the USGS study. Values of the horizontal conductivity were estimated for each unit on the basis of the specific capacity of the wells completed within that unit. The specific capacity of a well is the ratio of its discharge to its total drawdown. Although more precise methods are available, they require aquifer test data or core samples of the unit. In this case only the wells that had logs containing the necessary information were used.

Two different sets of equations were used to estimate the conductivity depending upon how the well was constructed. For wells that had a screened, perforated or open hole interval the modified Theis equation was used to estimate transmissivity values (Bedient et al., 1994).

$$s = \frac{Q}{4\pi T} \ln \frac{2.25Tt}{r^2 S} \quad \text{Eq 4.1}$$

s	= drawdown in the well, ft
Q	= well discharge, cu. ft per day
T	= transmissivity of unit, sq. ft/day
t	= pumping duration, days
r	= radius of the well, ft
S	= storage coefficient, dimensionless

A computer program was then used to solve the equation for transmissivity using Newton's iterative method. The hydraulic conductivity was then estimated by the following equation:

$$K_h = \frac{T}{b} \quad \text{Eq 4.2}$$

$K_h$  = horizontal conductivity, ft/day

$T$  = transmissivity from Eq. 4.1

$b$  = thickness estimated by the length of the open interval, ft

Using the length of the well screen to estimate the thickness may over estimate the value of  $K_h$ . This estimation is necessary because the equation assumes that virtually all flow into the well is horizontal. Any vertical flow to the well will cause an overestimation of the horizontal conductivity.

The second equation was used to estimate hydraulic conductivities for wells having only an open end. Bear (1979) provides an equation for the hemispherical flow to an open ended well just penetrating a hydrological unit. When modified for spherical flow to an open ended well within a unit, the equation becomes:

$$K_h = \frac{Q}{4\pi sr} \quad \text{Eq 4.3}$$

$K_h$  = horizontal conductivity

$Q$  = discharge

$s$  = drawdown

$r$  = well radius

Equation 4.3 is based on the assumption that flow can occur equally in all directions, i.e. the vertical and horizontal conductivities are equal. Due to the fact that unconsolidated deposits are typically layered, this is not likely true. However, the errors associated with this assumption are less than those that would occur by trying to fit the Theis equation to the open ended well geometry.

The individual well values calculated by the USGS can be found in Figure 4.3. The average value of the conductivity in each of the units was used in the initial MODFLOW model. The value of conductivity will vary within the unit itself and this variation will be estimated in the model calibration process. All of the average values, see Table 4.1, are similar in magnitude to values reported by Freeze and Cherry (1979) for similar materials. Specific capacity data was unavailable for the Whidbey confining unit and the value used for that unit was estimated as a reasonable value for a semiconfining unit.

Table 4.1: Average Horizontal Conductivities for the Hydrogeologic Units,  
Guemes Island

<u>Hydrogeologic Unit</u>	<u>Average Horizontal Conductivity</u>
Sc	23 ft/d
Wb	1.6 ft/d
Va	43 ft/d
Db	68 ft/d
Br	<1 ft/d

#### 4.1.3 Approximate Water Budget

The approximate water budget for Guemes Island can be found in Table 4.2. The elements of this budget that are of main concern to the modeling study are the groundwater withdrawal and the recharge. The precipitation was estimated by rain gages on the island and then adjusted with long term gages in Anacortes, Washington. The runoff was estimated as a residual and the evapotranspiration was estimated by the Thornthwaite energy-budget method, which uses a relationship between the precipitation, evaporation, and the temperature.

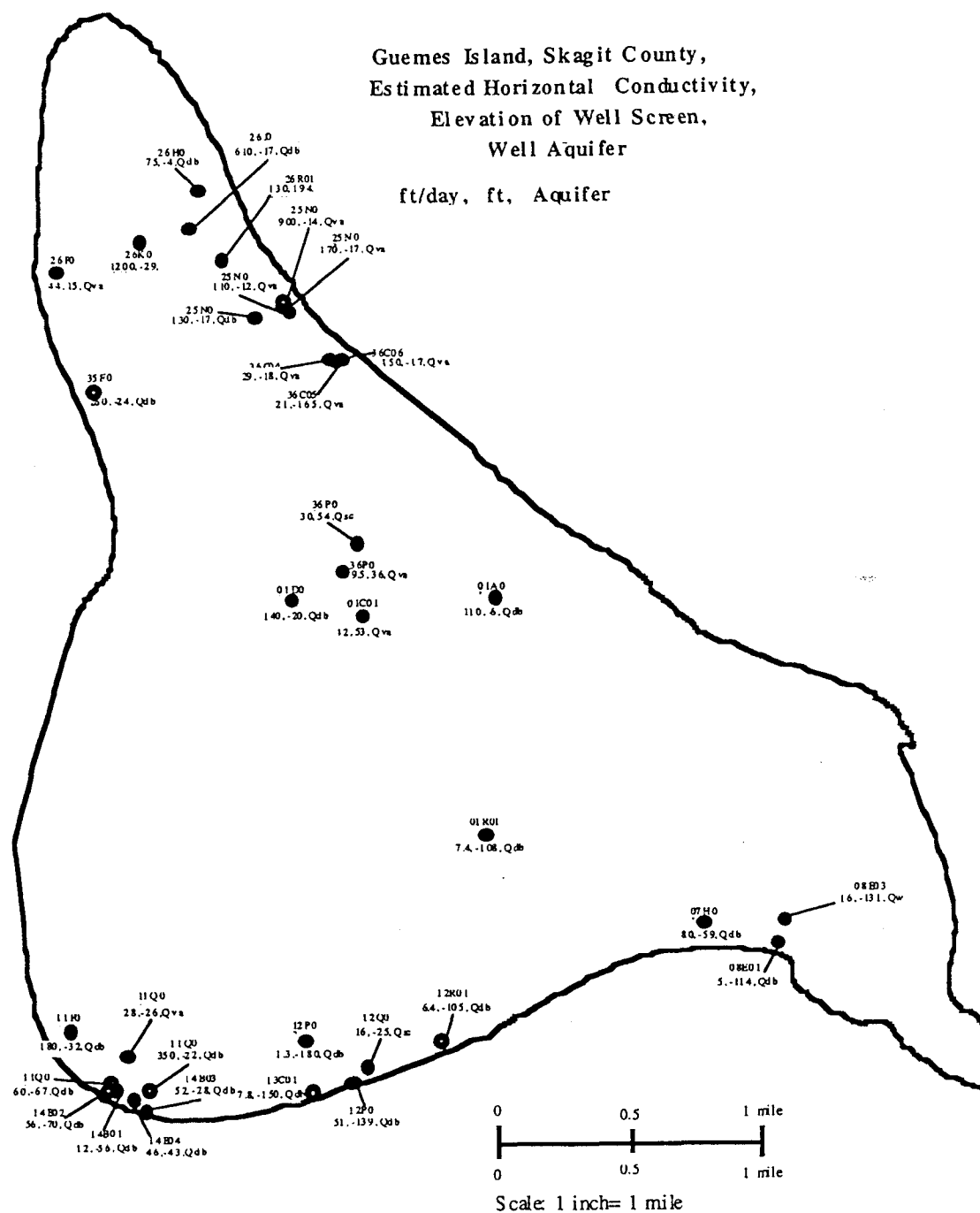


Figure 4.3: Estimated Hydraulic Conductivity Values

Table 4.2: Approximate Water Budget for Guemes Island

<u>Hydrologic Component</u>	<u>Estimated Quantity (inches per year)</u>
Precipitation	25
<u>Fate of Precipitation</u>	
Evapotranspiration	17
Recharge	6
Runoff	2
Total:	25
<u>Fate of Recharge</u>	
Withdrawal by wells	.2
Natural Discharge	5.8
Total:	6

The recharge value was estimated by using a relationship for recharge versus precipitation. This relationship is based on deep percolation below the root zone. Figure 4.4 shows the relationship, recharge vs. precipitation for different types of surface geology, that was used to estimate the recharge for this study. The recharge was estimated using a mixture of till and drift to simulate the surficial confining unit. The withdrawal by wells from the system was estimated from the well logs for each of the domestic self-supplied

wells as well from flow meters on the public supply systems. Actual well discharges for each of the wells in the Double Bluff aquifer can be found in Appendix D.

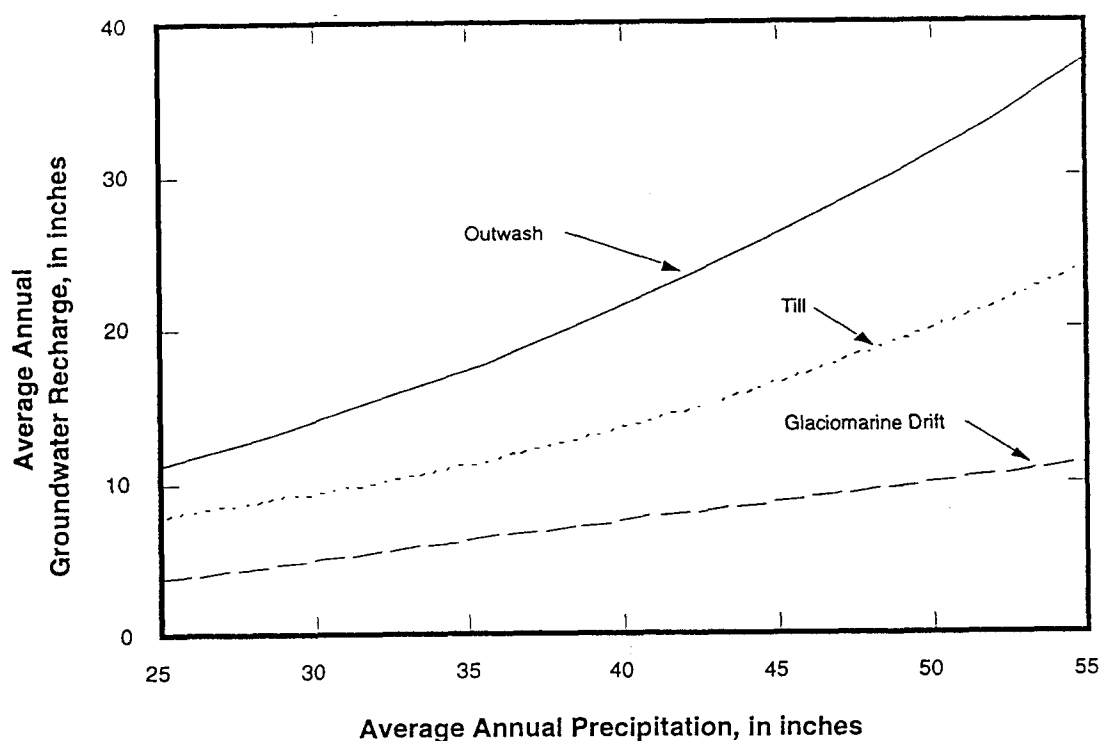


Figure 4.4: Relation of Precipitation to Groundwater Recharge on Guemes Island, Source: Kahle and Olsen, 1995

The value for the loss of recharge due to natural discharge is a residual value. Although the value for the pumping withdrawal may seem insignificant, the amount of recharge to reach the lower aquifers may be much less than the actual estimated recharge. Some of the recharge discharges along the exposed face of the western shore while some will percolate into the upper aquifers and discharge at their seepage face. The



actual amount of recharge that reaches the island's principle aquifer, the Double Bluff, depends on the conductivities of the overlying units and the amount of natural discharge occurring from those units. These natural discharges are dealt with in the full three dimensional model developed for this island. Although the Double Bluff aquifer is the main focus of the model and the future position of the saltwater interface in this aquifer is estimated for pumping scenarios within that aquifer alone, the upper units must be modeled in order to take into account the amount of natural discharge above the Double Bluff aquifer.

#### **4.1.4 Quality of Groundwater**

The quality of Guemes Island's fresh groundwater supply was investigated by the 1994 USGS study. In the initial study conducted in 1992, 24 wells were analyzed for concentrations of the major constituents. Appendix E summarizes statistically the concentration values of the common constituents, the average value of each constituent by hydrogeologic unit can also be found in Appendix E. During this study it was found that no primary MCL's were exceeded and that in general the fresh groundwater supply of Guemes Island is acceptable for domestic use at the present time.

The two constituents that are of concern in determining the presence of seawater intrusion are chloride and total dissolved solids. It was found that the SMCL for TDS, 500 mg/l, was exceeded in only 4 of the samples taken

and out of those four samples only two also exceed the SMCL of 250 mg/l for chloride. Figure 4.5 shows the areal distribution of chloride concentrations on Guemes Island as of June 1992.

The seasonal variability of chloride concentrations was investigated by a 12 month study, December 1991 through December 1992, involving 12 wells. It was determined by this study that the wells with the highest concentrations had the most seasonal variability, with the highest values occurring during the summer months as pumping rates increase and the amount of recharge decreases. This study also showed that seasonal changes in concentration in the Double Bluff aquifer were insignificant. Figure 4.6 shows some examples in the seasonal variability in chloride concentrations.

Water levels in the Double Bluff aquifer also do not fluctuate with the seasons, as they do in the upper units. This lack of fluctuation means that little error will be introduced into the Double Bluff aquifer by modeling the system as steady state.

Saltwater intrusion of Guemes Island's freshwater resources is one of the focuses of this research. The approach used in this study estimates the position of the saltwater interface and its movement due to changes in the stresses applied to the hydrologic system. The effects of these stresses on the individual well concentrations are not quantified using this modeling method. Based on existing data, it is the author's opinion that at the present time the quality of Guemes Island's fresh groundwater is excellent. It is also

OLDOW  
22.12 ± 0.25  
DAVE LAR  
71.61 ± 0.88  
HILL  
18.24 ± 17.13  
POTTER STATION  
152.67 ± 0.44  
MECRENS STUDIO  
101.71 ± 0.43  
SEA LAR  
78.94 ± 0.13

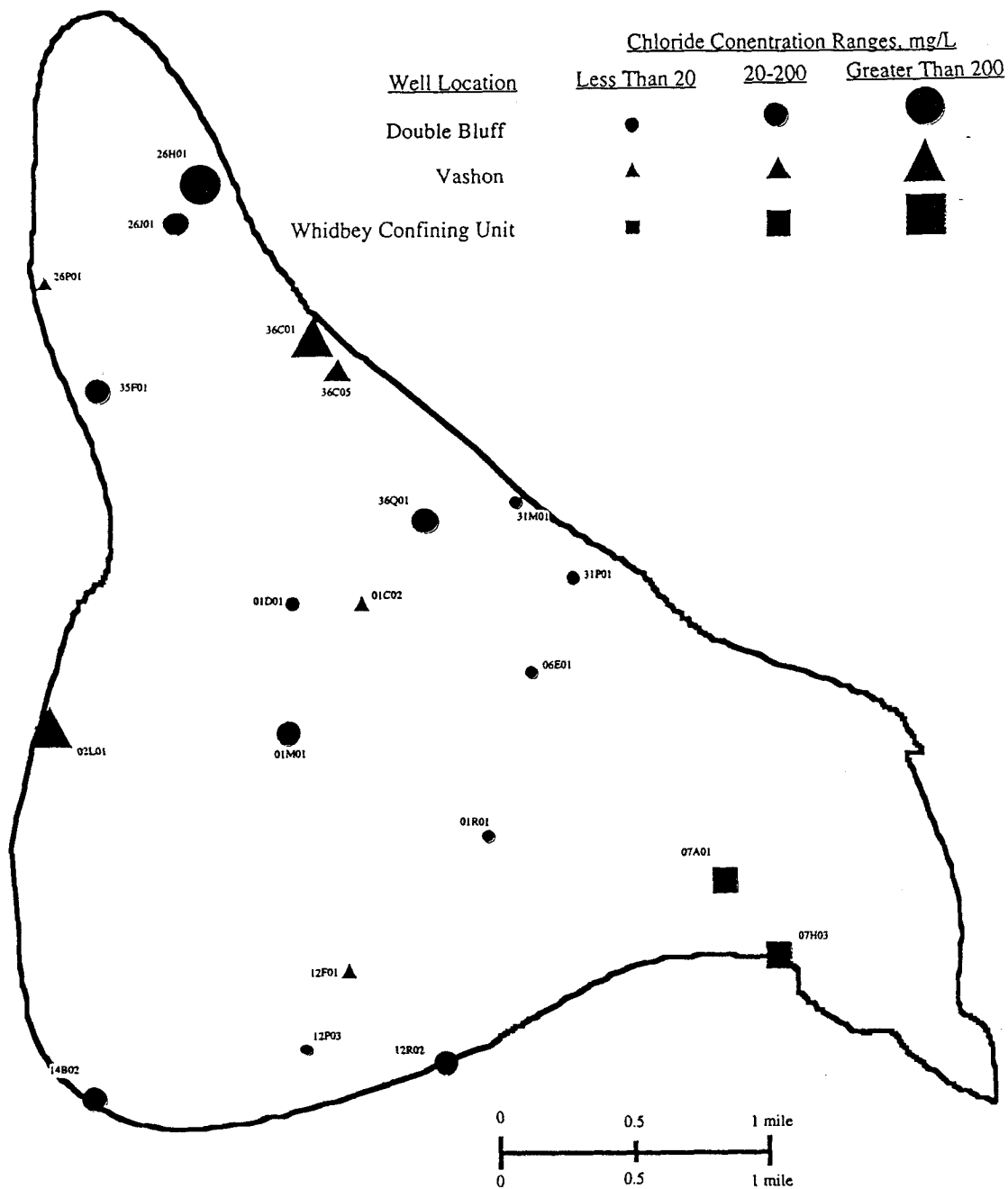


Figure 4.5: Areal Distribution of Chloride Concentrations, Source: Kahle and Olsen, 1995

the opinion of the author that although there may be some localized upconing in wells along the coast, that saltwater intrusion is not a major concern at this time. This thesis investigates the water resources of Guemes Island by calibrating a full 3-D model of the island and considering the future potential for movement of the saltwater interface.

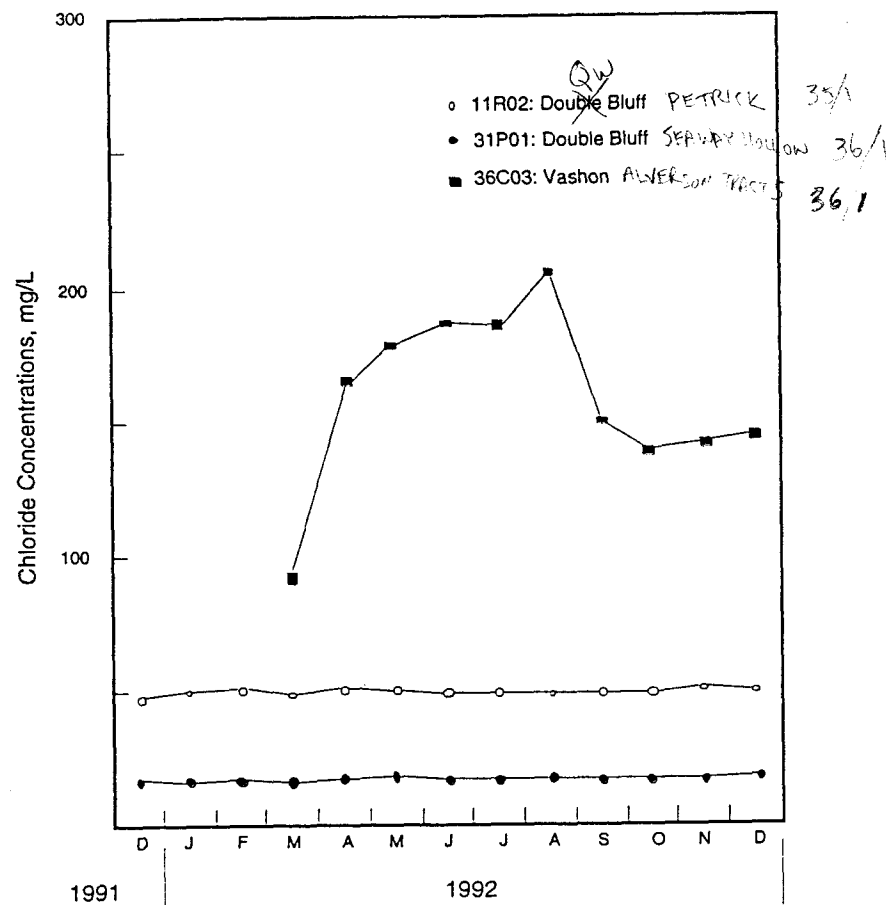


Figure 4.6: Seasonal Variation of Chloride Concentration in Select Wells

#### **4.2 ADDITIONAL DATA COLLECTED**

Before construction of the three-dimensional MODFLOW model could be completed and calibrated, two necessary sets of data were collected to compliment the data collected by the USGS in their study. The elevation of the underlying bedrock had to be estimated in order to determine the thickness of the Double Bluff aquifer unit. Although the saltwater interface underlies much of the island, the southeast corner of the island is a bedrock outcropping and in this region the bedrock cuts off the interface in some areas.

The second data set collected, an accurate head distribution within the Double Bluff aquifer, is vital not only in estimating the initial interface position but also in the calibration of the model. In the USGS study the depth to the water table from the top of the well casing was measured quite accurately. Using this data a distribution of the water levels in the Double Bluff aquifer was estimated. However, since there is only one benchmark on the remote island and it is heavily wooded, the elevation of the top of each well casing was estimated from a topographical map. This gave an error at each data point of roughly  $\pm 10$  ft. In an aquifer where head values range from 0 to 15 ft this estimation is insufficient in order to calibrate a flow model and any interface position estimation would only be within  $\pm 400$  ft.

#### 4.2.1 Data Collection

The field data was collected during a three week period, August 1995. The field data was collected and analyzed by the author, John Bradford, a Ph.D. student in the Department of Geology and Geophysics at Rice University, and Dr. John Oldow, former faculty member in the same department. Field data was collected in two steps. The first step used Global Positioning System (GPS) receivers to determine the lateral position and elevation of a number of points on the island. Readings were taken at the top of well casings in order to determine the head distribution in the Double Bluff aquifer. Readings were also taken at points along the main roads, approximately 500 ft apart, where gravity data would be taken. The second step of data collection involved taking gravimeter readings at the previously surveyed points on the roads.

#### 4.2.2 Elevation of Bedrock

The elevation of the bedrock underlying Guemes Island was estimated by the gravity survey. Gravity points were taken at each of the data points along the roads surveyed by GPS. The gravity data was modeled by John Bradford to obtain an estimation of the bedrock elevation underlying each point, see Figure 4.7. These data points were interpolated by the GMS system to the 37 by 47 grid used in the MODFLOW model of the island. The resulting map of the bedrock elevations in this area are shown in Figure 4.8. As expected the bedrock drops off sharply from the outcropping and will not

have an effect on much of the island as the saltwater interface will lie above it.

#### 4.2.3 Head Distribution in the Double Bluff Aquifer

The head distribution for the Double Bluff aquifer must be accurately mapped in order to compare the measured values, for calibration purposes, with those determined in the MODFLOW model. The head distribution determined was also used to estimate the present day position of the saltwater interface below Guemes Island by the Ghyben-Herzberg Relationship. The depth to the water table for each of the wells was measured by the USGS and the Guemes Island Environmental Trust in 1992. These depths were not measured again due to the fact that in a year long study it was determined that the seasonal heads in the Double Bluff aquifer vary less than a quarter of a foot. The elevation and lateral position of each well casing was determined by using GPS. Satellite readings were taken at or near each well casing and later compared to readings taken continuously at the base station. The elevation of each casing was determined by comparing its relative elevation to the base station to the relative elevation of the benchmark located at South Shore. The estimated accuracy of the elevation readings was determined to be about 0.1 m.

The actual wells surveyed in this study were chosen for two reasons. The first criteria was to get an adequate distribution on the island in order to

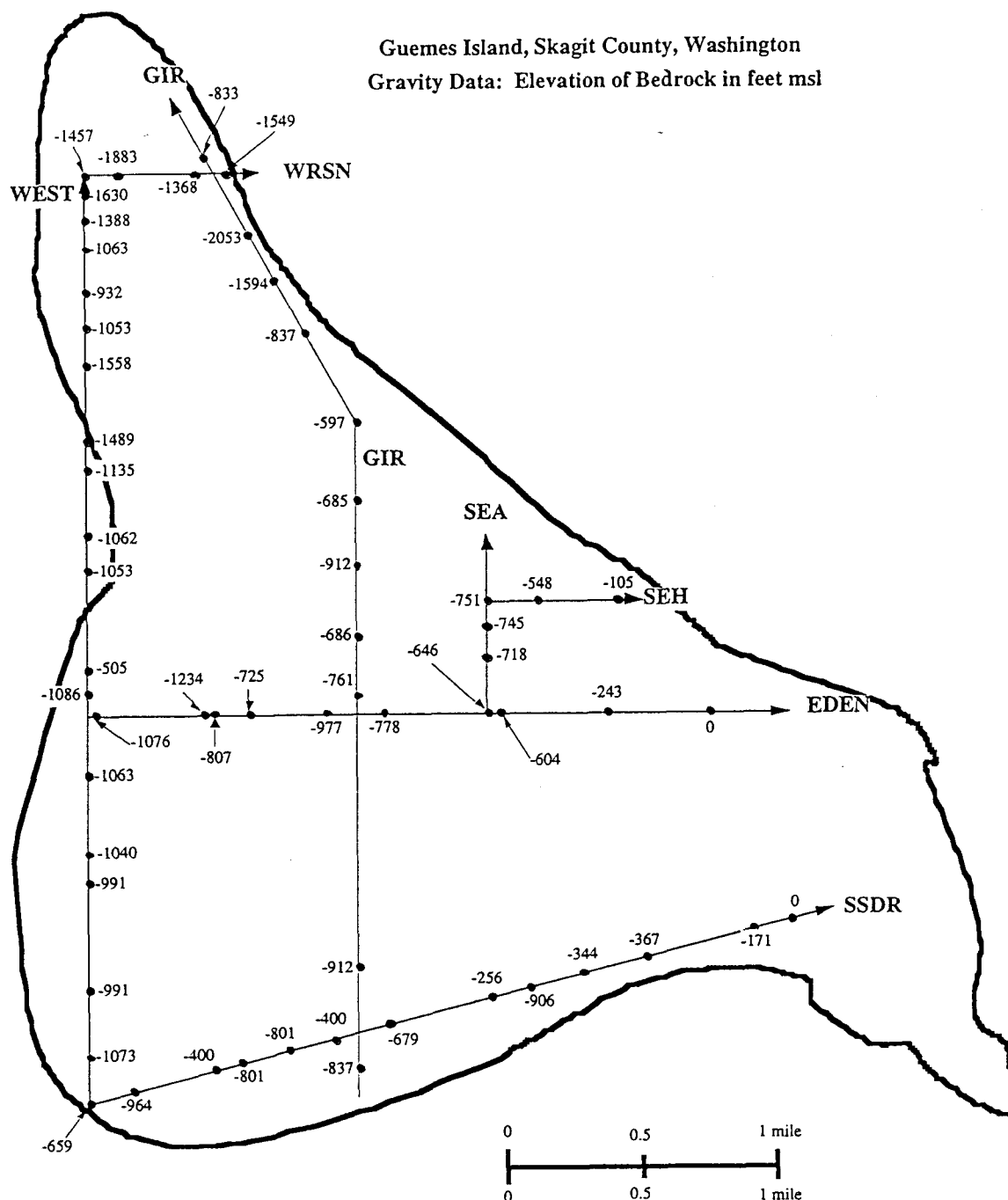


Figure 4.7: Point Elevations of Bedrock Estimated by the Gravity Survey



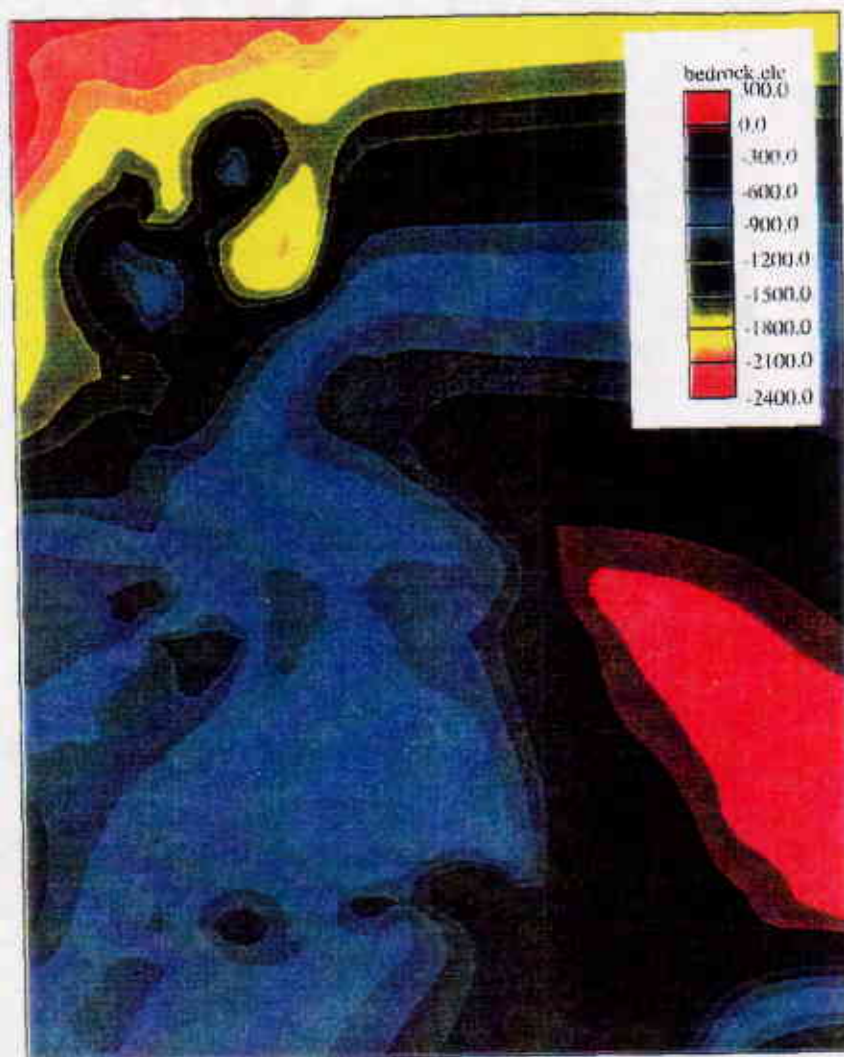


Figure 4.8: Bedrock Elevation Distribution Beneath Guemes Island

be able to accurately map the aquifer heads. The second criteria for well selection was the ability to get adequate satellite exposure. Some of the wells were surveyed at times of the day when a maximum number of satellites were overhead in order to increase the chance of a reading. Several of the readings were taken in an open area nearby and surveyed into the top of the well casing with a level and rod. The surveyed wells and the elevation of the freshwater head are shown in Figure 4.8. These data points were interpolated to the 37 by 47 grid and the resulting map of the head distribution in the Double Bluff aquifer is shown in Figure 4.9. It should be noted that in this map the interpolated values along the southeastern edge of the grid is cut off by the outcropping of bedrock shown by the grid outline.

#### **4.3 MODEL CONSTRUCTION AND GRID DESIGN**

The aquifer flow system has been conceptualized for MODFLOW. The USGS aquifer maps, the map of the bedrock elevation, and the head distribution were all used to set up the grid system and construct the model.

##### **4.3.1 Three-Dimensional Grid Layout**

The grid chosen for this model is 37x47x20. The xy dimensions were chosen in order to use a square grid system that fits the entire island within its boundary. Space was left along the edge of the island to accommodate the constant head boundary representing the sea. The xy dimensions of the grid

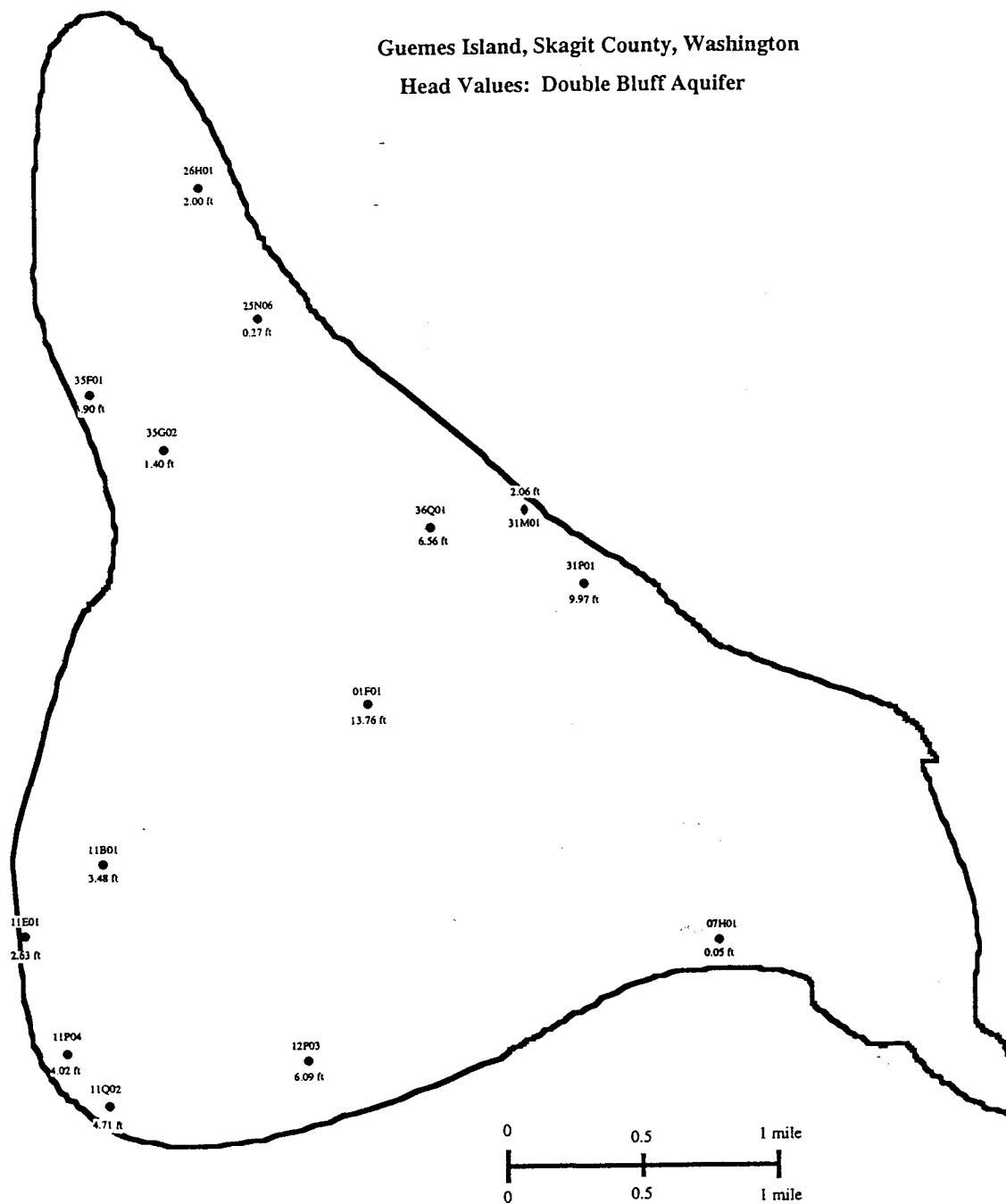


Figure 4.9: Measured Heads within the Double Bluff Aquifer

are 19536 ft by 24816 ft. The number of square grid cells in each direction are; 37 in the x, or east/west direction, and 47 in the y, north/south, direction. A total of 1739, 528 ft by 528 ft square cells, are used in each model layer. The grid layout for each layer and the location of the island in that grid can be found in Figure 4.10. The number of cells in each layer was chosen in order to be able to represent the aquifer system in detail while still maintaining a model system that has a reasonable computational time.

The number of model layers must also balance adequate detail of the flow system with computational time. A high number of model layers not only increases the computational time but also increases the number of input parameters to the model. Since the boundary conditions for each of the layers is different, due to the intruding saltwater, the modeling parameters must be added to each layer separately. During the calibration of the model this can add considerable time to the process. The z dimension of the model was chosen so that the upper layer would include the highest point of the surficial confining unit and the bottom layer included the lowest point on the saltwater interface. The model grid starts at an elevation of 200 ft and extends down to 600 ft below sea level. Twenty model layers were used in order to have a sufficient number of points along the saltwater interface in the Double Bluff aquifer. Each of these layers is 40 ft in thickness. The layers are small enough to estimate the fate of recharge in the upper layers and to adequately investigate three-dimensional flow in the Double Bluff aquifer.

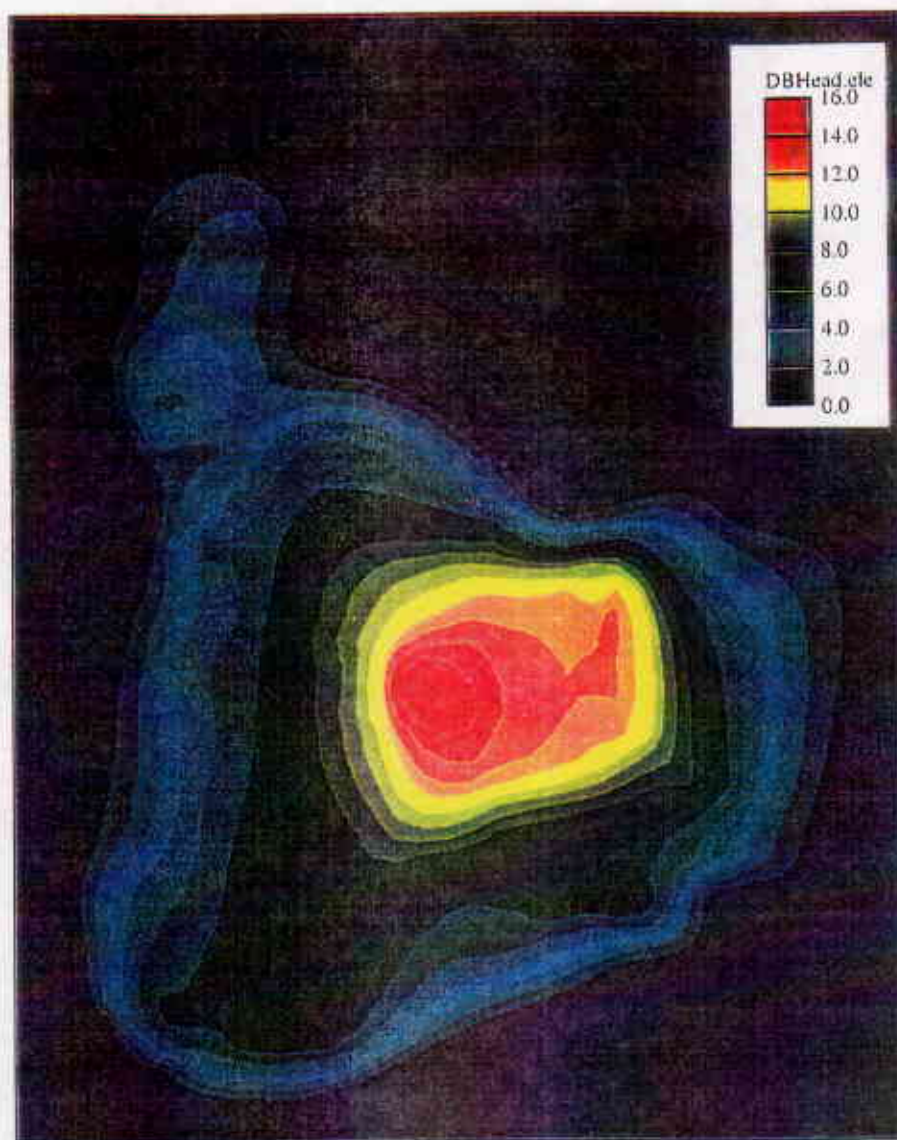


Figure 4.10: Measured Head Distribution: Double Bluff Aquifer

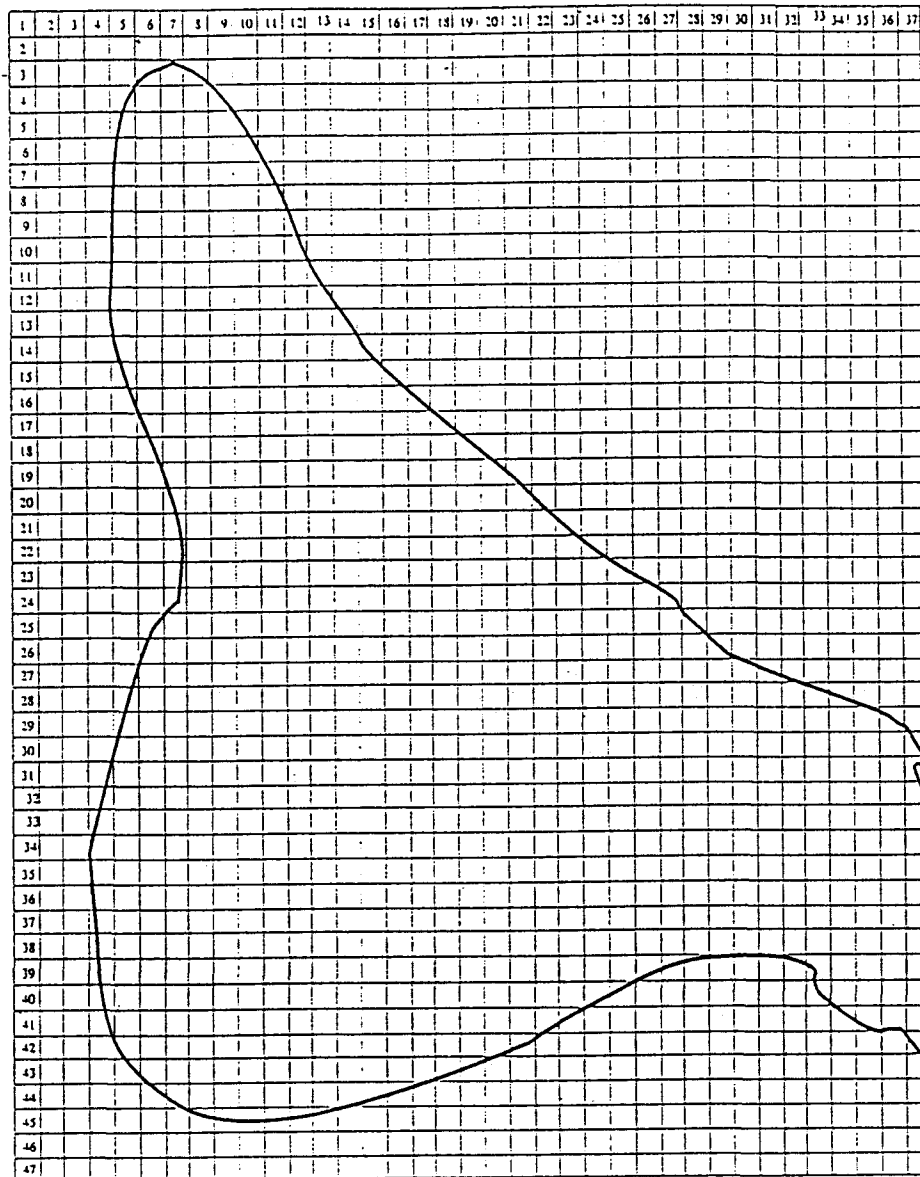


Figure 4.11: Grid Layout for MODFLOW Model: Guemes Island

#### 4.3.2 Representation of the Aquifer System in MODFLOW

The physical characteristics of the aquifer system, the areal shape of the island, the extent and shape of the hydrogeologic units, and the position and shape of the saltwater interface, are represented in the model grid. The conceptual model was built cell by cell in a brick framework, refer to Figure , with each individual cell representing a part of either the sea, one of the aquifers, the bedrock, or the intruding saltwater. The result is a model of the actual flow system for Guemes Island that is used in MODFLOW.

The extent and thickness of each aquifer was estimated from the maps developed by the USGS, see Appendix C. Horizontally the aquifer shapes were estimated by laying the grid over the maps. Vertically an aquifer started in a layer if its estimated top elevation at the center of the xy cell was greater than the elevation of the center of that layer and less than the center elevation of the layer above. The position of the bedrock was estimated from the gravity survey discussed earlier. In the original model, the position of the saltwater interface was estimated by using the measured head map, developed by the GPS survey, and the Ghyben-Herzberg relationship. The position within the grid of the top of the bedrock and the top of the saltwater wedge were determined the same way as that of the aquifers discussed above. Examples of the how the physical characteristics within a layer and within a

vertical cross section were conceptualized are shown in Appendix F , Figures F.1 and F.2.

#### 4.3.3 Boundary Conditions

There are three kinds of cells in this model system, refer to Figure 3.2. Active cells, which are denoted by a value greater than zero in the IBOUND array, represent all of the areas within the island above the saltwater interface and above bedrock. Heads within the active cells are solved for in each of the MODFLOW simulations. Constant head cells are used to represent the surrounding sea, these cells have a value less than zero in the IBOUND array and a value of zero in the starting head array. Constant head cells also are used to represent areas above sea level that are outside of the land mass at the elevation of that layer. The value of this constant head is equal to the elevation of the node in that particular cell. The saltwater interface and the bedrock are represented as a no flow boundaries, IBOUND value of zero. The boundary conditions in each layer is different. At the deeper layers the presence of saltwater dominates and much of the layer consists of inactive, no flow cells, representing the seawater. Examples of an areal and a vertical cross section of the boundary conditions can be found in Appendix F, Figures F.3 and F.4.



#### 4.3.4 MODFLOW Parameters

The conceptual model of the island flow system is used to build the MODFLOW model. The boundary condition and starting head for each cell is specified, as discussed in the previous section. The value of conductivity or transmissivity in a specific cell depends upon which hydrogeologic unit that cell represents. Conductivity values for each unit can be found in Table 4.1. The transmissivity is the conductivity value multiplied by the thickness of the layer, 40 feet in this model. The top layer of the model is unconfined. All layers below the top are specified as confined or unconfined depending upon the water level in that layer. The model will adjust the transmissivity value depending upon the static water level in the cell. Leakance between layers is accounted for by the VCONT term discussed in Chapter 3. The leakance value between two layers can be found in Table 4.3. Due to the layering effect in unconsolidated deposits the vertical conductivity is generally less than the horizontal. The vertical conductivity of a unit was estimated as ten percent of the horizontal (Bedient et al., 1994).

Table 4.3: Vertical Leakance Terms: Guemes Island

<u>Upper Layer</u>	<u>Lower Layer</u>	<u>VCONT</u>
Surfical Confining Unit	Surfical Confining Unit	0.0575
Surfical Confining Unit	Vashon Aquifer	0.0749

Surfical Confining Unit	Whidbey Confining Unit	0.0075
Surfical Confining Unit	Double Bluff Aquifer	0.0859
Vashon Aquifer	Vashon Aquifer	0.1075
Vashon Aquifer	Whidbey Confining Unit	0.0077
Vashon Aquifer	Double Bluff Aquifer	1.1317
Whidbey Confining Unit	Whidbey Confining Unit	0.004
Whidbey Confining Unit	Double Bluff Aquifer	0.0078
Double Bluff Aquifer	Double Bluff Aquifer	0.17

The other MODFLOW inputs included the pumping rate, the recharge, and the width of the seepage face. The recharge value of six inches per year estimated by the USGS was used along with pumping rates estimated in that study. The layer in which a well was placed depended upon the depth of the well casing. The width of the seepage face was estimated by Glover's potential theory, see section 3.3.4, as approximately 62 ft.

#### **4.4 MODEL CALIBRATION**

The MODFLOW model constructed must be calibrated. In this process the conductivity values within an aquifer are adjusted so that the head values produced by the model match those measured in the field within a specified limit of error. Since in this study there is only one set of head data, the steady state model is calibrated to that data. A sensitivity analysis will be used to test

the sensitivity of the calibrated model. This calibrated model can be used to predict the effect of future changes to the aquifer system.

#### 4.4.1 Calibration Process

The constructed model is adjusted in order to account for changes in conductivity within each layer. The calibration process involves both a qualitative and quantitative comparison of the head distribution produced by the model and the distribution measured in the field. Qualitatively, the head map produced is compared to the map generated by interpolation of the measured values. Quantitatively, the head values at individual wells are compared and the difference in the measured and generated value is computed.

Initially the model was run using average values of conductivity for each unit. The head distribution of the initial model run can be found in Figure 4.12. This distribution does not compare favorably with the map generated by the measured head values, Figure 4.10. The hydraulic conductivity within the layers is adjusted and the model rerun until the generated map, see Figure 4.13, closely images that of the interpolated head map and the generated head values at wells match those measured in the field. The conductivity is adjusted by raising conductivities in areas where the heads are above measured and lowering conductivities in areas where generated heads are below the measured heads. Increasing conductivity

values decreases resistance to flow toward the sea and lowers head, decreasing the values has the opposite effect on the system. A plot of the final adjusted hydraulic conductivities within the Double Bluff aquifer is shown in Figure 4.14.

The individual head values at 14 wells within the Double Bluff aquifer were compared and assumed calibrated when generated values were within 0.1 ft of the measured and the relative error was less than five percent, a common value used when calibrating flow data (Anderson and Woessner, 1992). Table 4.4 shows a comparison of the measured flow values with the final values generated by the calibrated flow model. All of the values are within the error limits and have a random distribution so that there is no apparent bias in any section of the model.

Hydraulic conductivity was the only parameter adjusted in the calibration process. The boundary conditions are set by the geometry of the system and the measured head values. Recharge is the only other parameter that could be adjusted in the calibration process. However, this value has a great effect on the head values throughout the island. In the steady state model the recharge accounts for all additions to the system. A small increase in the recharge will cause all heads within the system to rise dramatically. Due to this fact the recharge estimated by the USGS was used in the calibration process and only the conductivities were adjusted. Conductivity values within a single aquifer vary from region to region and the value at any

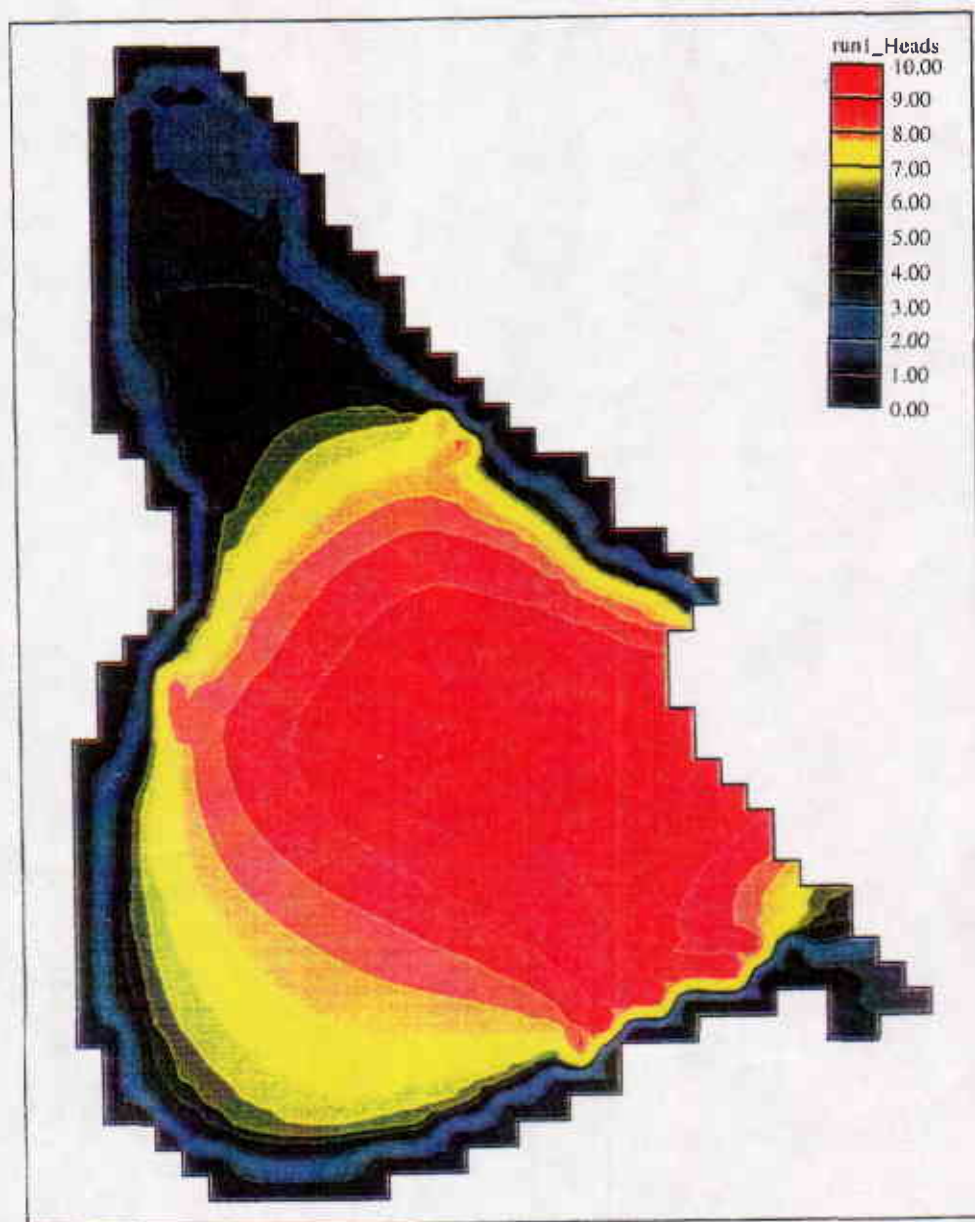


Figure 4.12: The Initial MODFLOW Run Using Average Values of Conductivity

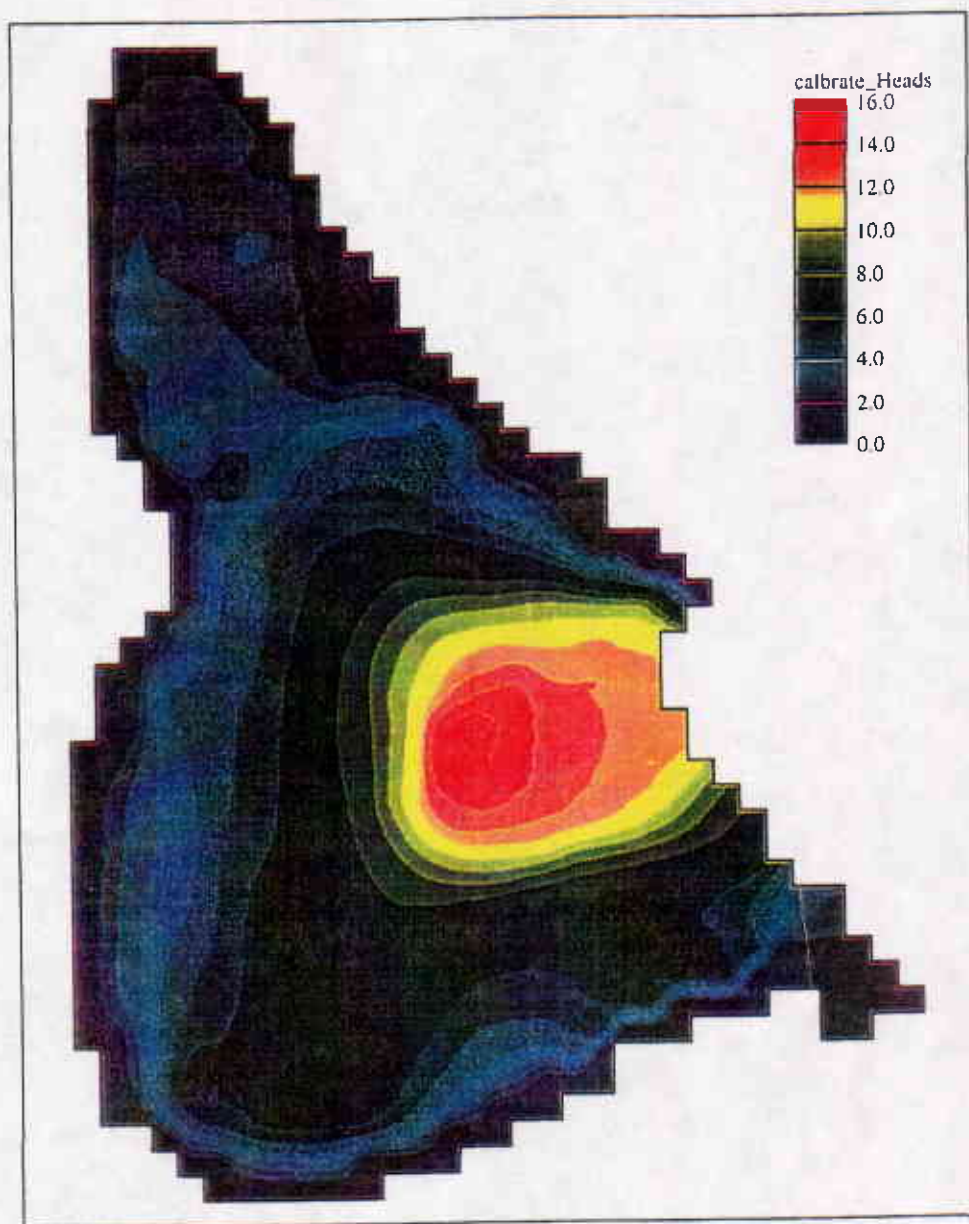


Figure 4.13: Calibrated Head Map: Double Bluff Aquifer

Table 4.4: Comparison of Generated and Measured Head Values

<u>Well #</u>	<u>Measured</u>	<u>Generated</u>	<u>Absolute</u>	<u>Relative</u>
	<u>Head</u>	<u>Head</u>	<u>Error</u>	<u>Error</u>
11Q02	4.71	4.7352	0.0252	0.54%
11P04	4.02	4.0629	0.0429	1.07%
11E01	2.63	2.5528	-0.0772	-2.94%
12P03	6.09	6.1147	0.0247	0.41%
11B01	3.48	3.4430	-0.0370	-1.06%
01F01	13.76	13.8047	0.0447	0.32%
07H01	0.05	0.0497	0.0003	-0.60%
31P01	9.97	10.0653	0.0953	0.96%
31M01	2.06	2.0010	-0.0590	-2.86%
36Q01	6.56	6.5427	-0.0173	-0.26%
35F01	3.9	3.8693	-0.0307	-0.79%
35G02	1.4	1.4090	0.0090	0.64%
26H01	2	1.9896	-0.0104	-0.52%
25N06	0.27	.2735	0.0035	1.3%

one point is not known with great certainty. The estimated conductivities used in this study were estimated from the well logs and there are sources of error in the method used, see section 4.1.2. The conductivity values can be

adjusted from the mean value and still be within a reasonable range. The adjusted conductivities in the Double Bluff aquifer range from 5 ft/day to 120 ft/day, well within the range of values measured in the field, see Figure .

There are sources of error in both the generated heads and the measured heads. The sparse information on the heads within the aquifer leads to errors in the interpolation of the head map. There is also error in the actual heads measured. The model constructed is a steady state model and therefore field measured data may reflect the presence of transient effects not represented by the model. The calibrated model may not be a unique solution to the system. However, by matching the heads in the Double Bluff aquifer both qualitatively and quantitatively the calibrated model can be used as a representation of Guemes Island's actual flow system.

#### 4.4.2 Sensitivity Analysis

The purpose of this section is to investigate the effect of changes in the calibrated conductivities on the flow system. The conductivities were adjusted and the effect on the root mean squared error observed. Figure 4.15 shows the calculated RMS for conductivities adjusted by a factor. The RMS is lowest at an adjustment factor, multiplier, of 1. The RMS increases as the factor increases or decreases the conductivity values. This is due to the fact



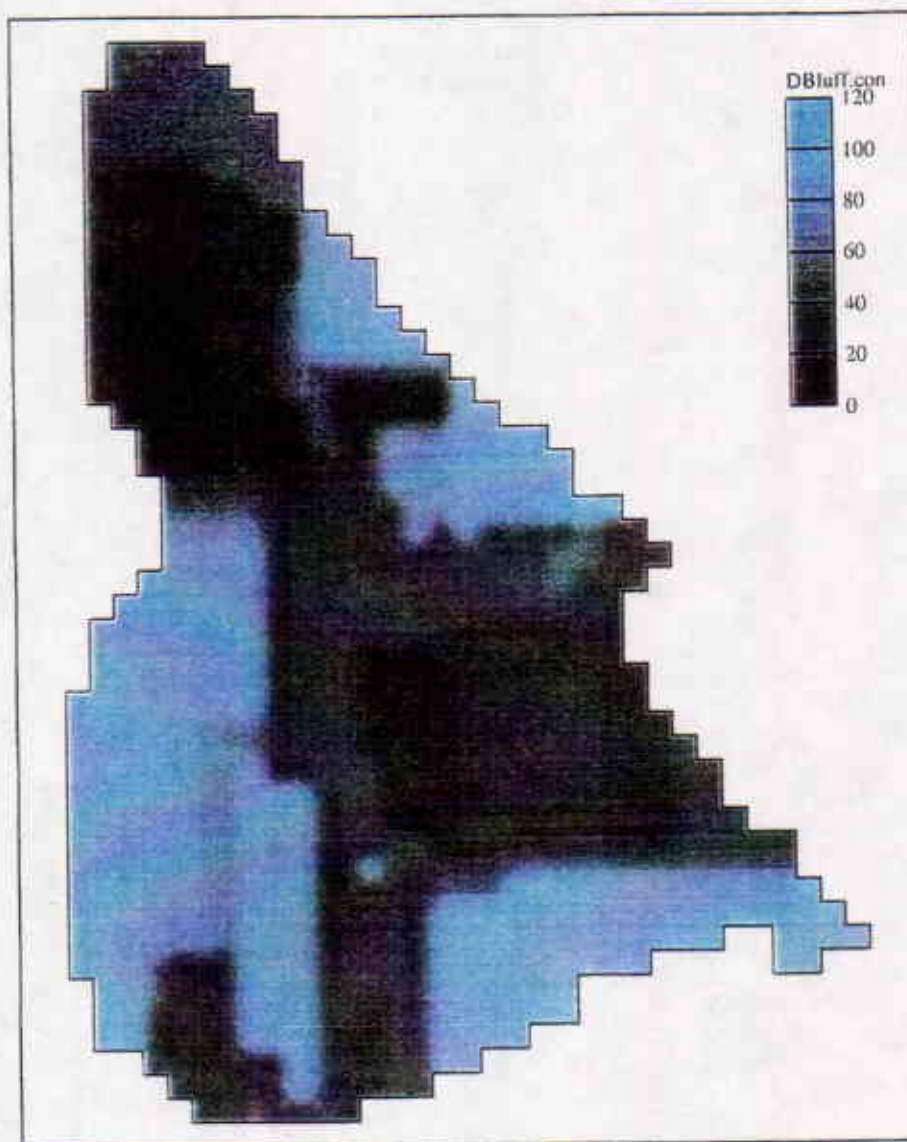


Figure 4.14: The Calibrated Conductivity Values: Double Bluff Aquifer

that by changing the resistance to flow the ability of the system to *mound* water changes. Increasing the conductivity allows more water to flow from the center of the island and discharge to the sea, causing the head values to decrease. Decreasing the conductivity has the opposite effect and more water is retained by the system.

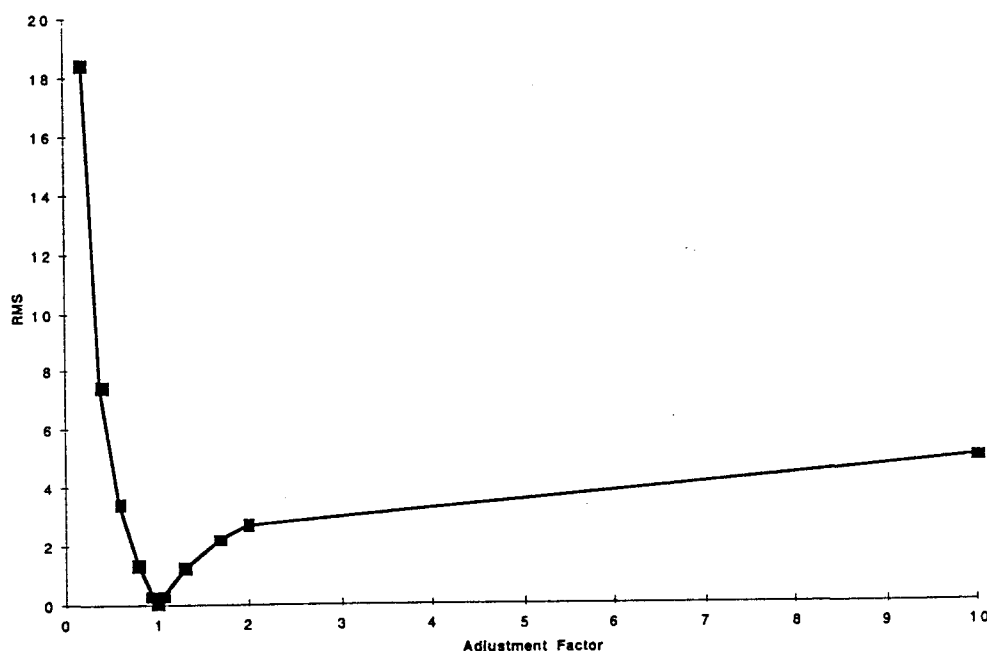


Figure 4.15: Sensitivity Analysis: RMS vs. Adjustment Factor

The sensitivity analysis shows that the system is best represented by the values of conductivity chosen in the calibration process. Any change in conductivity in only one region of the island causes the modeled head distribution shape to change and the head map no longer matches that generated from the measured values. This calibrated model is used in the

next section to predict changes in the freshwater head within the Double Bluff aquifer as pumping rates and patterns are adjusted.

#### ***4.5 FUTURE PREDICTIONS OF GROUNDWATER DEVELOPMENT***

The groundwater model of Guemes Island, constructed and calibrated in this chapter, is used to predict the future movement of the saltwater interface as the pumping rate on the island is increased. Six case scenerios were investigated in this study. The first three cases involve increasing the pumping rates of the existing wells, the last three keep the existing wells pumping at their current rate and add new community wells to the Double Bluff aquifer.

##### ***4.5.1 Case One***

The first case scenario simply doubled the pumping rates in each of the existing wells and calculated the steady state drawdown in the Double Bluff aquifer, see Figure 4.16. The drawdown values on much of the island were found to be insignificant. However, the drawdown along the northwest coast reached a value of 2.0 feet. In the area of greatest drawdown, known as Potlatch Beach, the water table is currently less than four feet. The drop in the water table will cause the position of the saltwater interface to rise 80 ft. The Potlatch Beach area is where the three well community system is located. These wells have the largest pumping rate of any wells on the island and

therefore doubling their pumping rate will have a large effect on the aquifer system in that area.

#### 4.5.2 Case Two

Since doubling the pumping rate of the Potlatch community system causes large drawdowns in that area, in this scenario these rates were only increased by ten percent. The pumping rates in all other wells were doubled. The generated drawdowns were decreased significantly from the those in case one. The maximum drawdown was calculated to be less than 0.4 ft. This maximum once again occurred in the Potlatch Beach area. The drawdown on the rest of the island is insignificant with the higher drawdowns in the section north of Potlatch beach and along the bedrock where the head is at a maximum, see Figure 4.17.

#### 4.5.3 Case Three

The third case further increased the pumping rates for all of the wells except those in the Potlatch community system. The wells were all increased to a value four times their original rate. As expected the drawdown on the island increased with the increase in the pumping rate, see Figure 4.18. The drawdowns and subsequent saltwater intrusion over most of the island was found to still be insignificant. The area of concern is the northern section of the island where the original heads are the lowest. The low head values in that area are most effected by the increase in pumping rate.

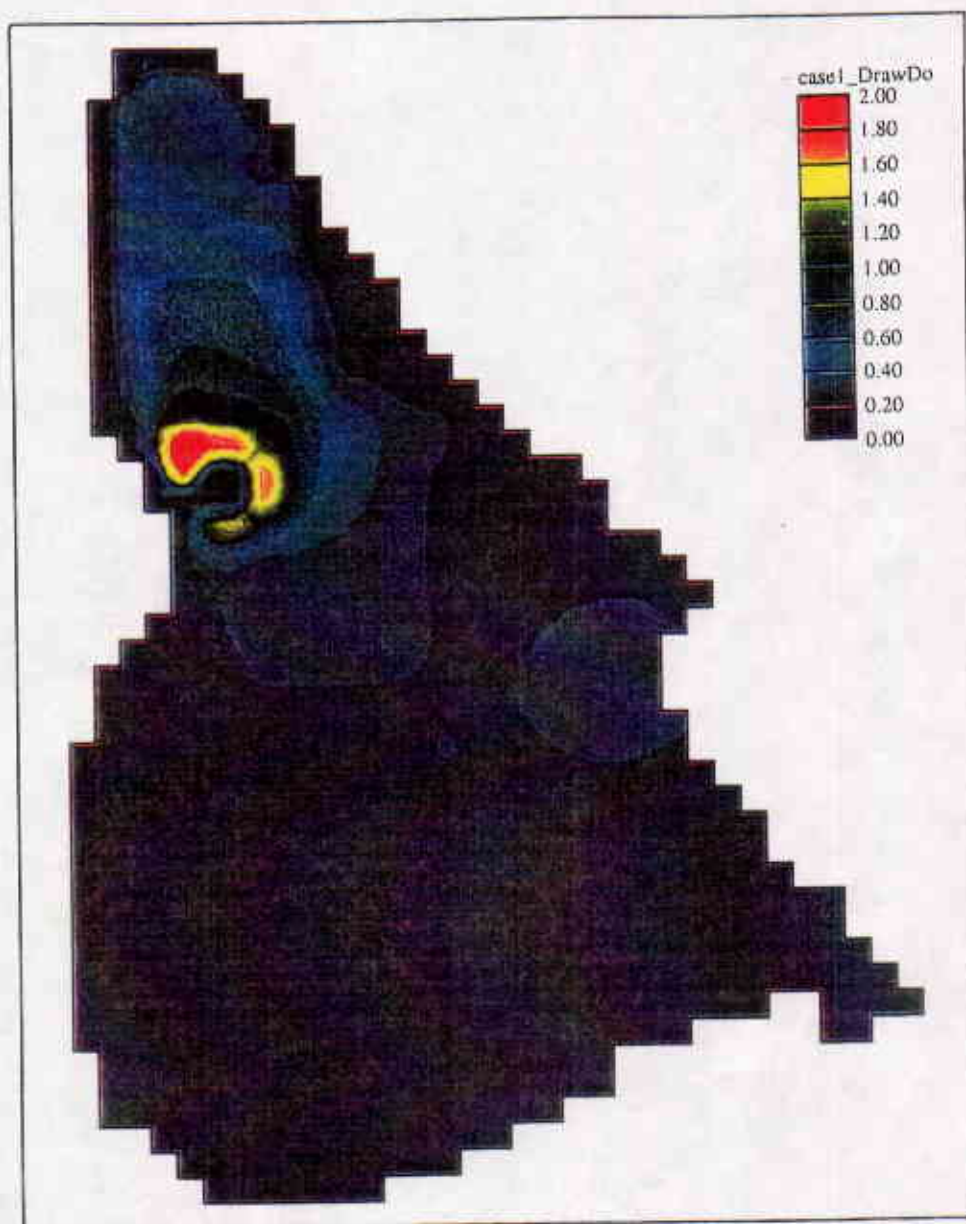


Figure 4.16: Drawdown in the Double Bluff Aquifer: Case 1

#### 4.5.4 Case Four

There is a large tract of land in the southwest corner of the island that is owned by a single land owner. This land is uninhabited at the present time but is a possible site for future construction. In order to accommodate possible new homes in this area, this scenario adds a three well community system to this area. The three wells are drilled into the Double Bluff aquifer to a depth 20 ft below the top of the aquifer in order to minimize the effects of upconing. The pumping rate for each well is the same as that used by a similar 32 connection community well. The three well system can provide water for approximately one hundred new homes. The new wells are located at cells: (10,39), (13,34), and (16,39), see Figure 4.11 for the location of these cells within the island.

The drawdown caused by the addition of these new wells to the aquifer system, Figure 4.19, effected only the southern portion of the island. The maximum drawdown located at one of the wells was less than 0.3 ft. The drawdown and saltwater intrusion caused by the addition of one hundred homes in this area of the island was found not to compromise the integrity of the freshwater resource.

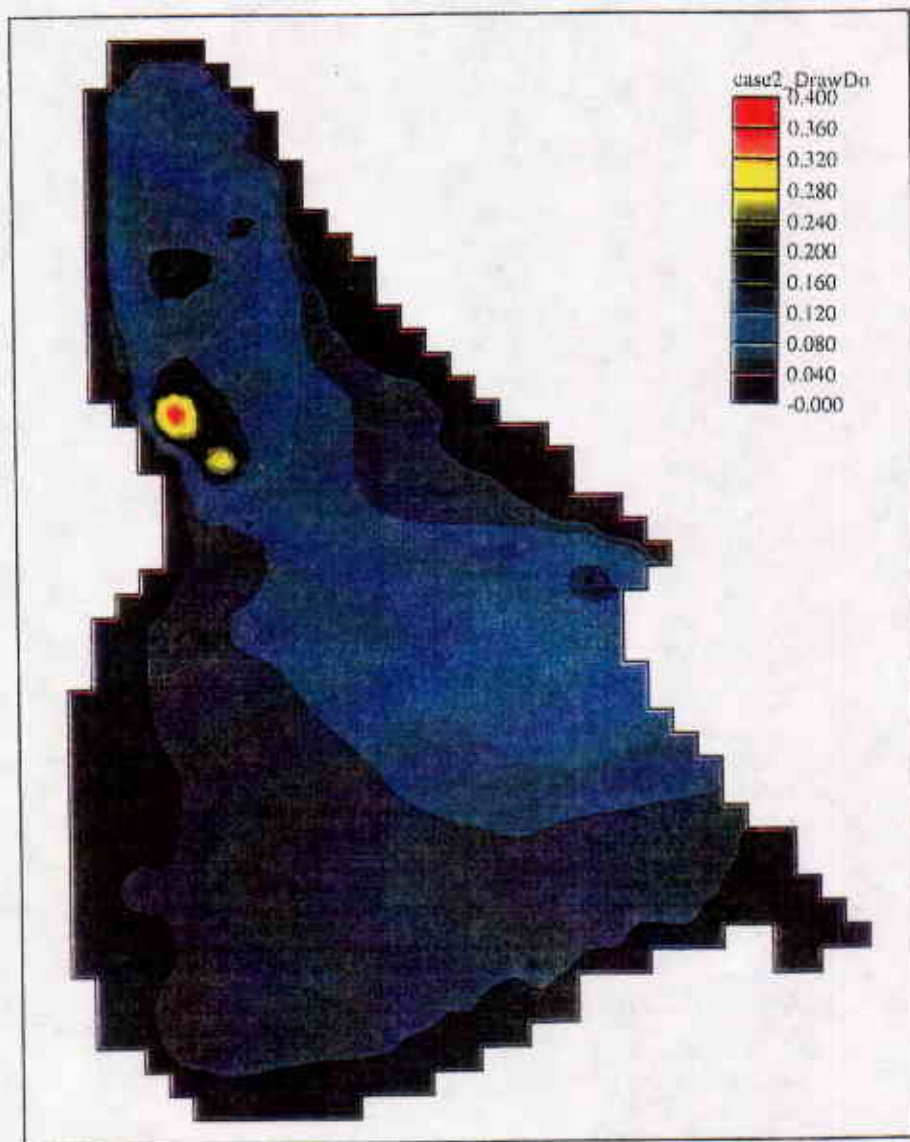


Figure 4.17: Drawdown in the Double Bluff Aquifer: Case 2



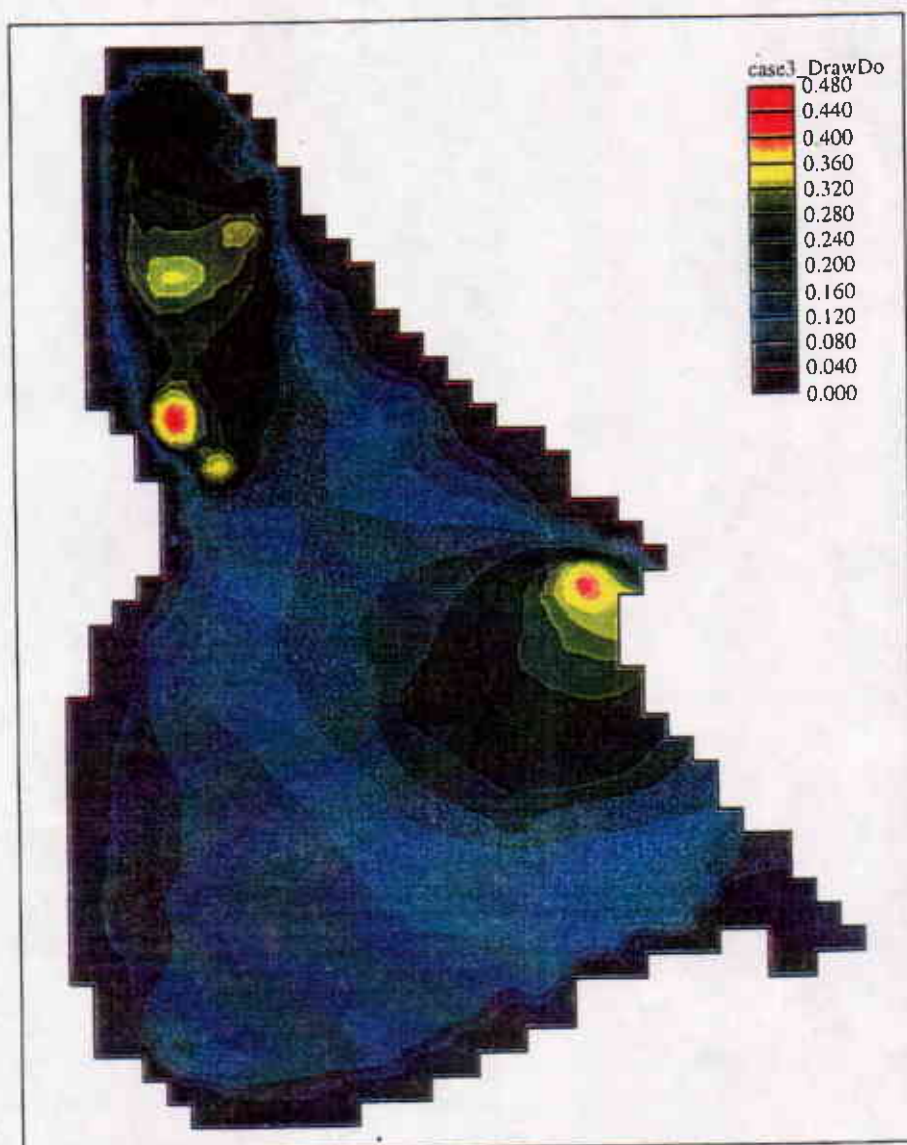


Figure 4.18: Drawdown in the Double Bluff Aquifer: Case 3



#### 4.5.5 Case Five

This scenario attempts to provide additional water to the northern section of the island, where drawdown caused by additional pumping of existing wells was found to be of concern. The three well system in the south remains in the scenario and two community wells, 20 connections each, are added to cells (12,16) and (21,13). These wells could provide additional water to the north shore or to Potlatch Beach. The drawdown caused by the addition of these wells was high around both wells, see Figure 4.20. The northern well caused the most drawdown in head, approximately 1.1 ft at the well itself. This area continues to be sensitive to additional pumping. Leaving the same pumping rates for all existing wells and adding only two community wells to the system has a significant effect on the system in the northern section of the island.

#### 4.5.6 Case Six

The last scenario uses the wells from cases four and five along with the addition of five extra community well systems, each with 20 connections. This addition will bring the total number of additional connections to 240. The new wells are located in the Double bluff aquifer at cells: (17,19), (19,24), (19,26), (26,36), and (23,38). The drawdown caused by the addition of these

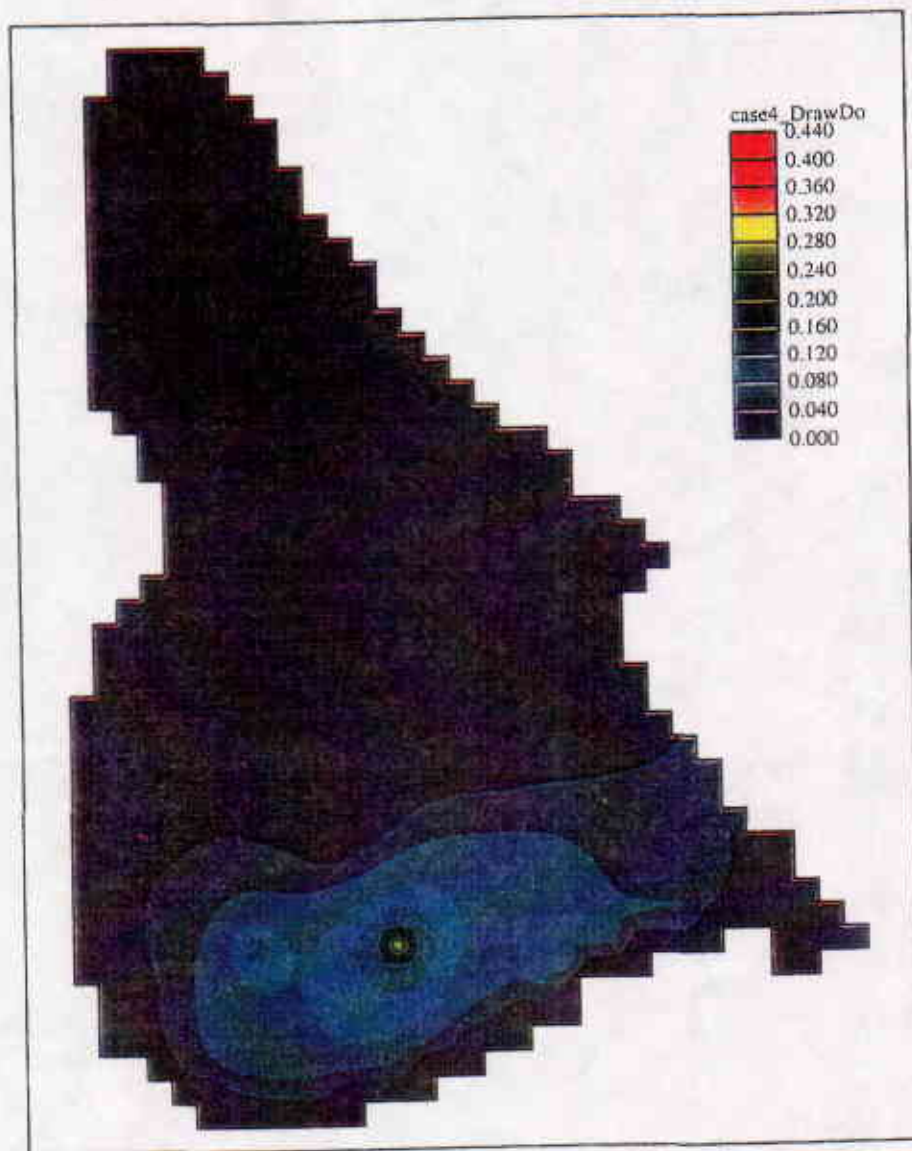


Figure 4.19: Drawdown in the Double Bluff Aquifer: Case 4

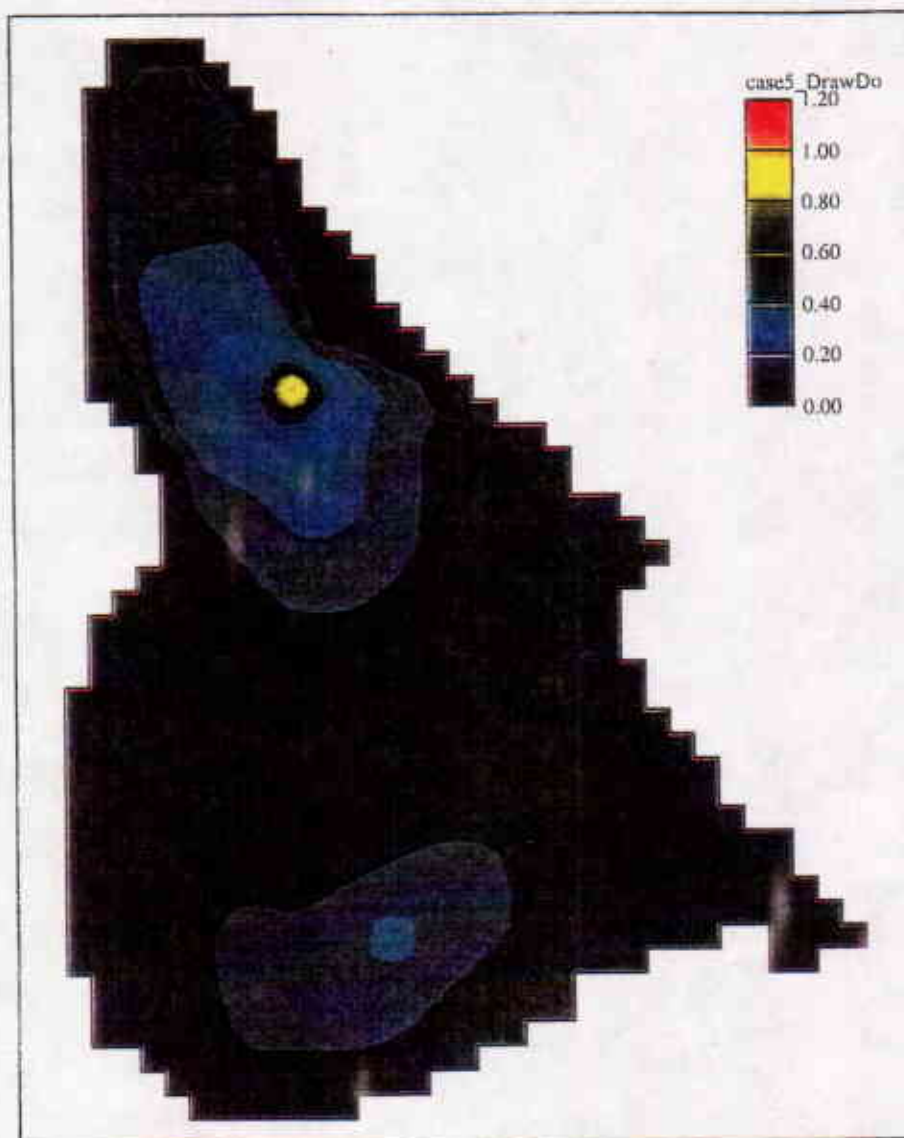


Figure 4.20: Drawdown in the Double Bluff Aquifer: Case 5

wells from today's head values can be found in Figure 4.21. The new area that has a significant drawdown is the southeast corner of the island. This corner like the section in the north of the island has low initial heads and the drawdown of between 0.4 and 0.5 will cause noticeable intrusion into that area. The well drilled in this corner has a pumping rate that can not be sustained without jeopardizing the integrity of the freshwater resource in that area.

#### **4.5.7 Freshwater Resources of Guemes Island**

The case study revealed that at the present time, based on available information, the quality of Guemes Island's fresh groundwater supply is excellent. Saltwater intrusion is not a major problem at the present time. There may be some localized areas of upconing but intrusion of the interface into the aquifer system is insignificant. The six case scenarios show that most of the island can sustain sizable growth while maintaining the integrity of the freshwater resources. The northern section of the island is the major exception. This part of the island has low head values at the present and the model shows that increasing the pumping rates in this area causes significant drawdown. Any additional wells to this area of the island should be carefully planned. Growth in this area may cause intrusion problems that will not only effect the new wells but also the wells currently in use. The southeast corner of the island also was effected by the addition of a community well.

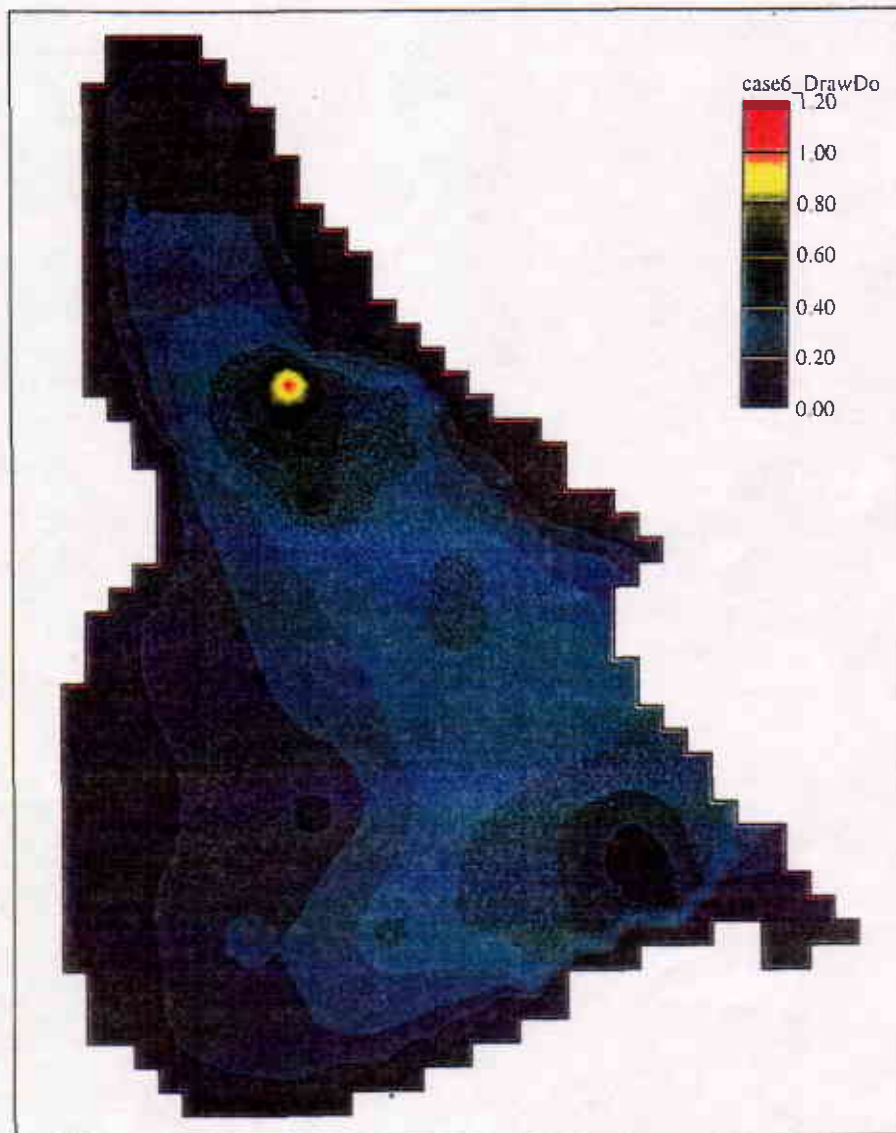


Figure 4.21: Drawdown in the Double Bluff Aquifer: Case 6

This area was not greatly effected by increasing the pumping rate of the current wells. Any large community system constructed in this region should use multiple wells in order to decrease the localized effects of drawdown caused by large pumping rates.

## 5. CONCLUSIONS

Saltwater intrusion is a concern in island and coastal aquifers that are in direct hydraulic connection with the sea. Managing freshwater resources in these areas requires careful planning in order to maintain the integrity of the resource. The interface between the saltwater and freshwater in these aquifers can be approximated by either a sharp-interface, immiscible fluid approach, or an approach that allows for mixing of the two fluids in a transition zone.

There is at the present time no single approach or model that can solve all intrusion problems. The sharp-interface model does not take into account the zone of the diffusion separating the two fluids. In some cases this zone may be quite large and viewing the interface as sharp can lead to model solutions inconsistent with observed values. Sharp-interface modeling can not determine the change in well discharge concentration caused by intrusion. However, it can be used as a water resources tool in approximating the effect of changes in aquifer stress to the position of the saltwater front.

Density-dependent flow modeling is a more accurate approximation to the actual flow system. It takes into account the zone of diffusion and can estimate concentration changes within the aquifer. However, this modeling approach is numerically intensive. Aquifer systems with complex geometry

and/or well patterns may require excessive computational time and cause large errors in the numerical output. Density-dependent modeling has also been shown to break down when the zone of diffusion is relatively small, as it is in many aquifers. In thin zones of diffusion, the steep concentration gradients cause numerical dispersion of the solution. An aquifer may have both interface types in different regions and either modeling approach may cause errors in portions of the aquifer.

The modeling method used in this thesis uses the sharp-interface approximation. The method uses a standard flow model to simulate the flow of freshwater within the aquifer system. The boundary separating the freshwater from the saltwater is modeled as a no flow boundary in the flow model. In order to accurately simulate flow along the boundary, a large number of layers within a single aquifer must be used in a 3-D model. The position of this interface is approximated using head values and the Ghyben-Herzberg Relationship. This method was tested against an analytical and numerical solution to a circular island containing a single unconfined aquifer. The method was found to compare favorably with the both solutions.

The advantage of this method is that it is as versatile as the standard flow model it uses to simulate the aquifer system. In island aquifer systems where vertical recharge to the aquifer system is the only source of freshwater, the full three-dimensional model can be used to estimate the fate of recharge



in the layers above the main water bearing aquifer(s). Once the flow model has been calibrated it can be used to investigate the effects of future withdrawals on the freshwater head, and consequently on the position of the saltwater interface.

A case study using this method was done on Guemes Island, Skagit County Washington. Based on the available data, there is no saltwater intrusion problem on the island at the present time but future freshwater withdrawals may be of concern. A three-dimensional model of the island was constructed and calibrated. The model was then used to investigate the effects of future freshwater withdrawals on the integrity of the freshwater resource.

The modeling study investigated the effects of six case scenarios on the position of the saltwater interface within the main water bearing aquifer. The study revealed that with large increases in pumping rates the northern region of the island is vulnerable to the intrusion of seawater. Potlatch Beach community is located in this area and is the largest community water system on the island. This system has lowered head values in that region and additional pumping will raise the position of the saltwater interface considerably.

The vulnerability of the northern region of the island does not mean that the island's freshwater resources are in jeopardy. The modeling study revealed that in general most of the Double Bluff aquifer, especially the

interior portions, can sustain substantial development with little effect on the position of the saltwater interface. With careful planning there is no reason why Guemes Island can not support future growth and still maintain the integrity of its freshwater resources.

Use of a standard flow model and simulating the position of the saltwater interface as a no flow boundary can be a valuable resource in investigating water resources in coastal areas. Although the method does not take into account the transition zone or localized changes in concentrations, the aquifer system can be modeled in detail and an estimation of the shape and position of the interface can be used to plan future development of the flow system. The complexity the saltwater intrusion problem and the necessity of managing these systems to maintain water resources, dictates the need for future advances in this field of study.

## 6. REFERENCES

- Anderson, M. P., and WW Woessner. (1992). *Applied Groundwater Modeling*, Academic Press, San Diego.
- Atkinson, S. F., G.D. Miller, D.S. Curry, and S.B. Lee. (1986). *Saltwater Intrusion: Status and Potential in the Contiguous United States*, Lewis Publishers, Chelsea, Michigan.
- Aucott, W. R. (1988). "The Predevelopment of the Groundwater Flow system and Hydrologic Characteristics of Coastal Plains Aquifers of South Carolina." USGS, Water Investigation Report 86-4347 .
- AWWA. (1990). "Water Quality and Treatment: A Handbook of Community Water Supplies." , F. W. Pontius, ed., McGraw-Hill, New York.
- Ayers, J. F., and H.L. Vacher. (1983). "A Numerical Model Describing Unsteady Flow in a Freshwater Lens." *Water Resources Bullentin*, 19(5), 785-792.
- Bear, J., and G. Dagan. (1964a). "Movin Interface in Coastal Aquifers." *J. Hydraul. Div. ASCE*, 90(HY4), 193-215.
- Bear, J., and G. Dagan. (1964b). "Some Exact Solutions of Interface Problems by Means of the Hodograph Method." *Journal of Geophysical Research*, 69(2), 1563-1572.
- Bear, J. (1979). *Hydraulics of Groundwater*, McGraw-Hill, New York.
- Bear, J., and I. Kapuler. (1981). "A Numerical Solution for the Movement of an Interface in a Layered Coastal Aquifer." *Journal of Hydrology*, 50, 273-298.
- Bedient, P. B., H.S. Rifia, and C.J. Newell. (1994). *Ground Water Contamination*, Prentice-Hall, Englewood, Cliffs, New Jersey.
- Bush, P. W., and R.H. Johnston. (1986). "Floridian Regional Aquifer System Study, In: Regional Aquifer-System Analysis Program of the USGS: Summary of Projects.", R.J.Sun ed., USGC Circ. 1002.

- Bush, P. W. (1988). "Simulation of Saltwater Movement in the Floridian Aquifer System, Hilton Head Island, South Carolina." USGS, Water Supply Paper 2331.
- Calvache, M. L. and A. Pulido-Bosch. (1991). "Saltwater Intrusion into a Small Coastal Aquifer." *Journal of Hydrology*, 129, 195-213.
- Chow, V. T. (1964). *Handbook of Applied Hydrology*, McGraw-Hill, New York.
- Cooper, H. H. (1959). "A Hypothesis Concerning the Dynamic Balance of Freshwater and Saltwater in a Coastal Aquifer." *Journal of Geophysical Research*, 64, 461-467.
- Cooper, H. H., et al. (1964). "Sea Water in Coastal Aquifers." USGS, Water Supply Paper 1613-C.
- Essaid, H. I. (1990). "A Multilayered Sharp Interface Model of Coupled Freshwater and Saltwater Flow in Coastal Systems: Model Development and Application." *Water Resources Research*, 26(7), 1431-1454.
- Fetter, C. W. (1972). "Position of the Saline water Interface Beneath Oceanic Islands." *Water Resources Research*, 8(5), 1307-1315.
- Freeze, R. A., and J. A. Cherry. (1979). *Groundwater*, Prentice-Hall, Englewood Cliffs, NJ.
- Glover, R. E. (1959). "The Pattern of Freshwater Flow in a Coastal Aquifer." *Journal of Geophysical Research*, 64, 439-475.
- Guswa, R. E., and D. R. LeBlanc. (1985). "Digit Models of Groundwater Flow in the Cape Cod Aquifer System, Massachusetts." USGS, Water Supply Paper 2209-.
- Hamilton, P. A., and J. D. Larson. (1988). "Hydrogeology and Analysis of the Groundwater Flow System in the Coastal Plain of Southeastern Virginia." USGS, Water Resources Investigation 87-4240.
- Handbook of Hydrology*. D. A. Maidment, ed, McGraw-Hill, New York.
- Henry, H. R. (1964). "Interfaces Between Saltwater and Freshwater in Coastal Aquifers, In: Sea Water in Coastal Aquifers." USGS, water Supply Paper 1613-C.

- Herbert, A. W., C.P. Jackson, and D.A. Lever. (1988). "Coupled Groundwater Flow and Solute Transport with Fluid Density Strongly Dependent Upon Concentration." *Water Resources Research*, 24(10), 1781-1795.
- Hickey, J. J. (1989). "Circular Convection During Subsurface Injection of Liquid Waste." *Water Resources Research*, 25(7), 1481-1495.
- Huyakorn, P. S., M.J. Unga, L.A. Mulkey, and E.A. Sudicky. (1987). "A Three-Dimensional Analytical Method for Predicting Leachate Migration." *Groundwater*, 25(5), 588-598.
- Huyakorn, P. S., Y.S. Wu, and N.S. Park. (1996). "Multiphase approach to the numerical solution of a sharp interface saltwater intrusion problem." *Water Resources Research*, 32(1), 93-102.
- Inouchi, K., Y. Kishi, and T. Kakinuma. (1985). "The Regional Unsteady Interface Between Freshwater and Saltwater in a Confined Coastal Aquifer." *Journal of Hydrology*, 77, 307-331.
- Inouchi, K., Y. Kishi, and T. Kakinuma. (1990). "The Motion of Coastal Groundwater in Response to the Tide." *Journal of Hydrology*, 115, 165-191.
- Johnson, M. J., D.J. Lundquist, J. Laudon, and J.T. Mitten. (1988). "Hydrogeology and Mathematical Simulation of the Pajaro Valley aquifer System, Santa Cruz and Monterey Counties, California." USGS, Water Resources Investigation 87-4281.
- Kahle, S. C., and T.D. Olsen. (1995). "Hydrogeology and Quality of Water on Guemes Island, Skagit County, Washington." USGS, Water Resources Investigation 94-4236.
- Kipp, K. L. J. (1987). "HST3D: A Computer Code for Simulation of Heat and Solute Transport in Three-Dimensional Groundwater Flow Systems." USGS, Water Resources Investigation 86-4095.
- Kohout, F. A. (1960a). "Cyclic Flow of Saltwater in the Biscayne Aquifer of Southeastern Florida." *Journal of Geophysical Research*, 65, 2133-2141.
- Kohout, F. A. (1960b). "Flow Pattern of Freshwater and Saltwater in the Biscayne Aquifer of the Miami Area, Florida." *International*

*Association of Science and Hydrology, Commission of Subterranean Waters*, 440-448.

- Konikow, L. F., and J.D. Bredehoeft. (1978). "Computer Model of Two-Dimensional Solute Transport and Dispersion in Groundwater." , USGS, Washington, D.C.
- Kontis, A. L., and R.J. Mandle. (1988). "Modification of a Three-Dimensional Groundwater Flow Model to Account for Variable Water Density and Effects of Mutiaquifer Wells." 1988, USGS.
- Kuiper, L. K. (1983). "A Numerical Procedure for the Solution of the Steady State Variable Density Groundwater Flow Equation." *Water Resources Research*, 19(1), 234-240.
- Kuiper, L. K. (1985). "Documentation of a Numerical Code for the Simulation of Variable Density Groundwater Flow in Three Dimensions." USGS, Water Resources Investigation 84-4302.
- Maas, E. V. (1984). "Crop Tolerance." *California Agriculture*, 38(10), 20-22.
- McDonald, M. G., and A.W. Harbaugh. (1984). "A Modular Three-Dimensional Finite Difference Groundwater Flow Model." 83-875, USGS, Washington, DC.
- Mercer, J., S. Larson, and C. Faust. (1980). "Simulation of Saltwater Interface Motion." *Ground Water*, 18(4), 374-385.
- Miller, M. R. (1980). "Regional Assessment of the Saline-Seep Problem and a Water Quality Inventory of the Montana Plains." 107, Montana Water Resources Research Center, Bozeman, Montana.
- Mualem, Y., and J. Bear. (1974). "The Shape of the Interface in Steady Flow in a Stratified Aquifer." *Water Resources Research*, 10(6), 1207-1215.
- Oberdorfer, J. A., J.P. Hogan, and R.W. Buddemeier. (1990). "Atoll Island Hydrology: Flow and Freshwater Occurrence in a Tidally Dominated System." *Journal of Hydrology*, 120, 327-340.
- Pinder, G. F., and H.H. Cooper Jr. (1970). "A Numerical Technique for Calculating the Transient Position of the Saltwater Front." *Water Resources Research*, 6(3), 875-882.

- Pinder, G. F., and R.H. Page. (1977) "Finite Element Simulation of Saltwater Intrusion on the South Fork of Long Island." *First International Conference on Finite Elements in Water Resources*, Princeton University, 2.51-2.69.
- Polo, J. F., and F.R. Ramis. (1983). "Simulation of Saltwater-Freshwater Interface Motion." *Water Resources Research*, 19(1), 61-68.
- Rielly, T. E., and A.S. Goodman. (1985). "Quantitative Analysis of Saltwater-Freshwater Relationships in Groundwater Systems: A Historical Perspective." *Journal of Hydrology*, 89, 125-160.
- Rielly, T. E., and A.S. Goodman. (1987). "Analysis of Saltwater Upconing Beneath a Pumping Well." *Journal of Hydrology*, 89, 169-204.
- Risser, D. W. (1988). "Simulated Water-Level and Water-Quality Changes in the Bolson-Fill Aquifer, Post Headquarters Area, White Sands Missile Range, New Mexico." USGS, Water Resources Investigation 87-4152..
- Rivera, A., E. Ledoux, and S. Sauvagnag. (1990). "A Compatible Single-Phase/Two-Phase Numerical Model: Application to a Coastal Aquifer in Mexico." *Ground Water*, 28(2), 215-223.
- Sanford, W. E., and L.F. Konikow. (1985). "A Two-Constituent Solute Transport Model for Groundwater Having Variable Density." USGS, Water Resources Investigation 85-4279.
- Shamir, U., and G. Dagan. (1971). "Motion of Seawater Interface in Coastal Aquifers: A Numerical Solution." *Water Resources Research*, 7(3), 1165-1174.
- Strack, O. D. L. (1976). "A Single Potential Solution for Regional Interface Problems in Coastal Aquifers." *Water Resources Research*, 12(6), 1165-1174.
- Strack, O. D. L. (1989). *Groundwater Mechanics*, Prentice-Hall, Englewood Cliffs, NJ.
- Taigbenu, A. E., J. A. Liggett, and A. H. -D. Cheng. (1984). "Boundary Integral Solution to Seawater Intrusion into Coastal Aquifers." *Water Resources Research*, 20(8), 1150-1158.

- Todd, D. K., and C.F. Meyer. (1971). "Hydrology and Geology of the Honolulu Aquifer." *Jour. Hydraulics Div. ASCE*, 97, 233-256.
- Todd, D. K. (1974). "Saltwater Intrusion and its Control." *Jour, of Amer. Water Works. Assoc.*, 66, 180-187.
- Todd, D. K. (1980). *Groundwater Hydrology*, 2nd ed., John Wiley & Sons, New York.
- USEPA, Office of Air and Water Programs. (1973). "Identification and Control of Pollution from Saltwater Intrusion." EPA-430/9-73-013.
- Voss, C. I. (1984). "A Finite-Element Simulation Model for Saturated-Unsaturated, Fluid-Density Dependent Groundwater Flow with energy Transport or Chemically Reactive Single-Species Solute Transport." USGS, Water Investigation Report 84-4369.
- Voss, C. I., and W.R. Souza. (1987). "Variable Density Flow and Solute Transport Simulation of Regional Aquifers Containing a Narrow Freshwater-Saltwater Transition Zone." *Water Resources Research*, 23(10), 1851-1866.
- Wilson, J. a. A. S. d. C. (1982). "Finite Element Simulation of a Saltwater/Freshwater Interface with Indirect Toe Tracking." *Water Resources Research*, 18(4), 1069-1080.
- Wirojanagud, P., and R.J. Charbeneau. (1985). "Saltwater Upconing in Unconfined Aquifers." *J. Hydraul. Eng. ASCE*, 111(3), 417-434.
- Wu, J., Y. Xue, P. Liu, J Wang, Q. Jiang, and H. Shi. (1993). "Seawater Intrusion in the Coastal Area of Laizhou Bay, China." *Ground Water*, 31(5), 740-745.
- Xue, J., X. Chunhong, J.Wu, P. Lui, J. Wang, and Q. Jiang. (1995). "A Three-Dimensional Miscible Transport Model for Seawater Intrusion in China." *Water Resources Research*, 31(4), 903-912.



## APPENDIX A

### MATLAB Code for Numerical Solution of the Circular Island

```
% Numerical Solution to the Interface Problem
%
% Author: Shawn M. Paquette
%
% Date: October 19, 1995
%
%

clear
delete salt.out
diary salt.out

x=17; % number of grid cells in the x-direction
y=17; % number of grid cells in the y-direction
delta=704; % x/y dimension of each of the square grid cells

% Set up the matrix of Boundry conditions to reflect the island in question
% zero values reflect constant head cells of 0 ft msl
% nonzero values reflect the island cells where the heads will be computed

int=[0 0 0 0 0 0 0 0 0 0 0 0 0 0 0 0 0
      0 0 0 0 0 0 1 1 1 1 1 0 0 0 0 0 0
      0 0 0 0 1 1 1 1 1 1 1 1 1 0 0 0 0
      0 0 0 1 1 1 1 1 1 1 1 1 1 1 0 0 0
      0 0 1 1 1 1 1 1 1 1 1 1 1 1 1 0 0
      0 0 1 1 1 1 1 1 1 1 1 1 1 1 1 0 0
      0 1 1 1 1 1 1 1 1 1 1 1 1 1 1 1 0
      0 1 1 1 1 1 1 1 1 1 1 1 1 1 1 1 0
      0 1 1 1 1 1 1 1 1 1 1 1 1 1 1 1 0
      0 1 1 1 1 1 1 1 1 1 1 1 1 1 1 1 0
      0 0 1 1 1 1 1 1 1 1 1 1 1 1 1 1 0
      0 0 1 1 1 1 1 1 1 1 1 1 1 1 1 1 0
      0 0 0 1 1 1 1 1 1 1 1 1 1 1 1 0 0
      0 0 0 0 1 1 1 1 1 1 1 1 1 1 0 0 0
      0 0 0 0 0 0 1 1 1 1 1 0 0 0 0 0 0
      0 0 0 0 0 0 0 0 0 0 0 0 0 0 0 0 0];
```

```

% Set up the values for the problem to be addressed

W=0.02; % Recharge in ft/day
Kavg=50; % Conductivity in ft/day
gs=1.025; % Density of seawater in kg/l
gf=1.0; % Density of freshwater in kg/l

% The matrix to be computed from the difference equation is  $h^2$  or the
% square of the hydraulic head

% initialize  $h^2$  matrix by assigning all interior head values to 100 ft
h=100*int;

maxerr=100; % initialize the maximum error
iter=1; % initial the iterations

while maxerr>0.001 & iter<10000
    iter=iter+1; % counting function for the number of iterations
    maxerr=0; % clears the maxerr from the last iteration so a new one can be
              % computed
    for i=1:x
        for j=1:y
            hold=h(i,j);
            if int(i,j)==0
                h(i,j)=0; % The head is 0 ft msl

            else
                % Solve the difference equation
                temp=0.25*(h(i+1,j)+h(i-1,j)+h(i,j+1)+h(i,j-1));
                h(i,j)=temp-(0.25*delta^2*(-2)*W)/(Kavg*gf/(gs-gf));
            end % if statement

            error=abs(hold-h(i,j)); % Solving for the stopping criteria
                                   % or the difference between new and
                                   % old estimation at this cell

            % Check to see if this error is larger than the previous max error

            if error>maxerr
                maxerr=error;
            end % if statement

        end % for with j
    end % for with i
end % while loop

```

```
end % for with i

end % while statement

disp('Head Values to the Numerical Solution')
disp(' ')
head=sqrt(h)
disp('Elevation of the Interface by Numerical Solution')
disp(' ')
interface=-(gf/(gs-gf))*head
contour(head,[0 2 4 6 8 10])
c=contour(head,[0 2 4 6 8 10 12]);
clabel(c)
axis('image')
xlabel('Cell Numbers in the X-Direction')
ylabel('Cell Numbers in the Y-Direction')
title('Hydraulic Head Values for the Num. Approx.: 17 X 17 Grid')

diary off
```

## APPENDIX B

### IBOUND Conditions for the MODFLOW Solution to the Circular Island

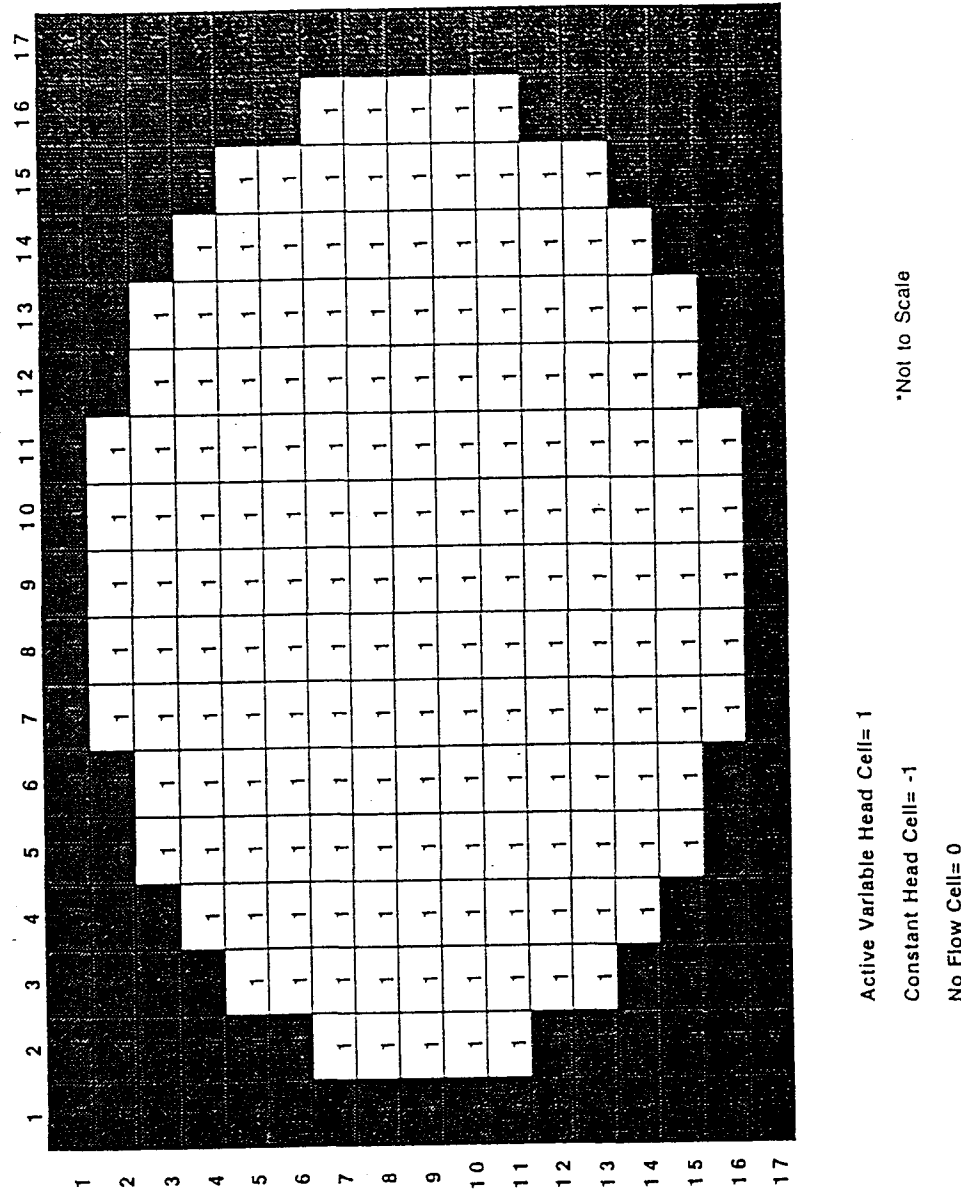


Figure B.1: IBOUND Conditions for Layer1 of the 17x17x20 Grid

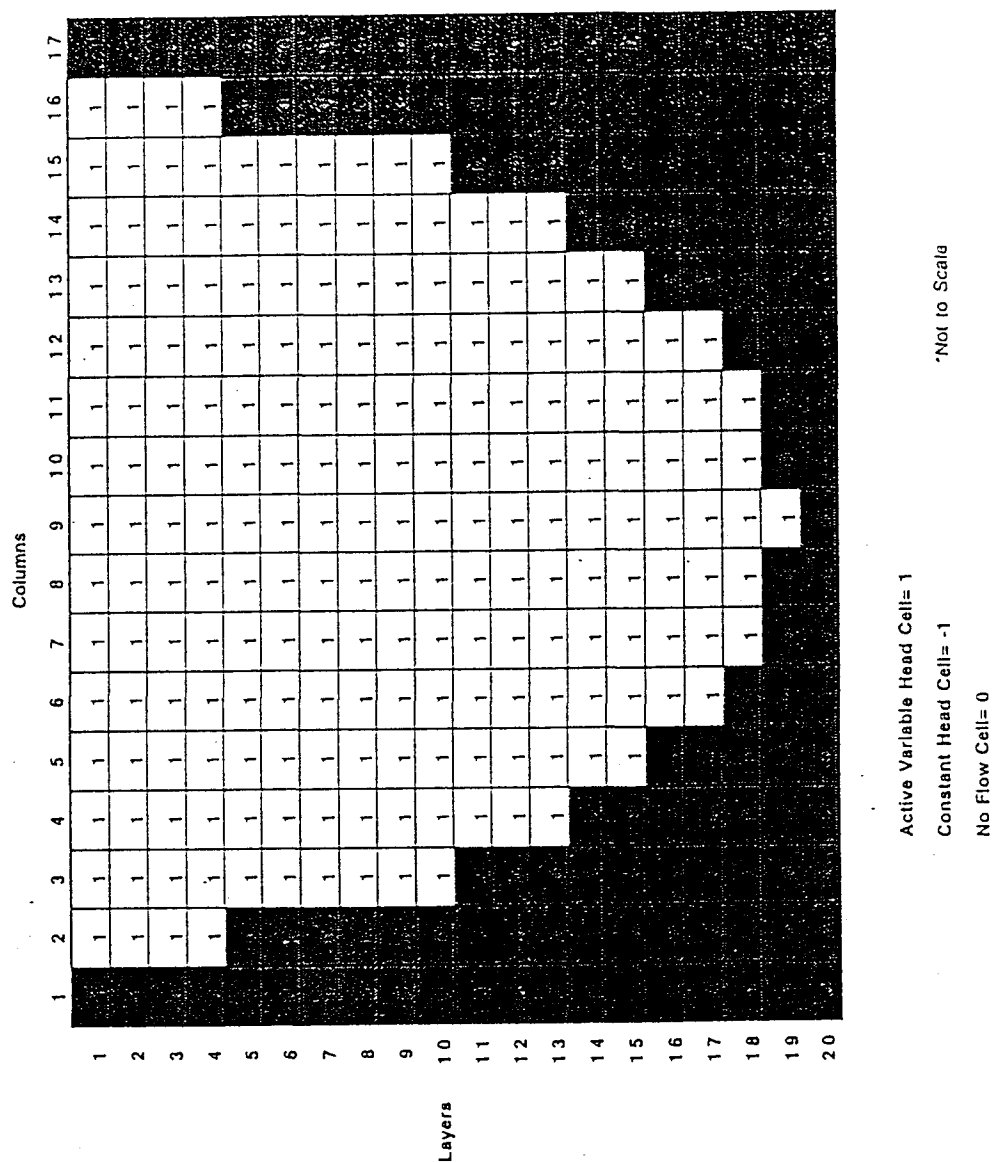


Figure B.2: IBOUND Conditions for Row 9 of the 17x17x20 Grid

## APPENDIX C

## Extent and Thickness of the Vashon Aquifer

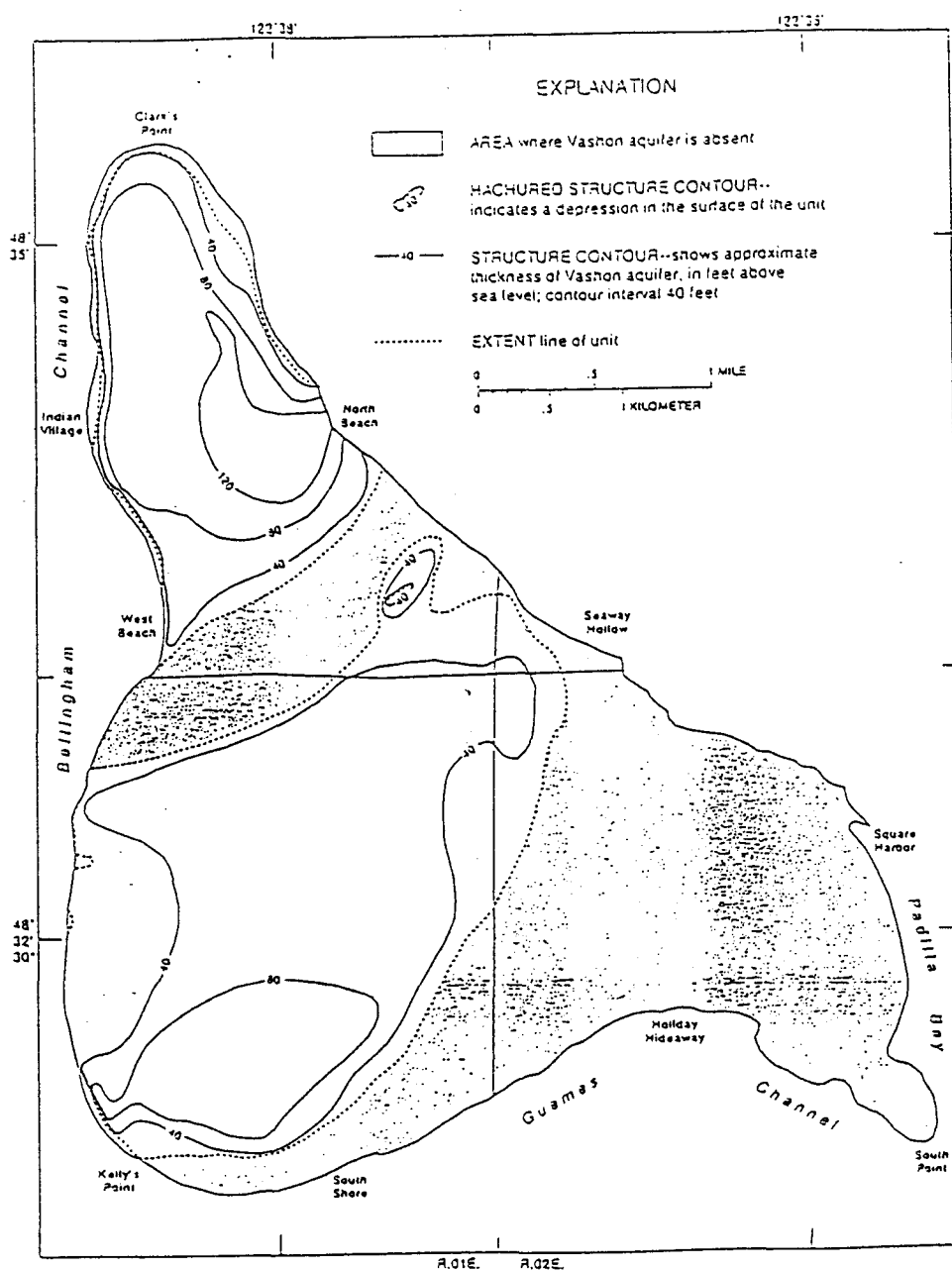


Figure C.1: Extent and Thickness of the Vashon Aquifer

## APPENDIX D

## Double Bluff Aquifer Well Information

Table D.1: Double Bluff Aquifer Well Information

Well Number	X Coordinate	Y Coordinate	Depth to casing (ft)	Estimated Withdrawl (gal/day)	Est. Withdrwl (cu. ft/day)	Layer In MOCFLOW
01A01	22	25	-6	145	19.35	6
01A02	22	27	-40	313	41.80	7
01O01	14	25	-20	218	29.12	5
01F01	17	29	-15	297	39.54	5
01H01	22	29	-25	146	19.51	7
01M01	14	30	-15	110	14.53	6
01R01	21	34	-108	328	43.88	9
02A01	10	25	-23	1680	224.49	7
02G01	8	29	-36	239	31.90	7
02L03	6	29	-77	75	9.97	8
02P01	5	32	-45	82	11.02	7
11B01	7	34	-30	131	17.47	7
11-E01	5	37	-55	2800	374.15	7
11L01	6	41	-50	278	37.19	7
11P01	6	42	-29	336	44.93	7
11P02	6	42	-40	281	37.57	7
11P03	6	41	-23	230	30.70	7
11P04	6	41	-32	147	19.59	7
11Q02	7	43	-67	115	15.43	8
11Q03	8	44	-22	99	11.95	7
11R01	9	44	-10	309	41.32	6
12H02	20	37	-141	174	23.27	10
12P03	14	42	-180	280	37.47	11
12P04	15	43	-139	108	14.16	9
12Q01	17	43	-134	260	34.75	9
12R01	19	42	-105	214	28.62	9
12R02	19	42	-97	344	45.93	8
13C01	15	43	-150	169	22.62	10
14A01	9	44	-25	227	30.34	7
14B01	7	43	-56	176	23.54	7
14B02	7	43	-70	169	22.63	8
14B03	8	44	-28	125	16.70	7
14B04	8	44	-43	92	12.23	7
06C02	25	26	-23	157	20.96	7
06-E01	23	27	-14	184	24.57	6
07H01	30	37	-27	112	14.92	7
08-E01	32	37	-114	92	12.23	9
25N01	13	12	-5	329	43.99	6
25N05	14	14	-145	184	24.58	10
25N06	13	14	-17	264	35.29	6
25H01	10	9	-4	336	44.92	6
26J01	10	11	-17	74	9.93	6
26K01	8	11	-29	216	28.90	7
26K02	7	11	-45	228	30.50	7
25R01	12	12	-29	235	31.45	7
35C01	6	15	-40	167	22.27	7
35F01	7	17	-24	6400	855.20	7
35G01	9	18	-18	9800	1309.52	6
35G02	9	19	-30	7560	1010.20	7
36Q01	19	22	-95	281	37.52	8
36R01	22	23	-14	90	12.09	6
31M01	22	21	-54	184	24.53	7
31M02	22	21	-14	232	31.00	6
31P01	24	24	-83	3360	448.98	8

## APPENDIX E

## Water Quality Summary of Guemes Island

Table E.1: Summary of Concentrations of Common Constituents, Guemes Island, June 1992

Constituent	Concentrations: (in mg/l unless otherwise noted)				
	Minimum	25th Percentile	Median	75th Percentile	Maximum
pH (standard units)	6.2	6.8	7.2	7.9	8.5
Dissolved Oxygen	0	<0.1	0.7	2.4	9.2
Specific Conductance (microS/cm)	221	266	352	586	1370
Hardness (as CaCO <sub>3</sub> )	63	91	120	170	270
Calcium	10	16	20	31	53
Magnesium	7.5	12	16	22	33
Sodium	10	13	19	72	200
Percent Sodium	9	18	26	53	85
Potassium	0.5	1.8	3.2	5.2	11
Alkalinity (as Ca CO <sub>3</sub> )	48	68	128	172	286
Sulfate	<0.1	10	22	36	82
Chloride	13	16	21	59	330
Fluoride	<0.1	<0.1	<0.1	0.1	0.3
Silica	13	28	30	35	50
Dissolved Solids	141	178	236	357	760
Nitrate (as nitrogen)	<0.05	<0.05	0.08	1.3	6.8
Iron (microg/l)	10	19	160	1170	7100
Manganese microg/l)	1	6	34	150	1500



Table E.2: Median Concentrations of Common Constituents by Unit, Guemes Island, June 1992

Constituent	Concentrations: (in mg/l unless otherwise noted)				
	Sc	Va	Wb	Db	Br
pH (standard units)	7.2	6.5	8.2	7.6	7.7
Dissolved Oxygen	0.4	2.4	<0.1	0.4	1.2
Specific Conductance (microS/cm)	347	242	557	345	500
Hardness (as CaCO3)	150	83	172	120	230
Calcium	38	18	33	19	42
Magnesium	13	10	21	18	30
Sodium	14	16	55	24	17
Percent Sodium	17	29	38	27	14
Potassium	1.9	1.6	5.7	3.7	4.2
Alkalinity (as Ca CO3)	142	61	247	135	194
Sulfate	18	29	22	12	50
Chloride	13	18	24	27	20
Fluoride	<0.1	<0.1	0.2	0.1	<0.1
Silica	13	30	29	32	30
Dissolved Solids	199	165	341	234	311
Nitrate (as nitrogen)	0.55	1	<0.05	<0.05	0.06
Iron (microg/l)	33	19	971	500	157
Manganese microg/l	36	3	54	150	20

